Evaluation of Non-Intrusive Monitoring for Condition Based Maintenance Applications on US Navy Propulsion Plants

by

William C. Greene

MBA, Warrington College of Business, University of Florida, 1996
B.S., Nuclear Engineering, University of Florida, 1988

Submitted to the Department of Ocean Engineering and the Department of Mechanical Engineering in Partial Fulfillment of the Requirements for the Degrees of

Master of Science in Naval Architecture and Marine Engineering

and

Master of Science in Mechanical Engineering

at the

Massachusetts Institute of Technology

June 2005

Signature of Author William C. Greene
Department of Ocean Engineering and the
Department of Mechanical Engineering
May 12, 2005

Certified by
Steven Leeb, Associate Professor of Electrical Engineering and Computer Science
Department of Electrical Engineering and Computer Science
Thesis Supervisor

Certified by David L. Trumper
David Trumper, Associate Professor of Mechanical Engineering
Department of Mechanical Engineering
Thesis Reader

Certified by
Timothy J. McCoy, Associate Professor of Naval Construction and Engineering
Department of Mechanical Engineering
Thesis Reader

Accepted by
Michael Triantafyllou, Professor of Ocean Engineering
Chairman, Department Committee on Graduate Students
Department of Ocean Engineering

Accepted by
Lallit Anand, Professor of Mechanical Engineering
Chairman, Department Committee on Graduate Students
Department of Mechanical Engineering

Evaluation of Non-Intrusive Monitoring for Condition Based Maintenance Applications on US Navy Propulsion Plants

by

William C. Greene

Submitted to the Department of Ocean Engineering and the Department of Mechanical Engineering in Partial Fulfillment of the Requirements for the Degrees of

Master of Science in Naval Architecture and Marine Engineering
and
Master of Science in Mechanical Engineering

ABSTRACT

The thesis explores the use of the Non-intrusive Load Monitor (NILM) in Condition Based Maintenance (CBM) applications on US Navy ships as part of the Office of Naval Research Electric Ship Integration (ESI) Initiative. The NILM is a device that measures an electrical component's performance by applying a single voltage and current transducer to a ship's existing power distribution system. The NILM was originally developed to monitor electrical power usage in buildings where it was noticed that it could disaggregate and report the operation of individual loads when many loads were present. The limits of this capability are explored by employing a signal processing script in MATLAB using component data gathered on the *USCGC SENECA (WMEC-906)*. The plausibility of using a few NILMs to provide machinery monitoring information for an entire engineering space, and the resulting opportunity to reduce sensor growth on future Navy ships is explored. Then efforts to monitor naval propulsion plant machinery with the NILM are discussed. Two NILMs were constructed and installed on selected individual components at the Naval Surface Warfare Center Philadelphia DDG-51 Land Based Engineering Site (LBES). Monitoring of the Fuel Oil and Low Pressure Air Service Systems was conducted during a week long certification of the pre-commissioning crew of the *USS BAINBRIDGE (DDG-96)*. Data collected was then used to explore the use of the NILM as a diagnostic device for shipboard systems through the evaluation of mechanical transients in the Fuel Oil system and a test leak inserted into the Low Pressure Air System. Additionally, a brief overview of the Multi-function Monitor (MFM), a type of electrical protection equipment installed on many US Navy ships, is provided. The MFM could provide a natural installation point on the ship's power distribution system to monitor a multiple loads. Finally, an evaluation of the NILM as an enabling technology for Navy CBM was conducted. The Integrated Condition Assessment System (ICAS) is the U.S. Navy's "Program of Record" for CBM and is currently installed on over 97 ships fleet wide. NILM data from individual components at the LBES was monitored simultaneously with ICAS and the results are compared.

Thesis Supervisor: Steven Leeb
Title: Associate Professor of Electrical Engineering and Computer Science

Thesis Reader: David Trumper
Title: Associate Professor of Mechanical Engineering

Thesis Reader: Timothy J. McCoy
Title: Associate Professor of Naval Construction and Engineering

Acknowledgements

I would like to thank Professor Steven Leeb of the Department of Electrical Engineering and Computer Science for being a very enthusiastic supervisor and not only sharing his expert knowledge on technical issues, but also providing sage advice on the thesis process.

I would like to thank Professor Timothy McCoy, of the former Department of Ocean Engineering for his encouragement, understanding and knowledge of all things electrical in the Navy.

I would also like to thank Professor David Trumper of the Department of Mechanical Engineering for reading my thesis and providing me with his guidance.

Throughout this research, many other individuals from several organizations provided invaluable operational and technical assistance. I would like to acknowledge the contributions and advice from these people with sincere appreciation.

The Office of Naval Research and Katherine Drew who provided funding for this research through the ONR Control Challenge Project.

The Granger Foundation for their support of the Massachusetts Institute of Technology Laboratory for Electromagnetic and Electronic Systems.

My fellow students on the LEES Navy Team:

Tom DeNuicci	Chris Laughman
Rob Cox	Jim Paris

The Naval Surface Warfare Center, Carderock Division, Philadelphia for their support, time and the use of their facilities.

Captain Larry Baun	Toni Checchio
Dan Devine	Frank Facciolo
Andy Cairns	Tom "Buck" Ryan
Lee Skarbeck	Jack Eplin

The crew of the Aeigis Training and Readiness Center Detachment (ATRCD), Philadelphia for their support, especially

GSCS(SW) Tim Wilson	GSM1 (SW) Butcher

The author hopes that this study will contribute to the Navy's continuing efforts to improve maintenance on ships and submarines, allowing them to take the fight to the enemy and bring their crews home safely.

This Thesis is dedicated to my wife Theresa Greene. Her love, understanding and support throughout the research and writing process made it possible.

Table of Contents

List of Figures

List of Tables

Page Intentionally Left Blank

Chapter 1 Introduction

1.1 The Need for Improvements in US Navy Condition Based Maintenance

Monitoring of machinery systems has become increasingly important in meeting the rapidly changing maintenance requirements of US Navy warships. As the pressure to reduce manning on ships increases, so too does the need for additional automation and reduced organizational level maintenance. Increased automation in the propulsion plant has led to rapid growth in the number of machinery sensors installed. Along with reduced manning, reductions in the size of the fleet and increased operating tempos are requiring maintenance providers to make repairs faster and ensure that equipment operates reliably for longer periods. In order to deal with these challenges, the Navy has made a policy shift to Condition Based Maintenance (CBM) from the previous Preventive Maintenance System (PMS). The Navy's program of record for CBM is called the Integrated Condition Assessment System (ICAS). This paper will evaluate the use of a new monitoring technology on US Navy propulsion plants, assess how it can be integrated with current CBM practices such as ICAS and determine if it can offer solutions to some of the challenges of machinery monitoring on Navy ships.

1.2 Non-Intrusive Machinery Monitoring

The Non-intrusive Load Monitor, or NILM, is a device developed at the Massachusetts Institute of Technology (MIT) Laboratory for Electromagnetic and Electronic Systems (LEES). It was originally conceived as an alternative to standard metering in the monitoring of electrical power usage in buildings. The NILM is a device that measures voltage and current at the electric utility service entry and generates spectral power envelopes such as the one shown in Figure 1-1. The NILM can determine the operating schedule of all of the electrical loads in a target system strictly from these measurements [1], [2].

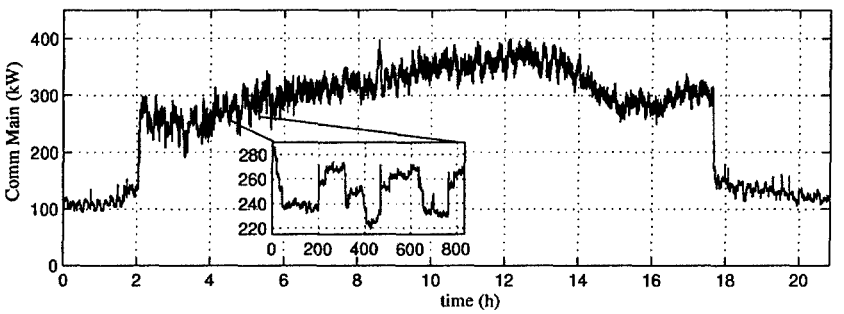

Figure 1-1: NILM Data from a Large Commercial Building

When connected to a power supply immediately upstream of a single component, the NILM will provide the power envelope of just that individual load. Figure 1-2 shows an auxiliary seawater pump being started and stopped. These power envelopes are characteristic of the physical task being performed by a load and can be used as "fingerprints" to identify individual loads. The NILM uses a transient event detector (TED) that can be trained to recognize these fingerprints during system installation. Once trained, the NILM can differentiate between the operations of individual loads, even when other loads on the same service are operating simultaneously. For example, the NILM can disaggregate and report the operation of individual electrical loads such as lights and motors from measurements of voltage and current made only at the electric meter where utility service is provided to a building [3], [4]. It can identify the operation of electromechanical devices in an automobile from measurements made only at the alternator [5].

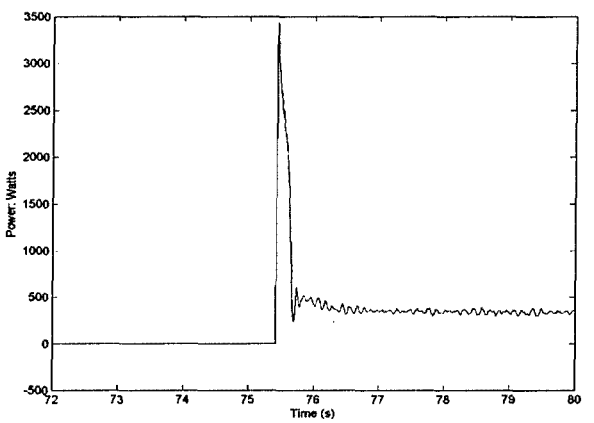

Figure 1-2: NILM Data from a Seawater Pump Startup

The NILM is in many ways an ideal entry point for measuring and collating useful information about any system that uses electromechanical devices. It requires a bare minimum of installed sensors, reducing expense and potentially enhancing system reliability. Because the NILM can associate observed electrical waveforms with the operation of particular loads, it is possible to exploit modern state and parameter estimation algorithms to verify the operation and "health" of electromechanical loads [4], [6-8]. The NILM can also monitor the operation of the electrical distribution system itself, identifying situations in which two or more otherwise healthy loads interfere with each other's operation through voltage waveform distortion or power quality problems [9], [10].

A group of researchers at LEES (designated the Navy Team) have recently begun to consider the application of the NILM to shipboard power systems and machinery monitoring [11], [12]. In theory, one or a small number of NILMs may be able to provide machinery monitoring information for an entire ship's propulsion plant, providing an opportunity to reduce sensor growth on future ships. The limits of this capability will be explored for the first time in this paper.

1.3 Current Research on Shipboard Applications of the NILM

1.3.1 Shipboard Installation

A complete NILM system consists primarily of commercial off-the-shelf (COTS) hardware and can be constructed for less than $1000. A typical shipboard monitoring system consists of a customized NEMA-type enclosure to house the measuring transducers for voltage and current at a point on the (typically three phase) power distribution system. The remainder of the NILM includes a Pentium-class computer, keyboard, monitor, data acquisition card (either PCI or USB) and an uninterruptible power supply (UPS). The computer executes the custom NILM signal processing software that disaggregates individual load events from the aggregate current and voltage data. Figure 1-3 shows a NILM on-board the *USCGC SENECA (WMEC-906)*, a 270-foot U.S. Coast Guard cutter.

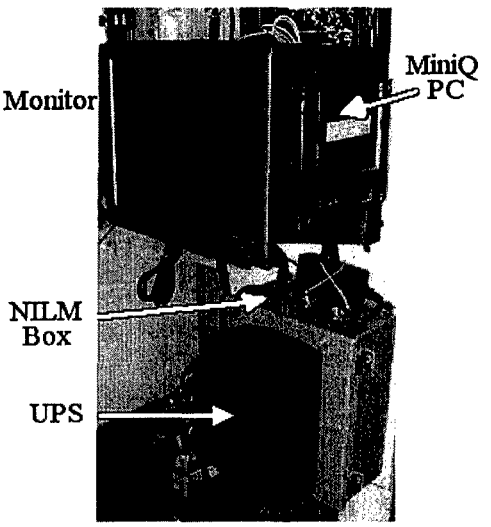

Figure 1-3: NILM Installation on the *USCGC SENECA*

The installation of the NILM is very simple and just involves lifting a few leads in the controller or power panel supplying the target component. The NILM itself operates off standard 120V AC power. Figure 1-4 shows a current transformer and voltage sensing line installed in a controller on the *SENECA*.

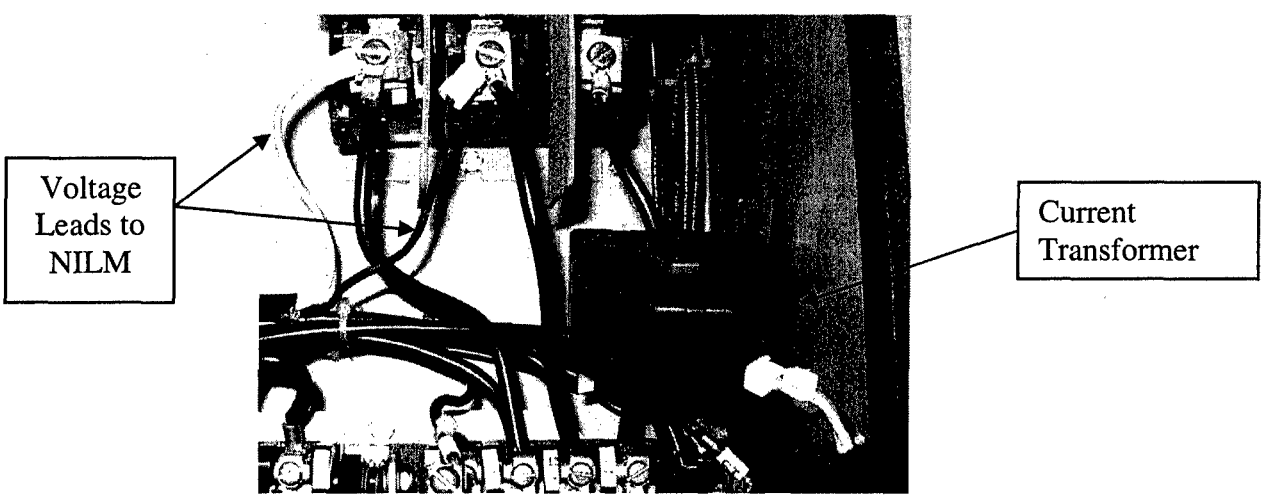

Figure 1-4: NILM Voltage Sensing Lines and Current Transformer

1.3.2 Initial Shipboard Testing

Several NILM systems were initially installed onboard the *SENECA* as discussed in reference [11]. Each of these systems was set up to monitor a relatively small collection of loads. For example, the NILM system shown in Figure 1-3 monitors a collection of four motors (two vacuum pumps and two transfer pumps) for the waste-water handling system. The NILM systems installed on the *SENECA* intentionally monitor collections of loads that are small and relatively easy for the NILM to recognize and disaggregate. The decision was made to monitor small sets of loads during field testing in order to focus on the development of diagnostic indicators for particular loads of interest to the LEES researchers and the ship's crew. Examples of results from *SENECA* are presented in Figures 1-5 through 1-8 below, including data from the auxiliary sea water (ASW) pumping system for heat loads, the waste-water vacuum pumps, and the rudder hydraulic steering gear.

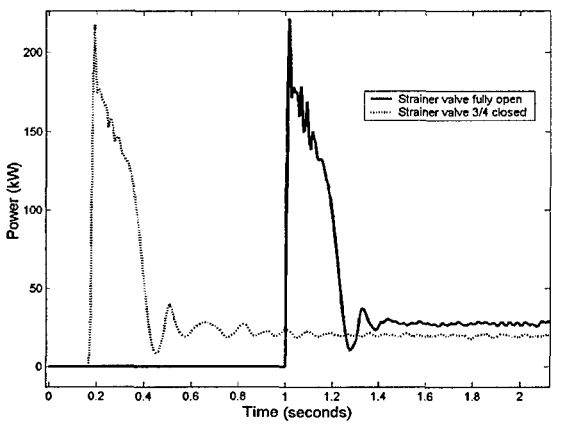

Figure 1-5: ASW Pump Starts with Inlet Flow Restriction

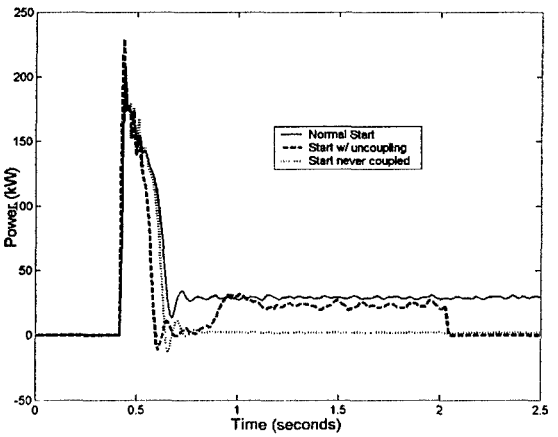

Figure 1-6: ASW Pump Starts for Various Levels of Motor and Pump Coupling

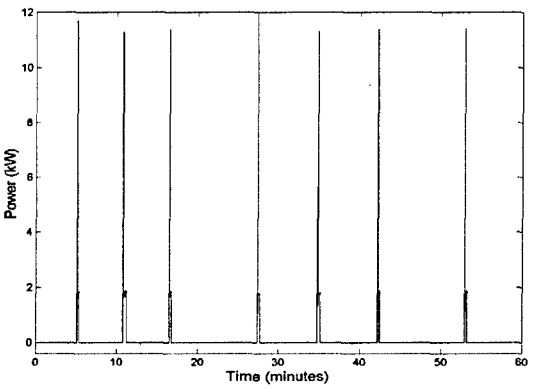

Figure 1-7: Sewage System Vacuum Pump Transients

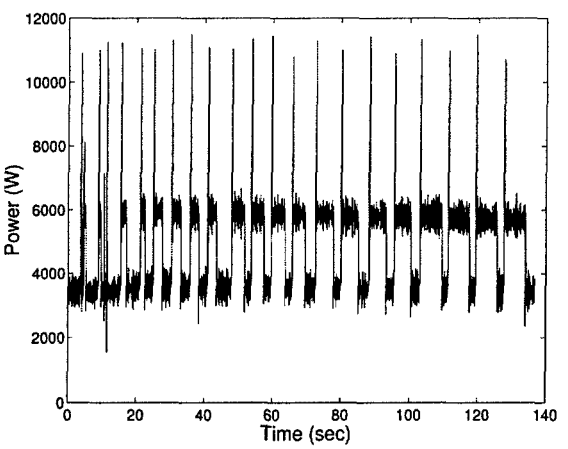

Figure 1-8: Steering Pump Transients

Using voltage and current inputs from the component's power supply, the NILM continuously computes spectral power envelopes that correspond to the harmonic content of the current waveform with respect to the phase of the voltage waveform. Harmonic current content at the line-voltage frequency corresponds, in steady-state operation, to conventional definitions of real and reactive power flow [1]. The graphs in Figures 1-5 through 1-8 illustrate the short-time harmonic content corresponding to real power flow during operation of the indicated loads. The NILM also computes reactive power flow and higher harmonic content, although these traces are not presented here. Notice in the above figures that different loads performing different physical tasks exhibit characteristic transient shapes that can be used to recognize the operation of particular loads. During installation on the *SENECA*, the NILM was trained to recognize individual components by making templates based on these transient patterns.

1.3.3 Development of Diagnostics from Shipboard Monitoring

In some cases, the figures in section 1.3.2 show both normal and pathological signatures, e.g., Figures 1-5, 1-6, and 1-7, for example, shows start-up transients for an ASW pump during normal operation and also during an impending failure of the motor-to-pump head mechanical coupling. The NILM can use the differences between "healthy" and "pathological" transient observations to recognize impending failures or maintenance needs. References [1], [3], [4], [6-9], and [11-13] discuss the adaptation of the NILM to perform diagnostic monitoring using a variety of approaches to signal processing and state and parameter trending.

Reference [12] follows the work of [11] on *SENECA*. Additional NILMs were installed and the data collected was used to develop metrics to diagnose several common shipboard system faults. The following is a summary of efforts in this area:

"D1" Cycling System Leak Identification – Initial data from the sewage system collected in reference [11] indicated that it is possible to differentiate between periods of heavy usage and fault conditions in cycling systems. The data suggested that in the presence of a leak, a "spike" will appear in the pump frequency distribution (how often the pumps cycle on and off). By

inserting numerous leak conditions, research in [12] was able to observe an increase in pump operating frequency as the size of the leak was increased.

"D2" Coupling Failure - Data collected from the *SENECA's* ASW System indicated that the NILM may be able to predict the failure of a flexible coupling linking the pump and motor components. Reference [12] tracked the frequency spectrum of the real power drawn by one of the *SENECA's* ASW pump motors during several successive starts from the installation of a new coupling until failure. It was observed that during the life of the coupling, a peak in the frequency spectrum of the real power at about 43 Hz begins to increase in magnitude until the coupling fails. A fifth order induction motor simulation with mechanical a model was used to validate these results.

"D3" Strainer and Heat Exchanger System Blockage – Research in reference [12] used frequency domain analysis of the power signature of *SENECA's* ASW Pump to identify the clogging of a sea water heat exchanger. This is a significant diagnostic as this fault is typically only detected by shutting down, draining and opening the system and then performing a time consuming manual inspection. Reference [12] also used the NILM to evaluate the performance of a new Reverse Osmosis (RO) Water Purification Plant installed on *SENECA* during the course of an entire 12 week patrol. It is hoped that a similar frequency domain analysis of the power signature of the RO pumps will help predict clogging to the water purification plant's osmotic membranes.

1.4 Research Objectives

There are three primary objectives of this research. The first objective is to explore the limits of the NILM in monitoring multiple loads simultaneously. To ameliorate the issues associated with the rapidly increasing number of sensors on naval vessels, a single NILM would ideally be able to perform load detection and CBM for more than just a few components. If a single NILM can monitor the loads in a reasonably sized engineering space, then significant economies of scale might be achievable. The development of a simulation to study these limits is presented in Chapter 2. The second objective is to test the NILM on a US Navy Propulsion Plant. This includes gaining access to a Navy facility, making long term installations of the NILM there, and

conducting machinery monitoring. Efforts in these areas are discussed in Chapters 3 and 4. Chapter 5 makes an initial evaluation of the Multi-function Monitor (MFM), a type of electrical protection equipment installed on many US Navy ships, to determine if it could be used as an installation point for the NILM. This goes hand in hand with Chapter 2, as a NILM collocated with the MFM would find a central entry point on the ship's power distribution system and would be able to monitor a significant collection of loads. The final objective is to introduce Navy's CBM program, ICAS, and demonstrate how the NILM might enhance its capabilites. This is the topic of Chapter 6.

Page Intentionally Left Blank

Chapter 2 Exploration of the Limits of Non-Intrusive Monitoring

2.1 Challenges Facing Future Machinery Monitoring Systems

In order to gain the optimal benefit from the use of CBM systems and smaller crews, it is imperative that ships be equipped with large sensor networks to provide information regarding component status. In the next few years, ICAS may have the ability to predict a fault on a particular machine or electromechanical load. With that ability, the ICAS could alert the ship's control system of the impending failure so that the load in question could be secured and an alternate unit could be brought on line [14]. To achieve this vision, the Navy is rapidly increasing the number of sensors installed on its ships. For example, a modern class of warship is the Arleigh Burke Class Destroyer (DDG-51), with the lead ship commissioned in July 1991. A typical DDG-51 has about 450 machinery and critical auxiliary sensors feeding ICAS, but more are being added through retrofitting. The San Antonio Class Amphibious Assault Ship (LPD-17) is the most recent class of US surface warship under construction with the lead ship christened in July 2003. The LPD-17 has between 1500-2000 machinery sensors [15]. Looking ahead, some estimates project the Navy's Future Surface Combatant (DDX) to have as many as 250,000 sensors, an increase of over two orders of magnitude from the number of sensors installed on LPD-17 [16].

These vast arrays of advanced sensors have brought about their own set of challenges to operators as well as the shipyards that build and maintain these vessels. The data communications wiring required for machinery monitoring systems "makes up a large part of the overall system complexity, cost and weight." One estimate for non-military industrial wiring of this kind is $5-10 per foot [17]. In addition to installation costs, cables are costly to maintain and increase the footprint of a sensor system: "They are vulnerable to damage and need to be removed and re-run whenever equipment needs moving, replacement or maintenance" [18]. Finally, the amount of power required for a network comprised of tens or hundreds of thousands of sensors is likely to be significant. As the number of shipboard sensors grows, the issues of cable cost, size, weight, maintenance, and power demand are magnified. To put things in perspective, the DDG-51 Class Destroyers already have 1,342,000 feet of cables to support

electrical power distribution, communications and sensors [19]. By introducing the NILM into a machinery space (shipboard propulsion plants are subdivided into machinery spaces) or a substantial section of a ship's electrical distribution system, it may be possible to mitigate the numerous economic and implementation issues associated with a large sensor network. Using data from field experiments conducted on-board the *SENECA* and additional laboratory tests, the following sections explore the feasibility of using the NILM to reduce the overall number of sensors in the propulsion plants on US Navy warships.

2.2 Investigating the Potential of the NILM

In order to monitor more loads, a NILM must be installed further upstream in the electrical power distribution network. As this is done, the NILM is said to become less "intrusive." Despite the obvious benefits presented by moving the NILM further from the component level, there is a trade-off involved. Specifically, as the NILM moves further upstream, it becomes increasingly difficult to identify the operation of individual loads from the measured aggregate current. A natural question arising from this situation is the following: "How 'non-intrusive' can the NILM be while still providing useful information about the operation of individual loads?"

The extent to which the NILM can be truly non-intrusive raises a direct trade-off between monitoring hardware expense and signal processing effort. That is, if several components are monitored by one NILM, sensor numbers will be reduced but signal processing demands will likely increase. To investigate the limits of monitoring multiple components with a single NILM, a simulation of a machinery space was developed using field data from the *SENECA*.

2.3 Development of a Machinery Space Simulation

Several NILM systems were employed on the *SENECA* to collect focused data on individual ship systems, including the ASW pumps, vacuum pumps, and steering gear hydraulic pumps. This data was collected with the NILM positioned close to small groups of loads of interest in order to search carefully for diagnostic indicators that could be used for CBM. In practice, a NILM might ideally be located in a major load center (or possibly in an MFM as discussed in Chapter 5) to monitor a larger collection of loads, with the data being displayed the ship's engineering

control center. Ideally, the NILM would not simply disaggregate and identify the operation of individual loads, but would also recognize key diagnostic indicators determined through close examination of the loads during the research phase.

For the "close" examination that has occurred during our early field tests, each NILM is configured with an input sensing range for current and voltage designed to take full advantage of the NILM's analog-to-digital (ADC) conversion resolution. Load data from these experiments, therefore, comes with a "scaling factor" of watts per ADC count tailored for those loads. Some of our observed component power ratings and scaling factors for the real power spectral envelope are shown in Table 2-1. The differences in scaling factors are a logical consequence of the very different sizes of the loads of interest, ranging from the smallest power consumer, a sewage vacuum pump, to the largest consumer, one of the ASW pumps. The vacuum pumps can be monitored with a higher input signal gain on the NILM data acquisition system, providing signals with the smallest watts per count resolution in our experiments. Conversely, the NILM monitoring the ASW pumps is configured with the lowest input signal gain, yielding the largest watts per ADC count in our field work.

Table 2-1: Power Ratings and Scaling Factors

Component	Rating (Hp)	Scaling Factor (watts/count)
#1 ASW pump	40	7.11
#2 ASW pump	40	7.11
#2 Vent Fan	15	0.642
#1 Sewage Vacuum Pump	1.5	0.619
#1 Sewage Discharge Pump	2	0.619
#1 Steering Pump	15	6.31
#2 Steering Pump	15	6.31

In practice, a genuinely "non-intrusive" NILM will employ a current sensor that is a compromise designed to permit observation of the largest power transients of interest while still providing the best resolution possible for the smallest transients of interest. To study the challenges that would be faced by a single NILM monitoring an aggregate current feeding all of the loads in Table 2-1, raw data observations of every load were put on a common scale. That is, base data from

individual load observations could be summed with high accuracy off-line in MATLAB. This summed data can be rescaled and digitally quantized to emulate the effect of observing the actual aggregate stream with a particular ADC front-end sampling the combined current signal. In other words, given the fine observations of small collections of loads made by several NILMs, it is possible to use this data to assemble one stream with the information content that would have been produced by a single NILM monitoring all of the loads of interest. The process is summarized in Figure 2-1 below.

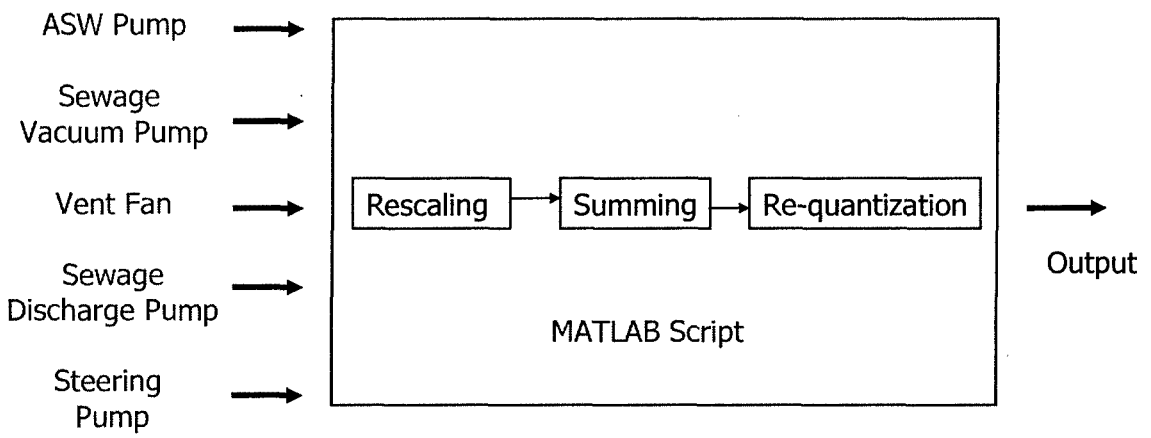

Figure 2-1: Multiple Component Monitoring Simulation

In Section 2.5, summed and re-quantized data will be used to determine the plausibility of using the NILM to monitor complex combinations of loads from a single point. For these experiments, the aggregate data was re-quantized using a simple scheme assuming that the real-power spectral envelope would be represented with 12 bits. In fact, this is a gross simplification. The NILM is able to employ significant signal processing and also 14-bit data conversion on the current and voltage measurements to enhance the input dynamic range. The simple 12-bit quantization used is a conservative choice.

As an example of this re-quantization procedure, consider a simulation representing a machinery space containing several of the components listed in Table 2-1. Evaluation of the component data reveals a maximum power that could be consumed by this collection of loads on an aggregate service, that is, a single utility feed for the collection of loads. A NILM monitoring this aggregate load would operate with a front-end ADC scaling that permitted full-range

observation from zero watts to this maximum power level. To create a conservative, quantized data stream representing what would be seen on the aggregate service, waveforms representing the sum of power consumed by these loads would be divided by this maximum power, and scaled in a range between zero and 4095 (the maximum number that can be represented by a 12-bit ADC). Finally, the "floor" function in MATLAB is applied to the data to account for quantization, thus eliminating decimal fractions and producing a hypothetical real power spectral envelope waveform consisting of integer values between 0 and 4095. The MATLAB script *"requant"* (Appendix A) helps perform the summing and rescaling, making it easy to conduct hypothetical studies using different collections of loads and assuming different operating schedules.

2.4 Waveform Recognition

With the ability to assemble realistic aggregate waveforms attributable to collections of loads of interest, the NILM can be easily tested off-line to determine the likelihood of successful load recognition. The TED for the NILM has evolved, and is discussed in several different incarnations in [1], [4], and [13], for example. The full TED employed in the NILM uses information from different spectral envelopes, and also at different points in time, in order to make a successful transient identification. This section describes a simplified approach to event detection using the MATLAB script *"recognition"* (Appendix A) that illustrates some of the tools used in the full NILM TED. It also provides quick, rough assessments of the likely success of the NILM in the anticipated aggregate load environment, as would be the case if the NILM was installed in a machinery space load center in a shipboard propulsion plant. The *"requant"* and *"recognition"* scripts may be employed to create a Machinery Space Simulation using the process described in Appendix B.

The simplified TED in the *recognition* script works as follows. Identifying a fast-varying section of an observed transient creates a "fingerprint" signature for a load of interest. Figure 2-2, for example, shows the start-up transient of one of the vacuum pumps onboard *SENECA*. A fingerprint template vector, t, consisting of N samples might be constructed by sampling a varying region of the transient, derived between 3.45 and 3.6 minutes, for example, in Figure 2-2.

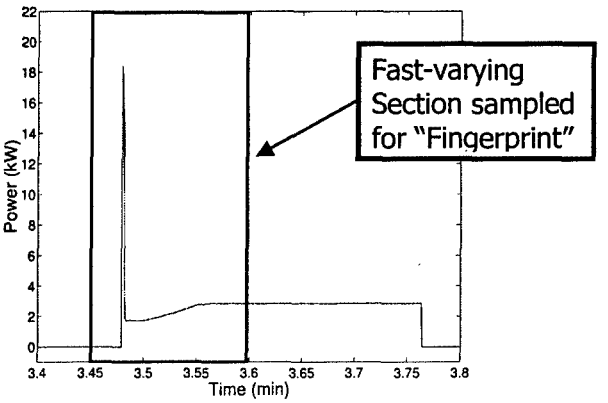

Figure 2-2: Vacuum Pump Start Transient

The vector, t, consists of elements:

$$t[i], \quad i = 0 \ldots N-1 \tag{2-1}$$

An "ac-coupled" and amplitude normalized version of this vector, designated *tac*, can be computed as:

$$tac = \frac{\left[t - \frac{1}{N} \sum_{i=0}^{N-1} t[i] \right]}{\left\| \left[t - \frac{1}{N} \sum_{i=0}^{N-1} t[i] \right] \right\|^2} \tag{2-2}$$

A transversal filter can now be used with this template, *tac,* to search an incoming data stream for the vacuum pump "fingerprint" [1]. Such a transversal filter would have an impulse response corresponding to the time-reversed samples of the vector *tac.* When the filter response is convolved with an incoming data stream, the output of the filter will be unity whenever the original template points, t, appear in the data stream. This process is illustrated in Figure 2-3 below.

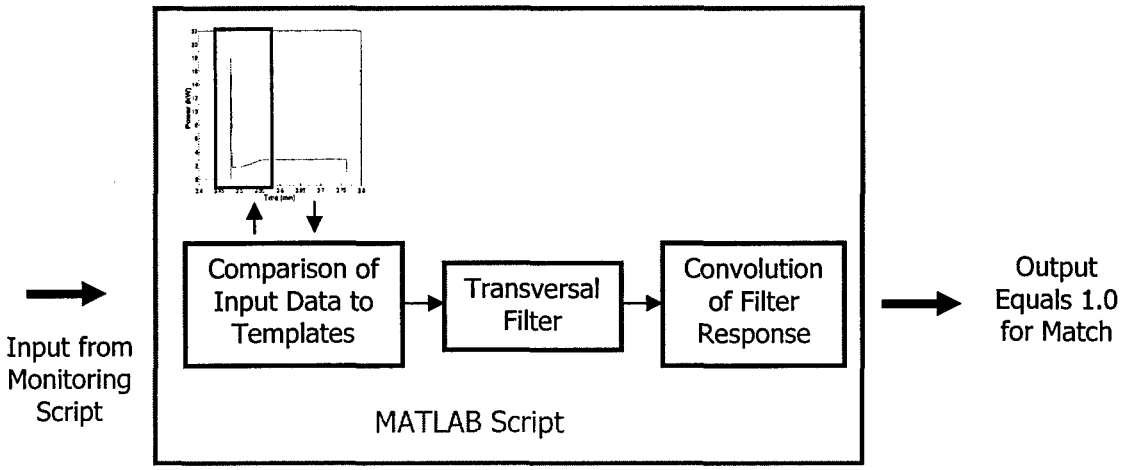

Figure 2-3: Simplified Transient Event Detection Algorithm

Essentially, this process computes the inner product between the ac-coupled and amplitude normalized template, *tac*, and a sliding window of data sampled from the incoming aggregate data stream. A unity output could indicate a perfect match. It could also indicate a window of data in the input stream with an unfortunately large norm and a different shape from the template. For this reason, a more sophisticated approach to detection is employed in the NILM TED. The simple approach described here illustrates a key computational component of the more sophisticated NILM TED, and also permits a rapid check of the reasonability of deploying the NILM to monitor a large collection of loads.

Five templates were developed for component start-up transients (Table 2-2).

Table 2-2: Target component templates

Template	Component
t1	#1 Sewage Vacuum Pump
t2	#1 Sewage Discharge Pump
t3	#2 Vent Fan
t4	#1 Steering Pump
t5	#1 ASW pump

A comparison was made of these templates with respect to the transients from which they originated and also with respect to transients used to develop templates for other loads. This comparison is presented in Table 2-3. When a template is compared to the entire signature from which it originated, the transversal filter output peaks at a match value of 1.0, as seen in the center diagonal of Table 2-3. When a template is compared with a signature of a different component, the result is a peak value other than 1.0. In reality, small variations in transients and noise from other loads make the case of a perfect match unlikely. Thus, it is necessary in practice to determine a range of peak values that can be considered to be a matching range. The values off the center diagonal in Table 2-3 provide some means for determining at least a crude set of boundaries. For example, these comparisons suggest that any peak value in the range from 0.9 to 1.1 could be considered a recognizable event.

Table 2-3: Waveform Match Values

Transient Signature	Templates				
	t1	t2	t3	t4	t5
Vacuum Pump	1.0	0.652	0.352	1.543	0.533
Discharge Pump	0.864	1.0	0.201	1.751	0.052
Vent Fan	1.267	0.6	1.0	2.073	0.065
Steering Pump	0.415	0.339	0.221	1.0	0.021
ASW Pump	16.5	13.26	5.48	28.41	1.0

2.5 Tests using *SENECA* Component Data

A total of seven tests were conducted using combinations of components from Table 2-1. The tests are grouped into three sets and are summarized in Table 2-4. The overall goal of these experiments was to determine if a target event could be detected against the background noise of the simulated engine room. The results of each test are described in this section.

Table 2-4: Description of Tests

Test Set	Test Number	Description
1	1	Recognition of vacuum pump starts against steady-state background components
	2	Recognition of discharge pump starts against steady-state background components
	3	Recognition of vent fan starts against steady-state background components
	4	Recognition of steering pump starts against steady-state background components
	5	Recognition of ASW pump starts against steady-state background components
2	6	Recognition of multiple and varying steering pump starts against steady-state background components
3	7	Recognition of sewage vacuum pump start against multiple steady-state components and transient events

Test Set 1

The first set of five tests was performed in order to evaluate the ability of the Machinery Space Simulation TED to identify a single target transient against a steady-state background signal. To implement these tests, a representative transient was added to a synthesized steady-state background signal at three different points in time. Figure 2-4 shows one such composite signal. A similar signal was created for each of the five loads listed in Table 2-2, and each of these was passed to the TED. The background signal used for each test was the same, and it was comprised of steady-state signatures produced by each of the following loads: the #1 ASW pump, the #2 ASW pump, the #2 Vent Fan with clean filters, and the #2 Vent Fan with blocked filters. A detailed description of the process used to sum the NILM data from individual loads and apply the templates in the Test Sets using the Machinery Space Simulation MATLAB scripts is provided in Appendix B. Table 2-5 lists the match values for each test case, and Figures 2-8 through 2-9 show the TED output waveform for a series of three component starts.

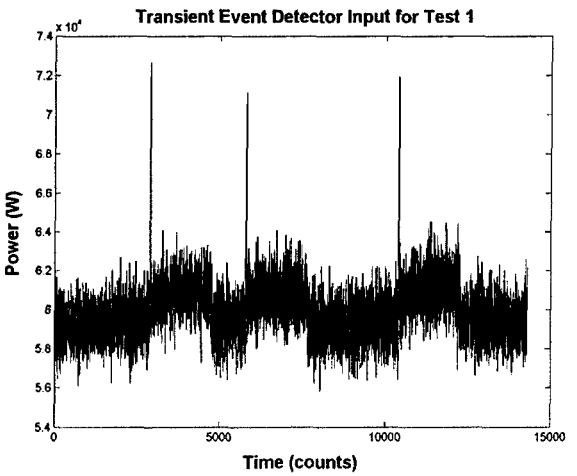

Figure 2-4: TED Input for Test 1 – Composite of 4 Steady-State Component Signatures and 3 Sewage Vacuum Pump Transient Signatures

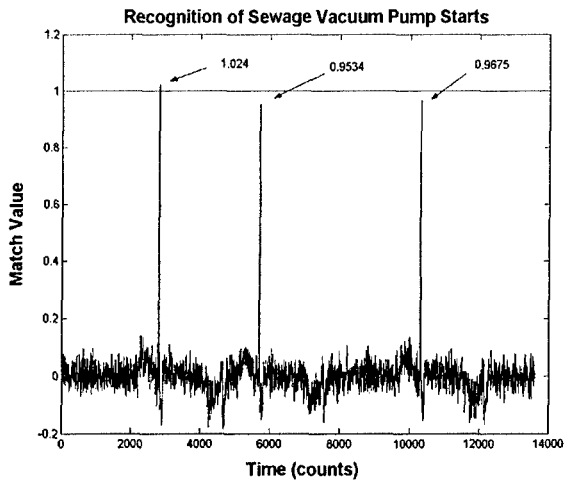

Figure 2-5: TED Output for Test 1 - Recognition of 3 Sewage Vacuum Pump Starts

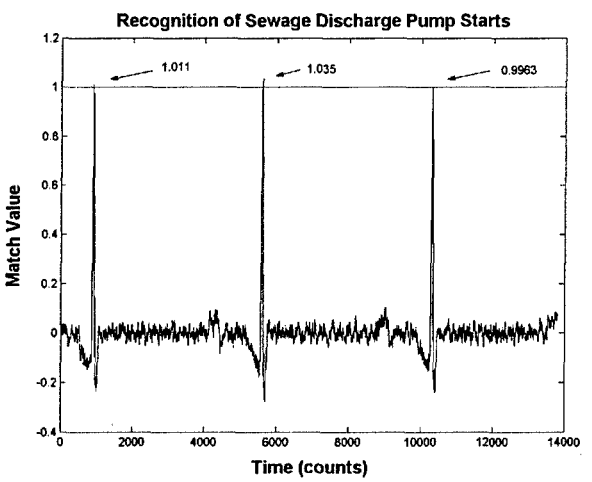

Figure 2-6: TED Output for Test 2 - Recognition of 3 Sewage Discharge Pump Starts

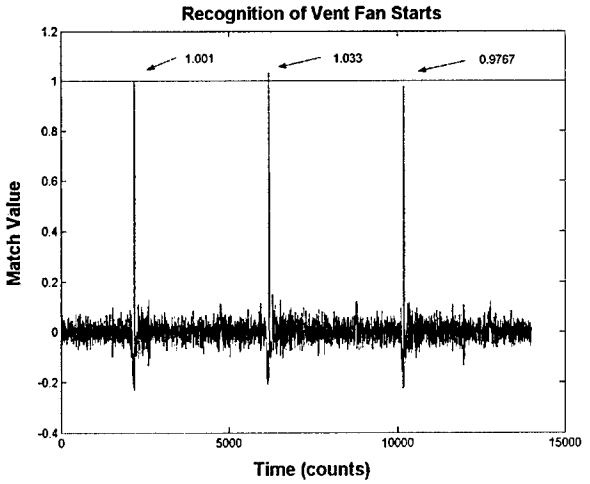

Figure 2-7: TED Output for Test 3 - Recognition of 3 Vent Fan Motor Starts

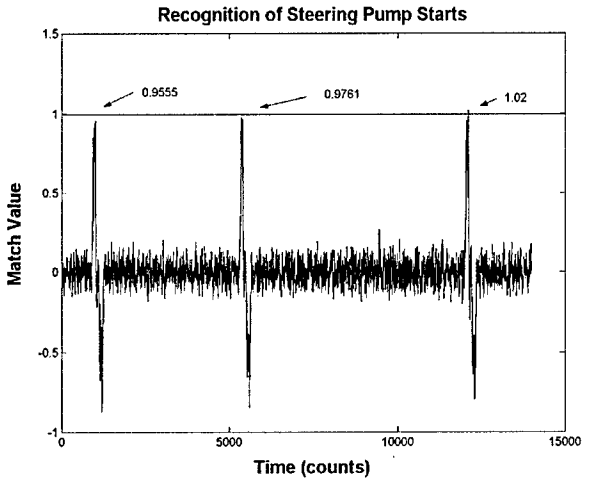

Figure 2-8: TED Output for Test 4 - Recognition of 3 Steering Pump Starts

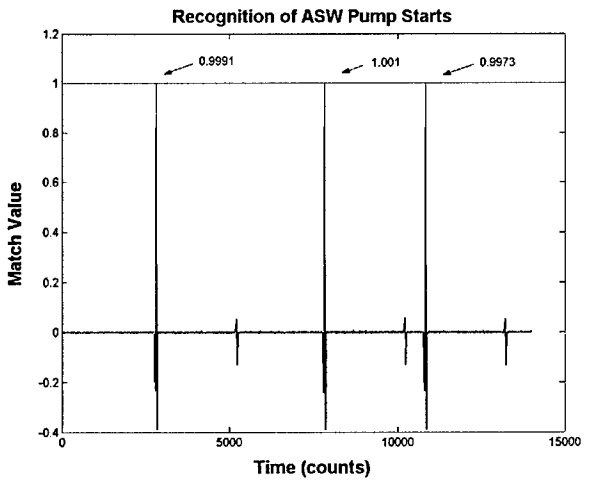

Figure 2-9: TED Output for Test 5 - Recognition of 3 ASW Pump Starts

The near-unity peak match values listed in Table 2-5 indicate that each of the loads can certainly be recognized individually while other loads are in steady operation. That is, a simple disaggregation of a load from a background stream of other loads operating in steady-state would be easily accomplished in this hypothetical scenario.

Table 2-5: Match Values for Tests 1-5 - Motor Starts Against Steady-State Background

Test/ Motor Start	Match Values			Mean
	Event #1	Event #2	Event #3	
1 Vacuum Pump	1.024	0.9534	0.9675	0.9816
2 Discharge Pump	1.011	1.035	0.9963	1.0141
3 Vent Fan	1.001	1.033	0.9767	1.0036
4 Steering Pump	0.9555	0.9761	1.0200	0.9839
5 ASW Pump	0.9991	1.001	0.9973	0.9991

Test Set 2

A second set of numeric experiments was conducted in order to evaluate the ability of a particular template to identify the operation of its associated load from several different transient events. In this case, instead of superimposing identical transients, the data used for this test were 16 different steering pump start transients recorded while the *Seneca's* rudder was fishtailing (i.e. the behavior shown in Figure 1-8). Although this test could have been performed with any of the loads listed in Table 2-2, the steering pump serves as an excellent example since our "real world" field data shows slight variability in the steering pump transient signature from start to start. Ultimately, this test should be repeated exhaustively for each load.

Each of the 16 different transients used in the second set of tests was added to the same synthesized steady-state background signature used in Test Set 1. Again, the component signals were processed using the Machinery Space Simulation (i.e. the engine room emulation and

waveform recognition processes described previously) and the output is shown in Figure 2-10. In this test, 12 of the 16 transients yielded peaks in the 0.9 to 1.1 match value range. The peaks of 4 of the 16 steering pump starting transients were slightly below the match bounds of 0.9 to 1.1. These four values are shown in Table 2-6.

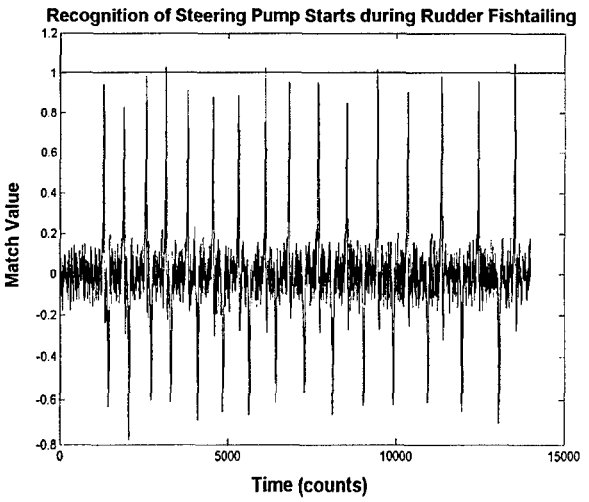

Figure 2-10: TED Output for Test 6 - Recognition of Multiple and Varying Steering Pump Starts against Steady State Background Components

Table 2-6: Match Values Exceeding Bounds of 0.9-1.1 for Test 6 - Recognition of Steering Pump Starts during Rudder Fishtailing

Pump Run	Peak Value	Deviation from Match Band
2	0.8306	0.0694
6	0.8820	0.0180
7	0.8880	0.0120
11	0.8488	0.0512

In this case, the simplistic approach to transient recognition is slightly stressed by the variability in the pump transients and the background signals. The match deviations are small, however, and the more sophisticated TED used in the full NILM would be able to recognize even the four transients referred to in Table 2-6. In fact, a template constructed not from a single observation but from the average of several training observations of the steering pump, would allow even the simple detection scheme to work in the anticipated match range with success.

Test Set 3

A final set of tests was performed in order to evaluate the ability of one template, the sewage vacuum pump template t1, to identify its associated transient against a background of both steady-state and transient component signatures. In this case, the sewage vacuum, sewage discharge, vent fan and ASW start-up transient signatures used to develop Table 2-3 were each separately superimposed on the synthesized steady-state signature used in Test Set 1 and 2. The TED output is shown in Figure 2-11. Here the Machinery Space Simulation TED easily determined that the only peak value in the matching range was due to the vacuum pump transient. Table 2-7 lists the peak match value for each transient.

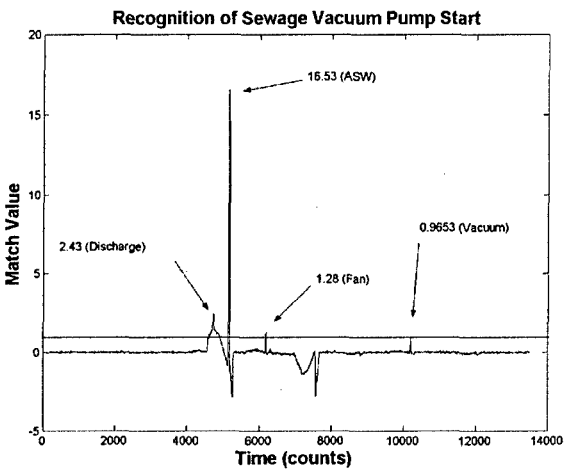

Figure 2-11: TED Output for Test 7 - Recognition of Sewage Vacuum Pump Start against Multiple Steady State and Transient Events

Table 2-7: TED Match Values for Test 7

Load	Match Value	Deviation from Match Band
Discharge Pump	2.430	1.330
ASW Pump	16.53	15.43
Vent Fan Motor	1.280	0.180
Vacuum Pump	0.9653	zero

Test Summary of Machinery Space Simulation using *SENECA* Component Inputs

The results of the first set of tests showed that start-up transients, even from a small component such as the 1.5 Hp sewage vacuum pump, consistently generate a match value inside the selected detection range of 0.9 to 1.1. The findings of the second set of experiments indicate that a single template will recognize many (12 of 16) similar transients generated by the same component. These results further indicate that the steering pump template would recognize all of the similar transients if the threshold were to be expanded slightly (by 0.0694) to include the outliers listed in Table 2-6. An examination of the column labeled t4 in Table 2-3 suggests that such a small change would not be likely to result in a false detection. The results of the final test demonstrate the use of a single template to recognize a component start-up against a more complex background of both steady-state and transient signatures. In this case the smallest component (the sewage vacuum pump) was still recognized.

2.6 Evaluation of Scale Factors in the Machinery Space Simulation

When observations are made at the individual component level, the data collected is inherently high quality data because the NILM is connected immediately upstream of the load and is configured based on the component's current rating to give us the best "look" at the data. In other words, we ensure the analog-to-digital converter fills up our collection window to provide the optimal signal gain. As the NILM is placed further upstream, larger capacity current sensors will be required. This will result in a much larger data window for the NILM. In this configuration, some of the fine details in the waveforms of individual components will be lost. The current sensor is selected primarily based on the sum of the current ratings of all the loads on the load center and the cable size where the transducer is to be installed. Future evaluation of the limits of the NILM will involve monitoring the lower quality aggregate signal of an entire load center and attempting to evaluate an individual load based on a high quality template developed from that load. These load centers can have ratings from several hundred to several thousand amperes and the large current sensors required are expensive and require significant electrical isolation to install.

In the previous section, the *"requant"* script provided an approximation of the effect of a larger current sensor by rescaling and re-quantizing the data from individual loads and associated high quality templates. The objective of this section is to employ a larger current sensor of known size and evaluate how this information can be used by the Machinery Space Simulation in predicting the ability of NILM to recognize individual components. Here the scaling and quantization of the individual loads is carried out by the larger current transducer and no simulation is required. However, in order to use a template collected with a smaller current transformer, the template data must be rescaled to a level comparable to the magnitude of the aggregate signal. This is accomplished by premultiplying each value in the template's array by an appropriate non-dimensional scale factor. This should not be confused with the power scale factor in Table 2-1.

Prior to running any tests, the scale factor for a signal collected by a system using an LA-55P vs. the same signal collected by a system using an LA-205S was estimated as follows:

The current measured by the current transducer is equal to the current seen by the load times the conversion factor K of the current transducer:

$$i_m = i_{load} K \tag{2-3}$$

The voltage measured by the NILM is equal to the current measured by the current transducer times the rating of the NILM's current resistor R. It should be noted that this measured voltage is what the NILM uses to calculate power:

$$v_m = i_m R = i_{load} KR \tag{2-4}$$

Therefore the scale factor should be equal to the ratio of the voltage measured by the system with the LA-55P to the voltage measured by the system with the LA-205S:

$$scale\_factor = \frac{v_{m,205}}{v_{m,55}} = \frac{i_{load} K_{205} R_{205}}{i_{load} K_{55} R_{55}} = \frac{K_{205} R_{205}}{K_{55} R_{55}} \tag{2-5}$$

Testing was accomplished through the use of the LEES Fluid Test System. This is a fluid system driven by a 0.5 Hp pump which is monitored by a single NILM using a LA-55P current transducer. The motor draws a steady state power of approximately 152 watts. Additional details

of the system can be seen in reference [11]. A single LA-205S current transducer (rated for 200A) was used to represent the larger current sensor needed if the monitoring of the Fluid Test System motor was conducted at a load center instead of immediately upstream of the individual load. This transducer was installed on the same phase of the Fluid Test System pump motor as the LA-55P and data was recorded simultaneously from both sensors. The use of a second current sensor required setting up an additional channel of monitoring. The components used in the three channel NILM configuration are listed in Table 2-8.

Table 2-8: Fluid Test System NILM Configuration

Channel	Measurement	Measuring Resistor Ratings	Reference Resistors	Current Transducer Conversion
1	Voltage	36Ω (pins 34-68)	62Ω (pins 34-26)	
2	LA-55P Current	56Ω (pins 33-67)	62Ω (pins 33-26)	1/1000
3	LA-205S Current	62Ω (pins 32-66)	36Ω (pins 32-26)	1/2000

Using the information in table Table 2-8 and equation 2-5, the scale factor was calculated:

$$scale\_factor = \frac{(1/2000)(62\Omega)}{(1/1000)(56\Omega)} = 0.5536 \qquad (2\text{-}6)$$

Raw current and voltage data was collected manually (i.e. using commands in the LINUX shell vice using the NILM menu prompts, see reference [12] for a detailed procedure) and then the data files were run through the NILM processing software (PREP) off-line. The motor installed on the Fluid Test System pump was operated in the system's normal configuration with both the LA-55P and LA-205S current transducers providing data. The pump was started and run in steady state for two minutes. Then five startup transients were generated by starting the pump and allowing it to run for approximately ten seconds. The results of this test are shown in Figure 2-12 for the LA-55P and in Figure 2-13 for the LA-205S. A detailed view of the fourth start in these two figures is shown in Comparing these figures illustrates the loss of resolution that results from the use of a larger current transducer.

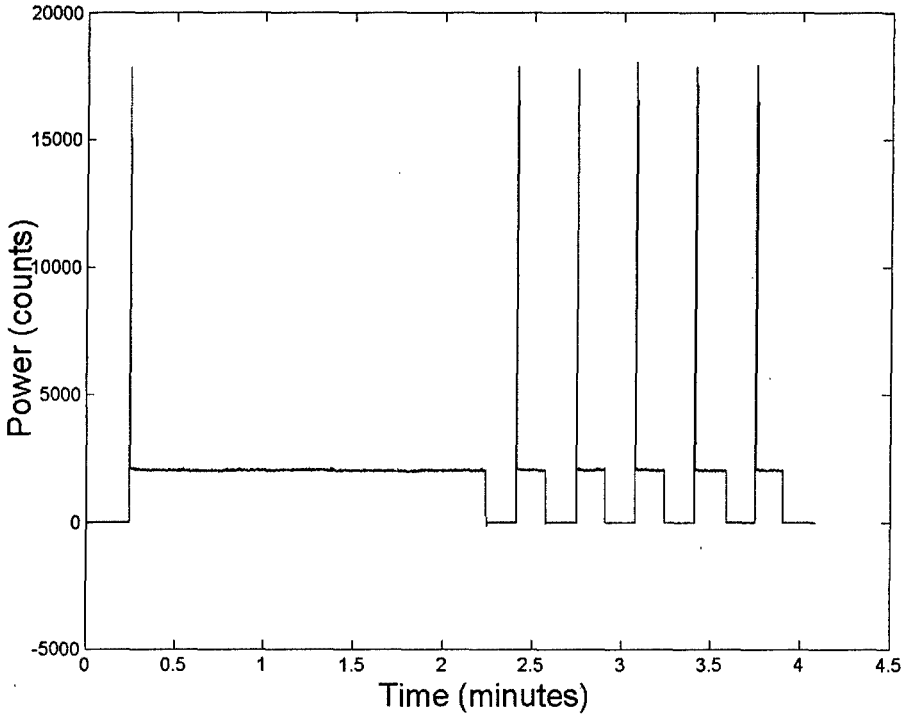

Figure 2-12: Fluid Test System Motor Data from an LA-55P Current Transducer

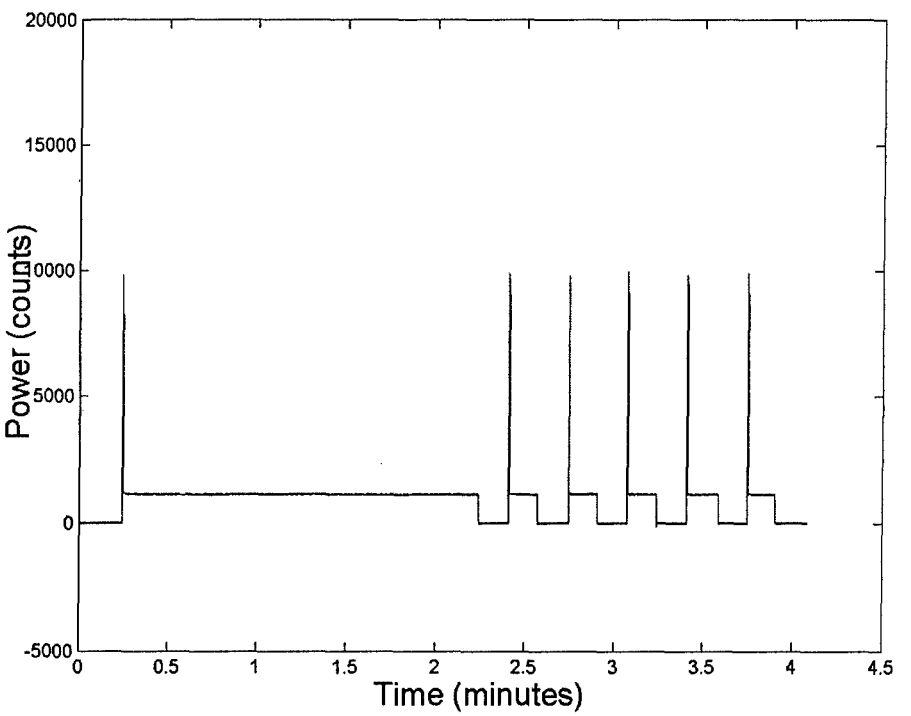

Figure 2-13: Fluid Test System Motor Data from an LA-205S Current Transducer

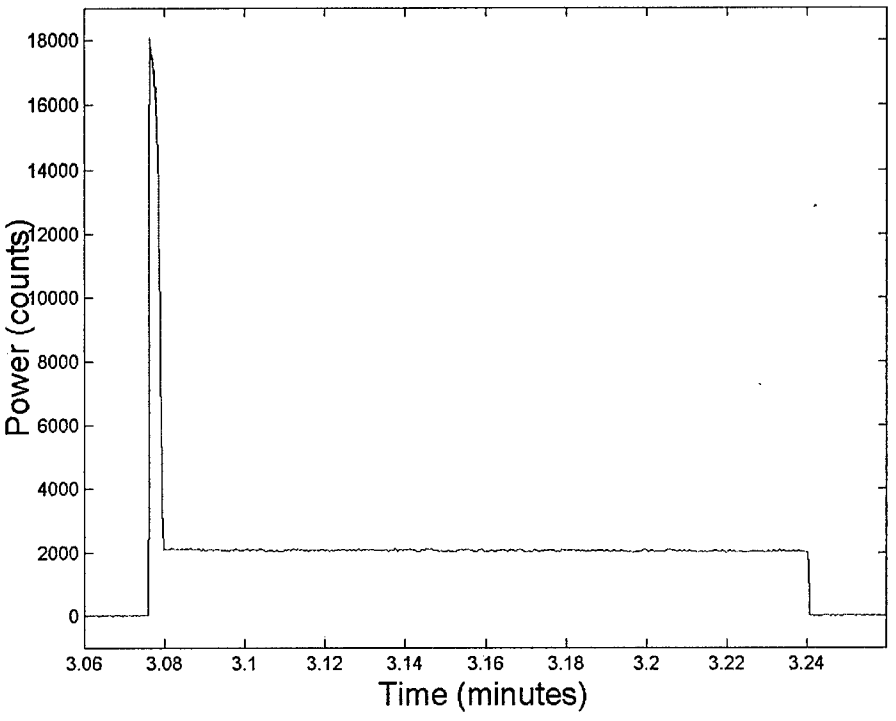

Figure 2-14: Detail of Fourth Motor Start in Figure 2-12

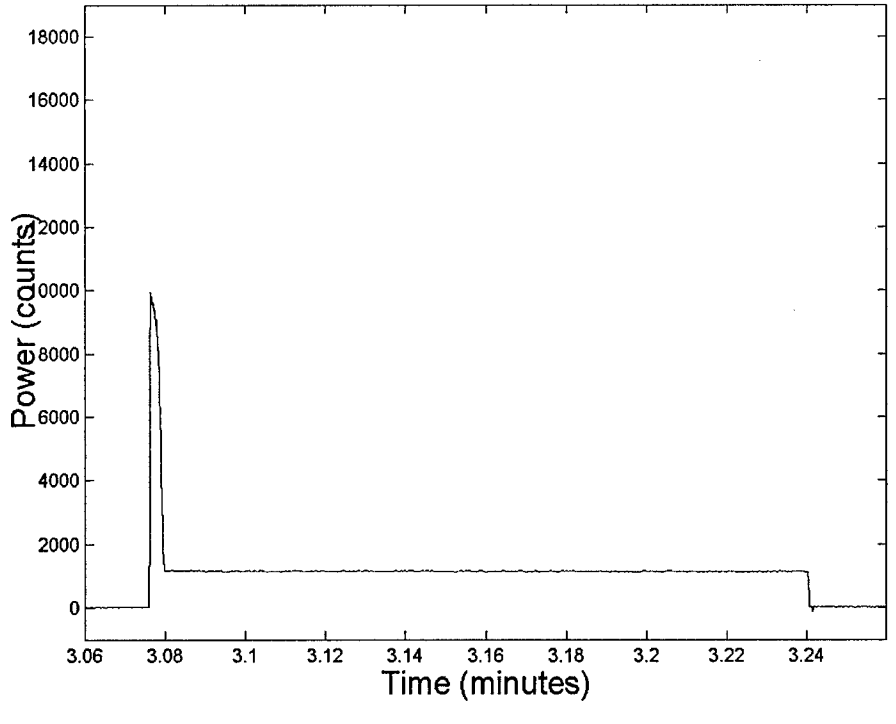

Figure 2-15: Detail of Fourth Motor Start in Figure 2-13

The simultaneous collection of data from both current sensors allows the high quality template to be re-scaled based on a scaling factor computed directly from the ratio of measured steady state power using the LA-55P to the measured steady state power using the LA-205S. The same ratio was also evaluated for the mean peak power from each of the six starting transient. The values are shown in Table 2-9.

Table 2-9: LA-55P to LA-205S Scaling Data

	Calculated	Mean Steady State Power	Mean Peak Power (over 6 starts)
LA-205S		1135.2	9853.8
LA-55P		2048.6	17903
Scale Factor	0.5536	0.5541	0.5501

The mean peak power provides a check that indicates the rescaling should be valid for both transient and steady state conditions. The differences in the three scale factors in Table 2-9 may be attributable to a combination of the limited sample size of the measured data and the accuracy of the resistor and current sensor ratings. These ratings are as follows: 1% for the 56Ω resistor, 5% for the 62Ω resistor, 0.65% for the LA-55P and 0.8% for the LA-205S. The resistors were measured and the actual values were found to be 56.1Ω and 61.7Ω. Using these values the calculated scale factor is 0.5499. It is anticipated that when averaged over many data runs, the scale factor derived from both measured steady state and peak power would approach this value.

The waveform recognition script from the Machinery Space Simulation was then used to determine the quality of the Fluid Test System motor signature when it is collected using an LA-205S. As mentioned above, since the effect of the larger CT is known, the *requant* script does not need to be called. Instead, the high quality template data from the LA-55P is scaled using the measured scale factor of 0.5541 from the ratio of mean steady state power. This data is then entered as the "section" in the *recognition* script. Note that this script has previously been applied to a group of loads summed together, but in this case the actual aggregate signal from the LA-205S was used, intentionally limited to one load. The quality was measured using the match values discussed in Section 2.4 and the results are shown in Figure 2-16. The match values are tabulated in Table 2-10 and have a tight range around 1.0, with a maximum deviation of 0.0222.

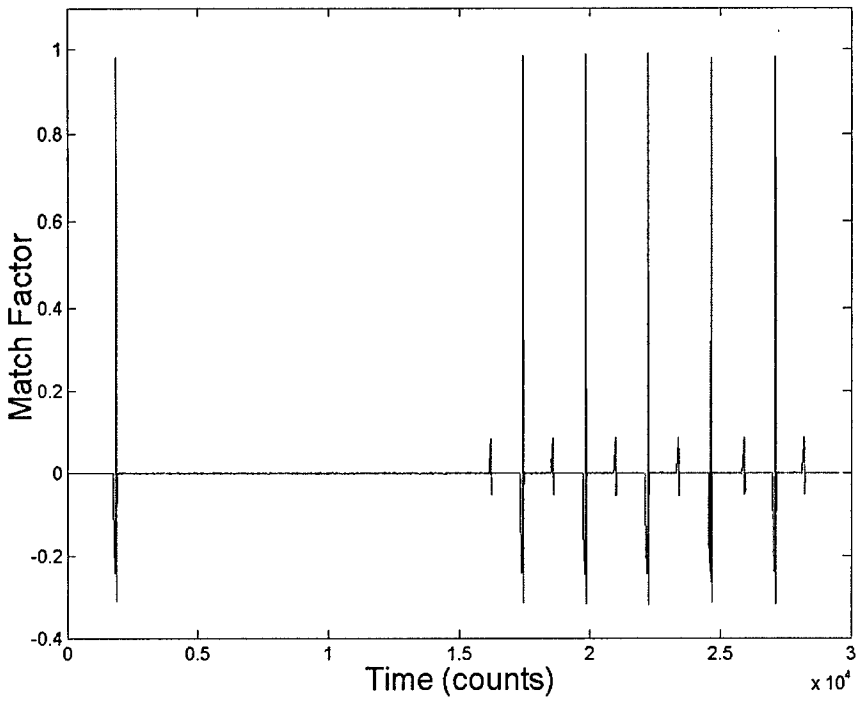

Figure 2-16: Recognition of Fluid Test System Pump Start using an Aggregate Signal from an LA-205S and a Template from an LA-55P

Table 2-10: Match Values for Figure 2-8.

Event	Match Value
Start 1 (Steady State Run)	0.9798
Start 2	0.9843
Start 3	0.9892
Start 4 (Template Source)	0.9907
Start 5	0.9778
Start 6	0.9833

2.7 Conclusion

The above testing illustrates several important points. First, scale factors based on current transformer conversion factors and resistor ratings can be employed along with the Machinery Space Simulation to make rapid estimates of the limitations of the NILM in monitoring multiple components. Next, the match factors produced by the simulation may be utilized as a tool to measure and compare the quality of disaggregated signals. Finally, time does not appear to be a factor in using a high quality template to identify a component in aggregate signals collected by a larger scale current transducer. This concept is illustrated in Section 2.6 which shows that the template generated using the fourth motor start in Figure 2-12 still provides recognition of transients that occurred at other times in the data collection sequence.

The data analysis in this chapter provides the first indications that the NILM with a full TED could successfully monitor large collections of loads on a warship. A typical trade-off is also apparent. The most minimal monitoring installation might attempt to use one or two NILMs at the generating points on a ship to track all loads. This provides the least expensive arrangement in terms of installation effort and hardware expense. It also places the highest possible burden on the TED software, and plainly could lead to misidentifications. Alternatively, individual monitoring of every load provides accurate information (to the extent that the large network of sensors are all working) at the expense of substantial sensor installation and maintenance costs. In the coming year the LEES Navy Team hopes to continue field tests and refine the understanding of just how "non-intrusive" the NILM can be while still providing acceptable performance.

Chapter 3 The DDG-51 Land Based Engineering Test Site

3.1 Background

The long range goal of the LEES Navy Team is to test the NILM on a US Navy warship. However, for a variety of reasons, the timelines for the approval and testing of new technologies on commissioned warships are generally very long. In 2003, the LEES research team spent almost a year trying to get authorization to test the NILM on a DDG-51 Class Destroyer (Figure 3-1), but ultimately this effort was unsuccessful. As an alternative, testing was pursued at the Navy's Surface Ship Engineering Complex located at the Naval Surface Warfare Center, Carderock Division (NSWCCD) in Philadelphia, Pennsylvania (site of the former Philadelphia Naval Shipyard). This site includes a full scale land based Navy propulsion plant used for equipment and software testing as well as for training the commissioning crews of new DDG-51 Class Destroyers.

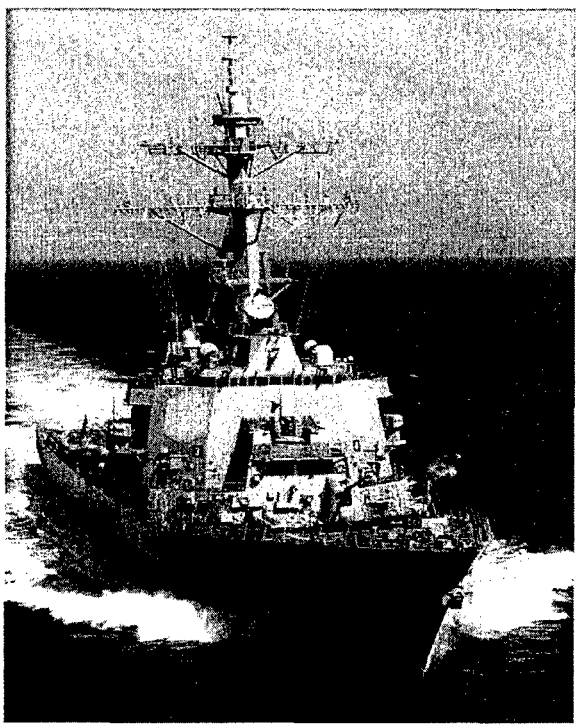

Figure 3-1: DDG-51 Class Destroyer

3.2 Plant Overview

The NSWCCD Surface Ship Engineering Complex houses more than one dozen test facilities, engineering sites and laboratories, including the DDG-51 Land Based Engineering Site (LBES). The mission of the LBES is to provide a test and evaluation platform as well as life cycle management and in service engineering support for Navy surface combatant ships. The DDG-51 LBES, which started operations in 1988, is located in a former naval aircraft assembly building that is 100ft wide, 680ft long and 51ft high and. The LBES is designed to replicate the Number Two Main Engine Room on the DDG-51 Class of Destroyers and consists of four levels (Figure 3-2 and Figure 3-3) [20]. The major equipment includes two LM2500 Gas Turbine propulsion engines (GTMs) along with associated support equipment (Lube Oil, Fuel Oil, High and Low Pressure Air, Cooling Water). The main engines drive a full scale propulsion train complete with main reduction gear, shafting and bearings. The LBES is also equipped with the DDG-51 Machinery Control System (MCS) that provides centralized monitoring and control of the propulsion, electrical, and auxiliary systems.

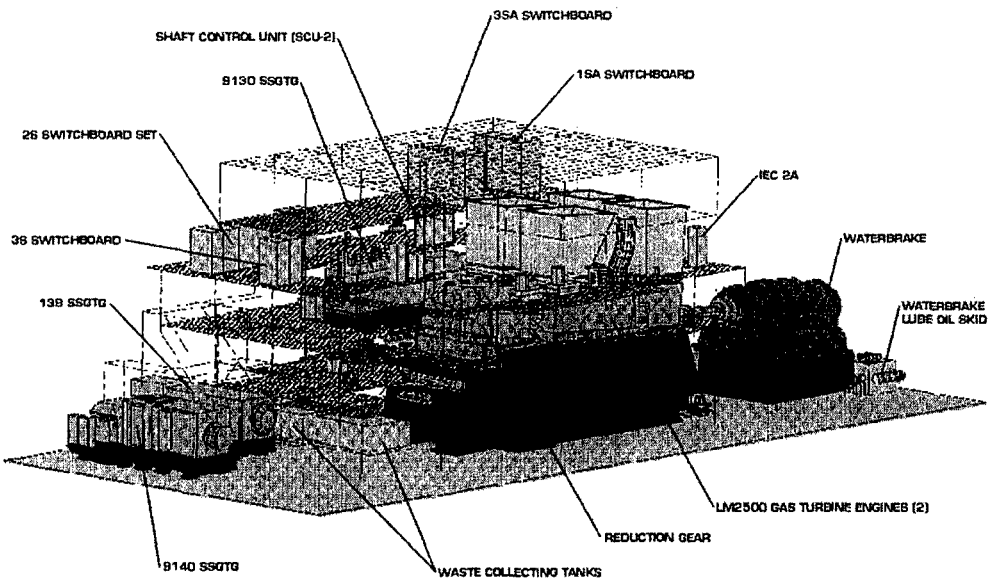

Figure 3-2: DDG-51 LBES Perspective 1

There are some significant differences between the land based facility and the machinery spaces on the DDG-51 Class Destroyers. The LBES has a full Zonal Electrical Distribution System (ZEDS), which represents the entire shipboard electric plant of a DDG-51 (Figure 3-4). This includes three Ship's Service Gas Turbine Generators (GTGs) and all eleven MFM-IIIs (see Chapter 5). The Number 2 Main Engine Room on the DDG-51 houses only one GTG. The ZEDS is physically collocated with the propulsion plant, but they are electrically independent. The ZEDS is set up to supply several large load banks to allow for flexibility in testing and does not supply the propulsion plant auxiliary systems (lube oil pumps, air compressors, etc). These loads are supplied by the power from the regional utility. The LBES also has no propeller, so to simulate the resistance of the ocean on the propulsion train, a large water brake is installed at the end of a shortened shaft. The LBES employs a shore based fresh water cooling system instead of the traditional Sea Water Service System tied to separate fresh water/sea water heat exchangers. The LBES is also not equipped with many of the habitability and support systems necessary for a

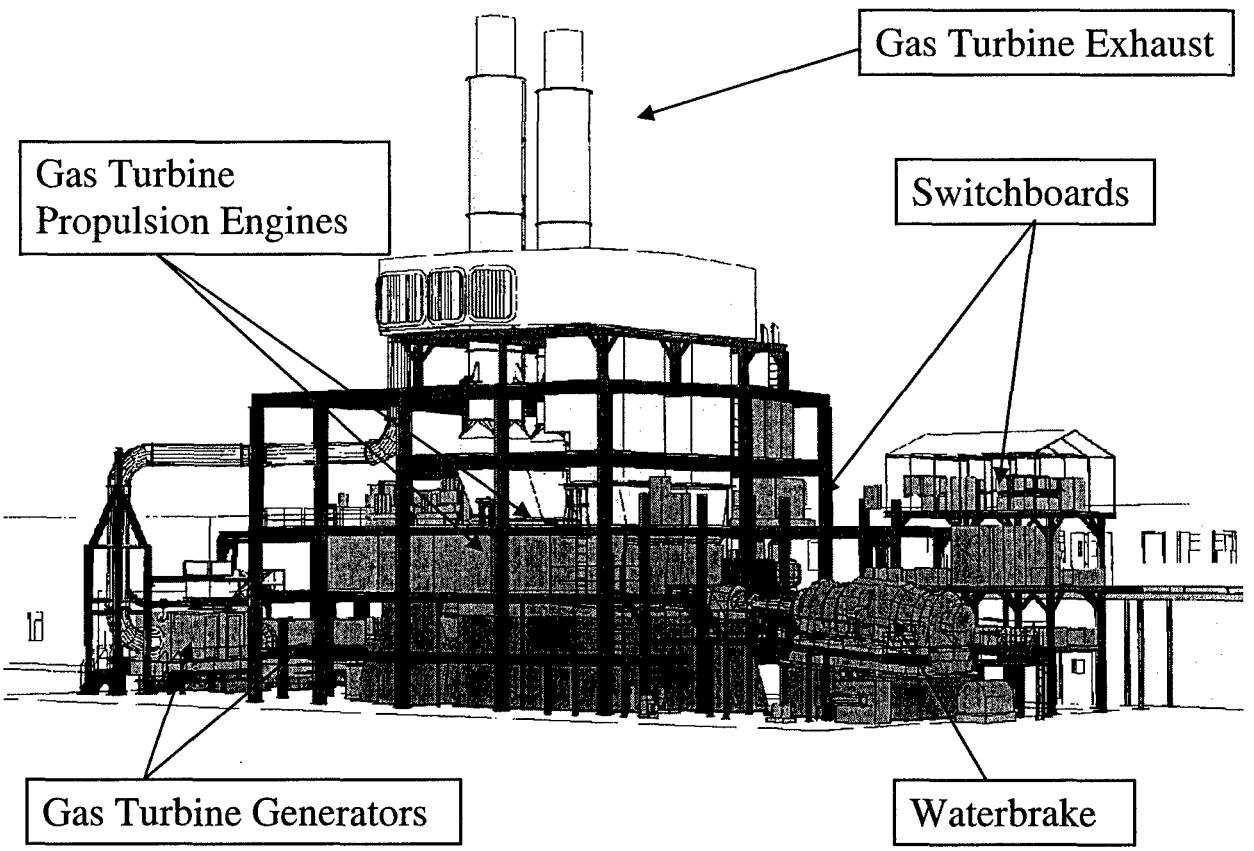

Figure 3-3: DDG-51 LBES Perspective 2

ship at sea, such as sewage, fire main, air conditioning, refrigeration and some air loads such as the Prairie and Masker acoustic silencing systems. Many of these secondary systems are present at the NSWCCD Surface Ship Engineering Complex, but are set up in separate stand alone test facilities.

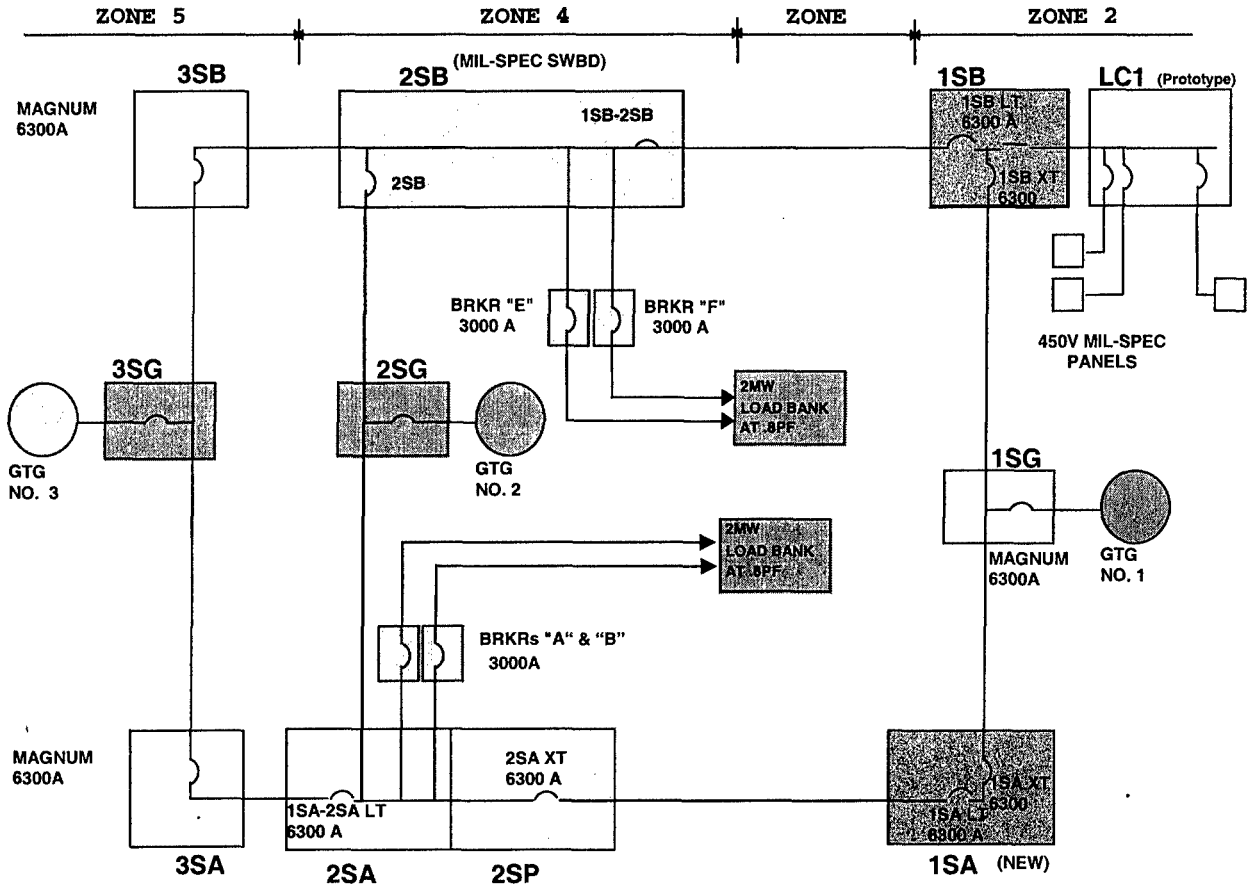

Figure 3-4: LBES Electrical Plant Configuration

General information on the systems in the following sections was obtained from references [21] and [22], and was revised based on component technical manuals and discussions with site engineers where noted to reflect the DDG-51 LBES configuration. Detailed drawings for selected LBES systems are included in Appendix C.

3.3 Fuel Oil Service System

The purpose of the LBES Fuel Oil Service System is to provide clean and filtered fuel oil to the two GTMs and three GTGs. The flow paths can be traced on the drawing in Appendix C and are summarized as follows:

1. Fuel Oil Pumps take suction on the Fuel Oil Service tank and discharge to the propulsion turbine fuel supply header. A stop check valve prevents back flow through the off service pump.
2. An air pilot operated unloading valve is set to maintain 25 PSIG in the propulsion turbine's fuel supply header is located at the service pump's common discharge. The unloading valve discharge returns fuel to the service tank when demand is less than 100%.
3. The fuel is then directed through a service heater, pre-filter and filter/separator to remove particulates and moisture.
4. Some of the fuel is then feed to the GTMs, with the remainder directed to the fuel service head tank and gravity feed tank.
5. Fuel from the gravity feed tank is directed to the three SSGTGs as needed.

The system is equipped with two motor operated pumps. Normal operation is one pump, the fuel heater, one pre-filter and one filter/separator in operation. Figure 3-5 shows the LBES fuel oil pumps with the purification equipment in the background. The specifications for the pump and motor are shown in Table 3-1 and Table 3-2 [23].

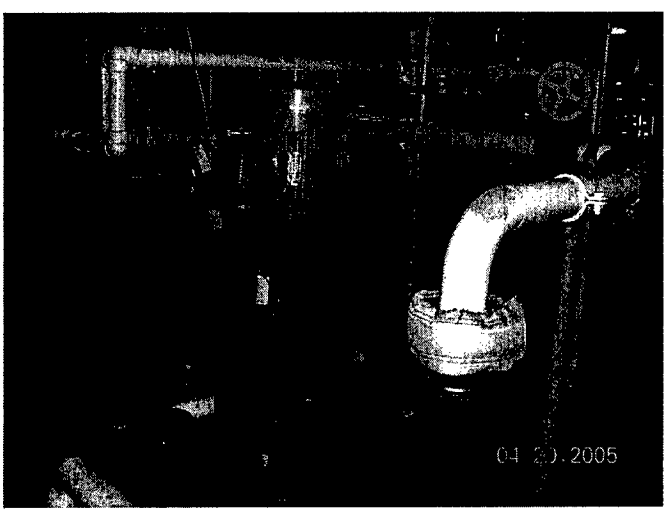

Figure 3-5: LBES Fuel Service Pumps.

Table 3-1: Fuel Oil Service Pump Reference Data

Number of Pumps	2
Type	Positive Displacement Rotary Vane
Capacity	36/72 GPM
Discharge Pressure	110 PSI
Suction Lift	10 inches Hg
Pump Speed	260/520 RPM
Type of Drive	Two Speed Helical Reducer
System Pressure	150 PSIG

Table 3-2: Fuel Oil Service Pump Motor Reference Data

Motor Type	Squirrel Cage Induction	
Power Requirements	440 Vac, 3 Phase, 60 Hz, 5.75/7.5FLA	
Conductor Type/Diameter	LSTSGU-3/0.06 inches	
Motor Horsepower	3.75/7.5 HP	
Motor Speed	900/1800 RPM	
Stator Windings	Low Speed	High Speed
Number of Poles	8	4
Connection	Delta One Circuit	Wye Two Circuit

The 2A Fuel Oil Service Pump was monitored by a NILM installation at the motor controller panel (Table 3-3). The motor controller uses the following logic:

1. With the lead pump in low, if header pressure drops below 20 PSIG for two seconds, the standby pump shifts to high speed.
2. With pump(s) in high speed, if the header pressure does not recover, or stays below 20 PSIG for five seconds, both pumps are commanded to off (this is most likely designed to limit the fire hazard in the event of a fuel oil system rupture).
3. With pumps in local control, the pump logic is disabled.

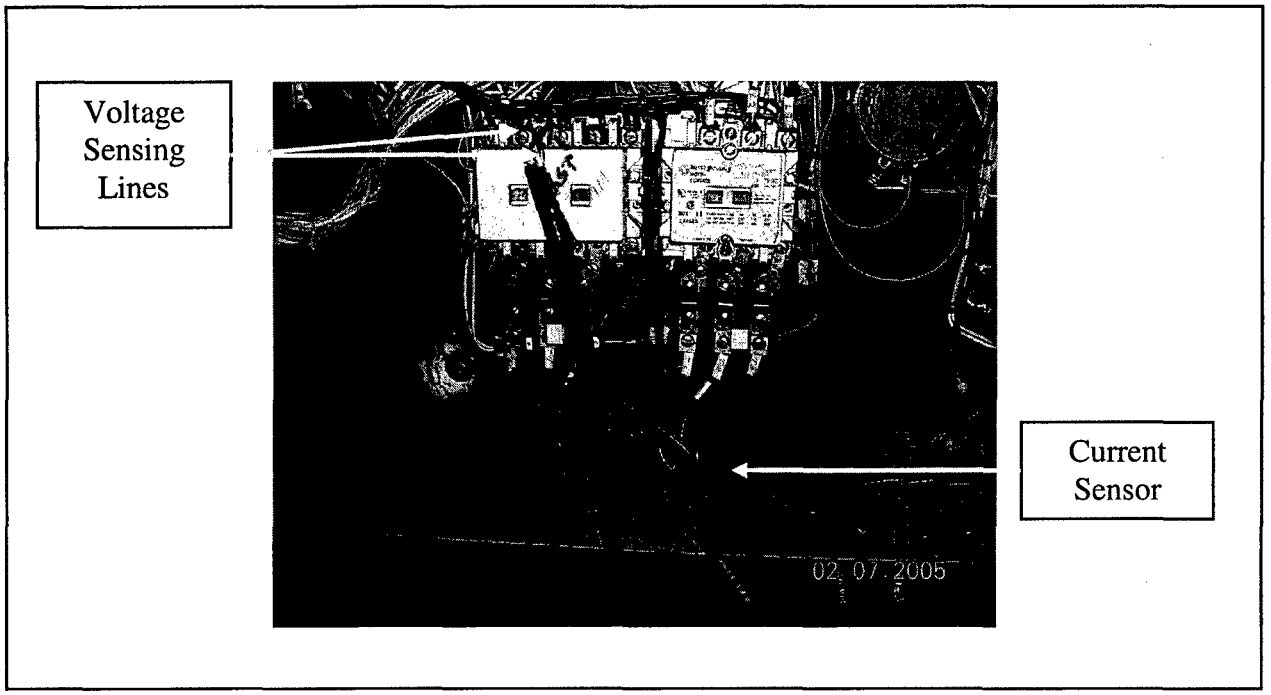

Figure 3-6: 2A Fuel Oil Pump Controller with NILM Sensors Installed

The NILM was configured as follows:

Table 3-3: NILM Configuration for Fuel Oil Service Pump Monitoring

NILM Channel	Measurement	Resistors	Reference Resistors	Transducers	Current Transducer Conversion
1	Voltage	180Ω (pins 34-68)	62Ω (pins 34-26)	LEM LV-25P	2500/1000
2	Current	62Ω (pins 33-67)	62Ω (pins 33-26)	LEM LA-55P	1/1000

NILM voltage sensing was connected line to line across phase 1 and phase 2 (terminals L1 and L2) of the fast speed motor contactor as shown in Figure 3-6. A jumper installed between the low speed and high speed contactors provides voltage in either speed. The low and high speed inputs to the third phase (terminals T3 and T6) were run through the current transducer to allow monitoring of both speeds. The pump was operated per the test plan titled Non-intrusive Load Monitor and ICAS Component Monitoring in Appendix D. The spectral power envelope of five low speed pump starting transients is shown in Figure 3-7.

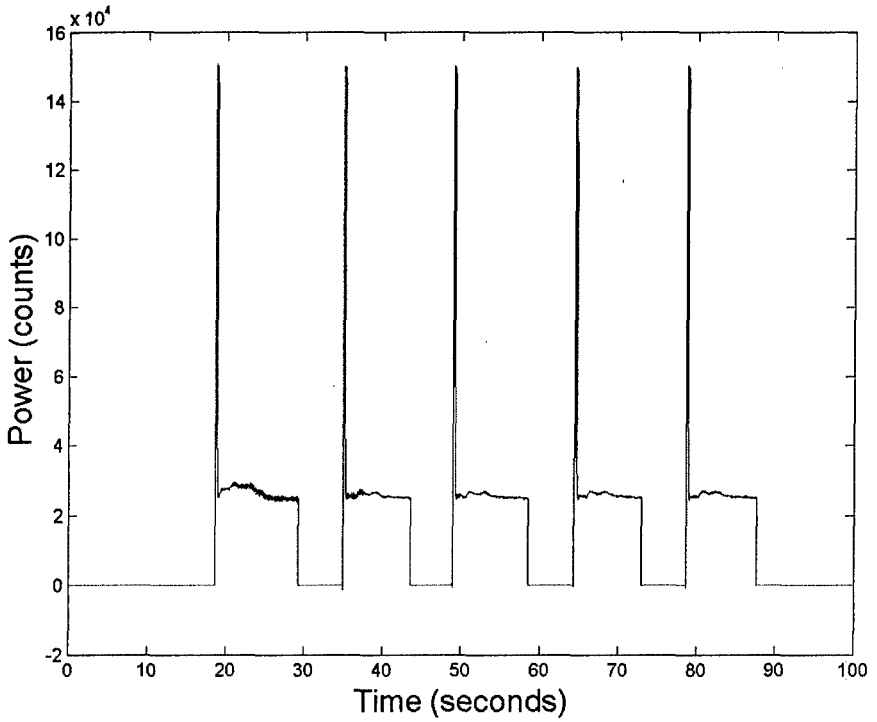

Figure 3-7: 2A Fuel Oil Service Pump Starts in Low Speed

The first start of the series in Figure 3-7 shows a slightly larger variation in the power spectrum while the pump settles into steady state operation. This phenomenon can also be seen in the first few seconds of the next starting transient, be then it disappears. The pumps were stated for this test after the system had been idle for several hours. It is possible that this phenomenon is caused by a dry impeller as the pump initially gains suction on the fuel oil service tank (a similar signature appeared on the initial 2B Lube Oil Pump start). This hypothesis could be verified by further testing.

Another interesting phenomenon that was observed was an intermittent mechanical transient (loud chattering) of FS-V016, a lift check valve which is located at the discharge of the 2B Fuel Oil Service Pump. The transient occurred periodically when the 2A pump was started in fast speed and lasted for several seconds. This observation is explored further in Chapter 4.

3.4 Lube Oil Service System

The purpose of the Lube Oil Service System is to deliver clean, filtered lube oil at the proper temperature and pressure to the main propulsion reduction gear assembly, its associated components (i.e. clutches, bearings, couplings, turning gear, gear mesh, etc.) and its separate thrust bearing in order to prevent excessive friction and heat. The system also transports oil to and from the Lube Oil Storage and Conditioning Assembly (storage tank, filters, and coolers). The flow paths can be traced on the drawing in Appendix C and are summarized as follows:

1. Lube Oil Pumps take suction on the Main Lube Oil Sump. An unloading valve at the discharge of the attached pump bypasses oil directly back to the sump as necessary to maintain a pressure of 14.5 PSIG at the hydraulically most remote bearing.
2. Lube oil is then directed by an air operated 3-way temperature regulating valve (LOS-VO-52) either to the Lube Oil Coolers or to the header to supply loads (reduction gear and thrust bearing).
3. After the cooler, some of the oil is directed to the synthetic oil coolers to provide cooling for the separate GTM lube oil system. It is then returned to the header.
4. After passing though the loads, the header returns the lube oil to the sump.

Table 3-4: Lube Oil Service Electric Drive Pump Reference Data

Number of Pumps	2
Type	Screw
Capacity	225/560 GPM at 100PSIG
Discharge Pressure	100 PSI
Suction Lift	10 inches Hg
Efficiency %	58.0/67.5
BHP	24.3/51.6
RPM	880/1780
Liquid	Lube Oil 2190 TEP

The primary motive force for the Lube Oil Service System is an attached pump that is driven off the reduction gear. The pump has a capacity of 693GPM at 168 shaft RPM and 75PSIG. It is capable of meeting all system demands from full power (168 RPM) down to 116 RPM. Below

this level, two electric motor driven screw type pumps (designated 2A and 2B) are used to provide lube oil flow. Pump and motor data are provided in Table 3-4 and Table 3-5 [24]. The Lube Oil Service Pumps, header and duplex strainers are pictured in Figure 3-8. The reduction gear housing can be seen behind the pumps.

Table 3-5: Lube Oil Service Pump Motor Reference Data

Motor Type	Induction
Power Requirements	440 Vac, 3 Phase, 60 Hz, 61/72FLA
Conductor Type/Diameter	LSFSGU-50/0.26 inches
Motor Horsepower	30/60 HP
Motor Speed	900/1800 SYN
Stator Windings	
Number of Poles	2
Connection	Delta One Circuit

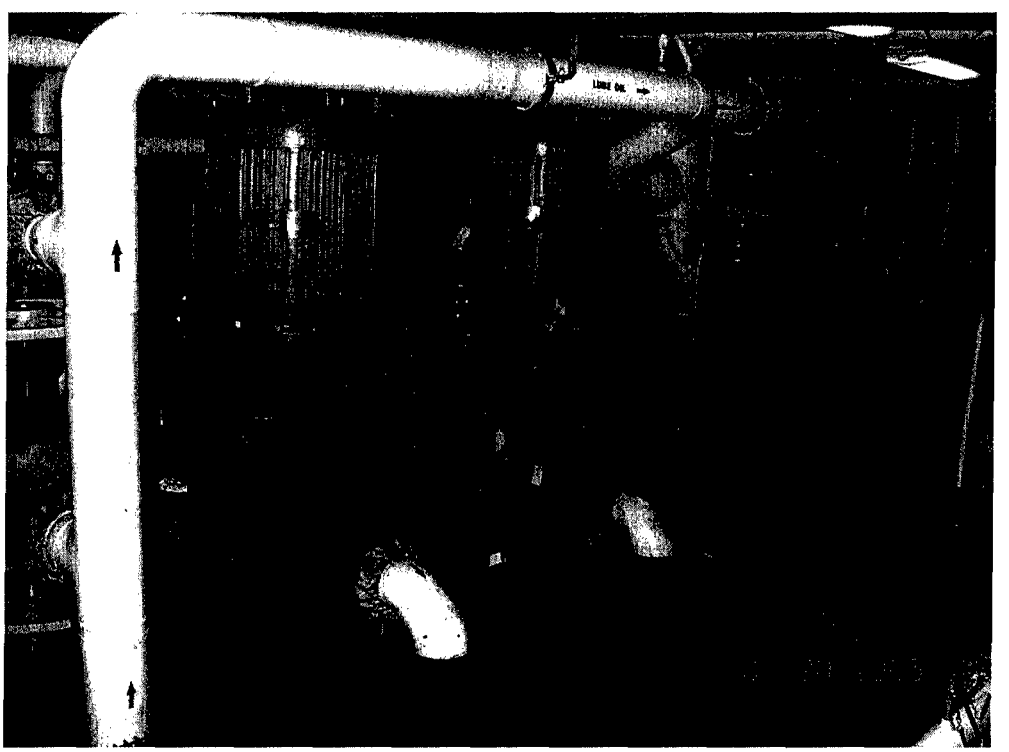

Figure 3-8: 2B Lube Oil Service Pump

The 2B Lube Oil Service Pump was monitored by a temporary NILM installation at the motor controller panel (Figure 3-9). The motor controller uses the following logic:

1. With both pumps off, if the most remote bearing pressure drops below 13 PSIG, the pump selected as "lead" will start in low speed.
2. With the lead pump in slow, if the most remote bearing pressure drops below 11.5 PSIG, the lead pump will cycle to high speed.
3. If the pressure drops below 10 PSIG, the standby pump will start in high speed.

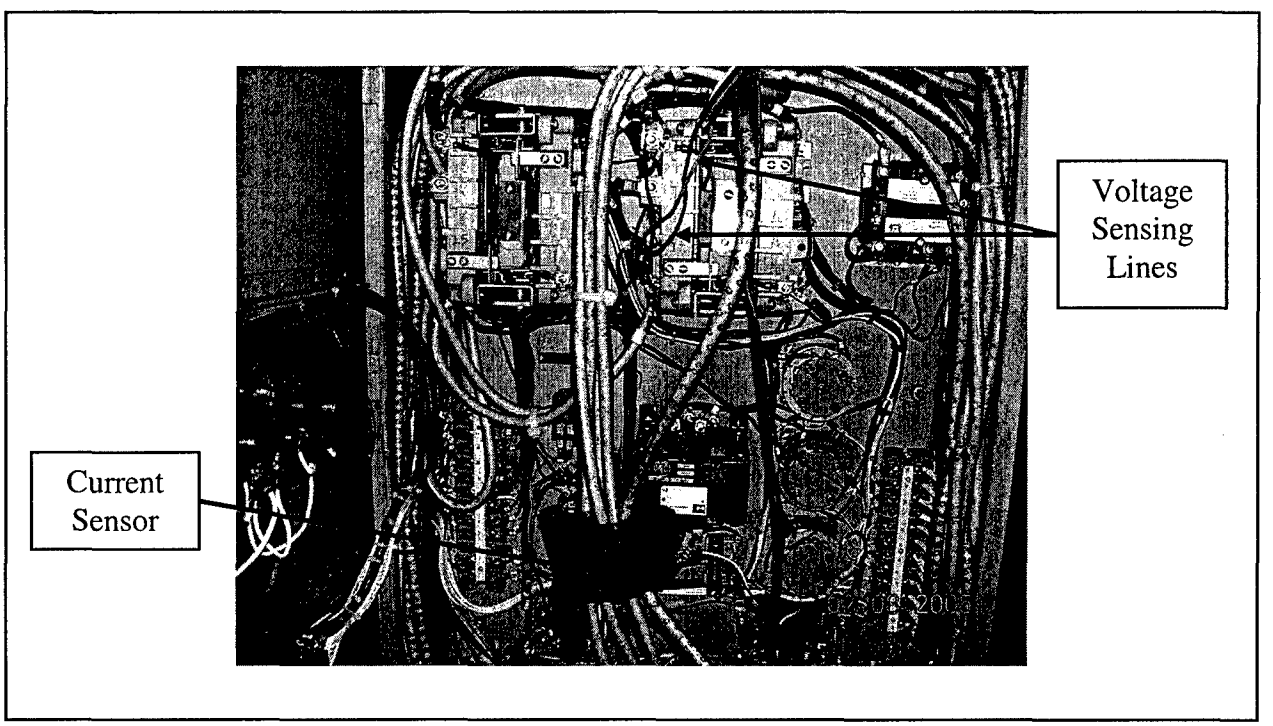

Figure 3-9: 2B Lube Oil Pump Controller with NILM Sensors Installed

The NILM was configured as follows:

Table 3-6: NILM Configuration for Lube Oil Service Pump Monitoring

NILM Channel	Measurement	Resistors	Reference Resistors	Transducers	Current Transducer Conversion
1	Voltage	180Ω (pins 34-68)	62Ω (pins 34-26)	LEM LV-25P	2500/1000
2	Current	36Ω (pins 33-67)	62Ω (pins 33-26)	LEM LF-505S	1/5000

NILM voltage sensing was connected line to line across phase 1 and phase 2 of the fast speed motor contactor as shown in Figure 3-9. As in the fuel oil pump motor controller, jumpers installed between the low speed and high speed contactors provide voltage in either speed. The low and high speed inputs to the third phase were run through the current transducer to allow monitoring of both speeds. The pump was operated per the test plan titled Non-intrusive Load Monitor and ICAS Component Monitoring in Appendix D. The spectral power envelope of five low speed pump starting transients is shown in Figure 3-10.

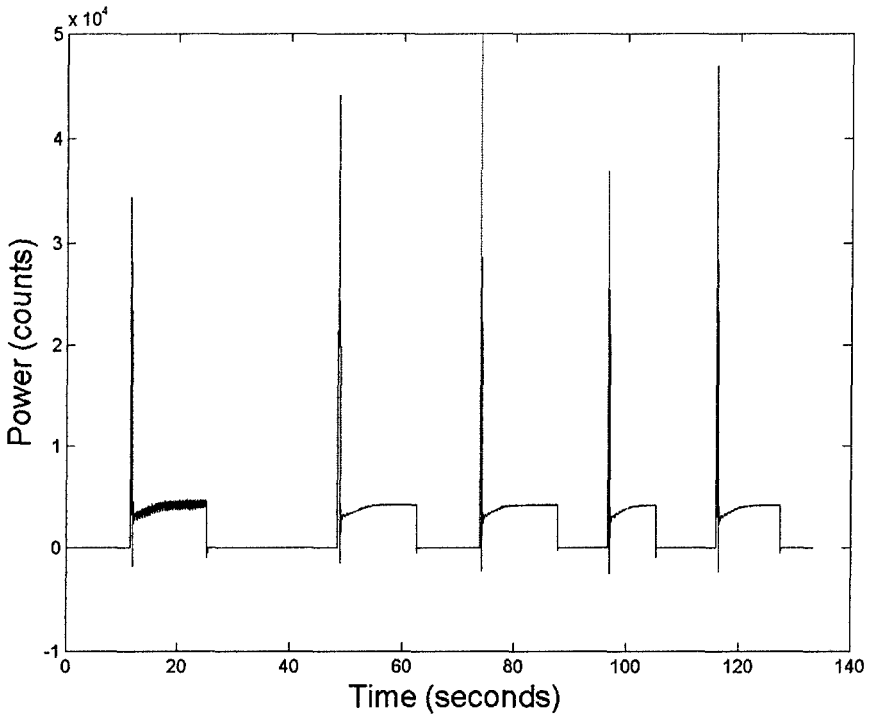

Figure 3-10: 2B Lube Oil Service Pump Starts in Low Speed

Figure 3-10 illustrates the same variation in power magnitude during the first start of the series. The 2B Lube Oil Service Pump had again been idle for several hours before the test and this observation may be caused by the same dry impeller phenomenon postulated in Section 3.4.

3.5 Low Pressure Air Service System

The purpose of the LBES Low Pressure Air Service System is to provide clean, dry low pressure air at 125 PSIG throughout the plant for service, control, and pneumatic power. The air flow path can be traced on the drawing in Appendix C and is summarized as follows:

1. The compressor takes suction on the atmosphere in the LBES machinery space and discharges compressed air to the service header.
2. The air then enters a dehydrator to remove moisture and particulates.
3. After the dehydrator, the air is stored in a receiver that maintains a relatively constant supply of compressed air service to the loads on the downstream header.

The Low Pressure Air Compressor or LPAC is powered by a 30 horsepower electric motor and generates 125 PSI compressed air. The Low Pressure Air Service System is normally augmented by a shop air system that operates at approximately 80 PSIG. If system pressure drops below 80 PSIG, shop air is directed to the service air header through a check valve. The shop air isolation (ALP-V002) and check valve (ALP-V003) join the header just upstream of the compressor discharge. Figure 3-11 shows the LBES LPAC and controller while Figure 3-12 [25] shows a cutaway view of the compressor. The specifications for the compressor and motor are shown in Table 3-7 and Table 3-8 [25].

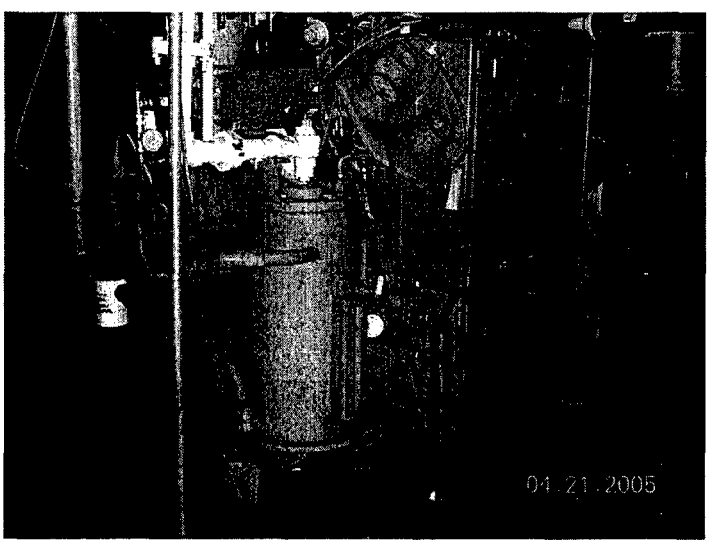

Figure 3-11: LPAC and Controller

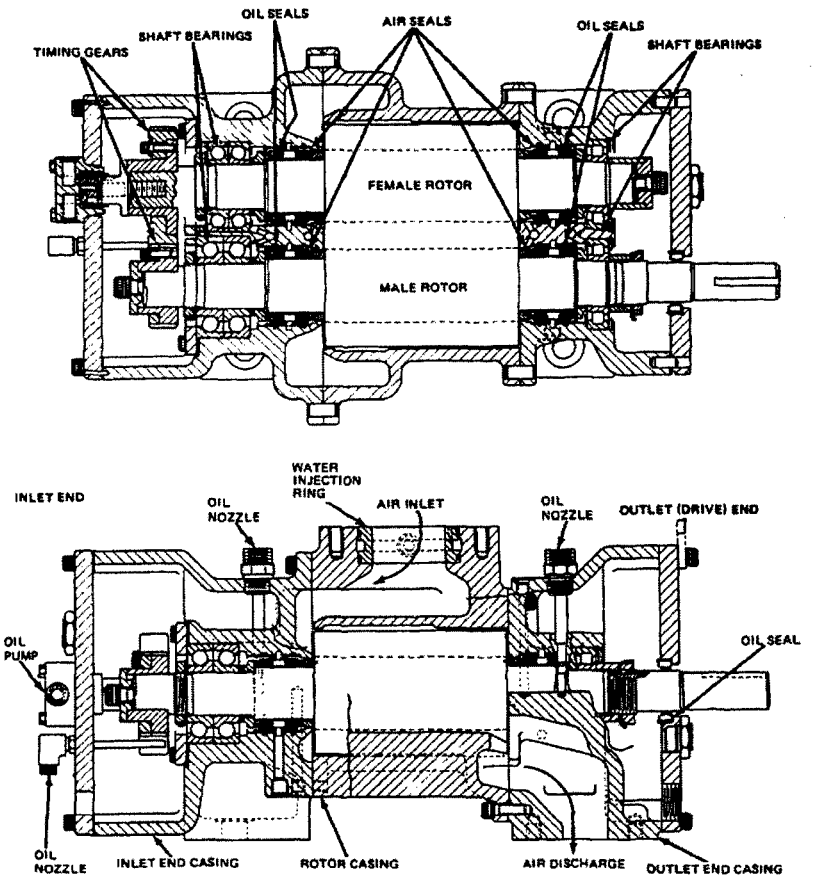

Figure 3-12: Cutaway View of Compressor

Table 3-7: Compressor Reference Data

Model	NAXI 100-4A
Manufacturer	Ingersol-Rand Company
Type	Single Stage, Positive Displacement, Axial Flow, Helical Screw
Power Requirements	440 Vac, 3 Phase, 60 Hz, 35 FLA
Discharge Pressure Settings	115/120/125 PSIG
Capacity	100 SCFM (at 125 PSIG)
Brake Horsepower	28.8 Maximum
Motor Speed	3600 RPM
Modes of Operation	Local Manual/Automatic

Table 3-8: Motor Reference Data

Motor Type	"P" Induction
RPM Synchronous	3600
RPM Full Load	3535
Motor Horsepower	35 HP
Rotor Type	Squirrel Cage

The LPAC motor controller uses the following logic in Automatic 125 PSIG operation:

1. The compressor is started in the automatic mode by switching the OFF/ON selector to ON.
2. As described in reference [25] "When the compressor discharge pressure reaches 125 PSIG, the discharge pressure switch actuates the solenoid-operated unloader valve. The solenoid valve opens to recycle discharge air through a bypass line back to the compressor inlet to prevent the continued build-up of pressure in the air receiver. As shown in Figure 3-13, the opening of the solenoid valve also applies discharge air pressure to the air cylinder operator. The air cylinder piston extends to mechanically shut the butterfly valve located in the compressor air intake pipe. Shutting off the air intake to the compressor effectively unloads the unit."
3. The compressor will operate for 10 minutes unloaded and then automatically shut down.
4. When receiver air pressure drops below 110 PSIG, the compressor will automatically be reloaded if the unit is operating unloaded, or automatically be restarted and loaded if the unit is shut down.

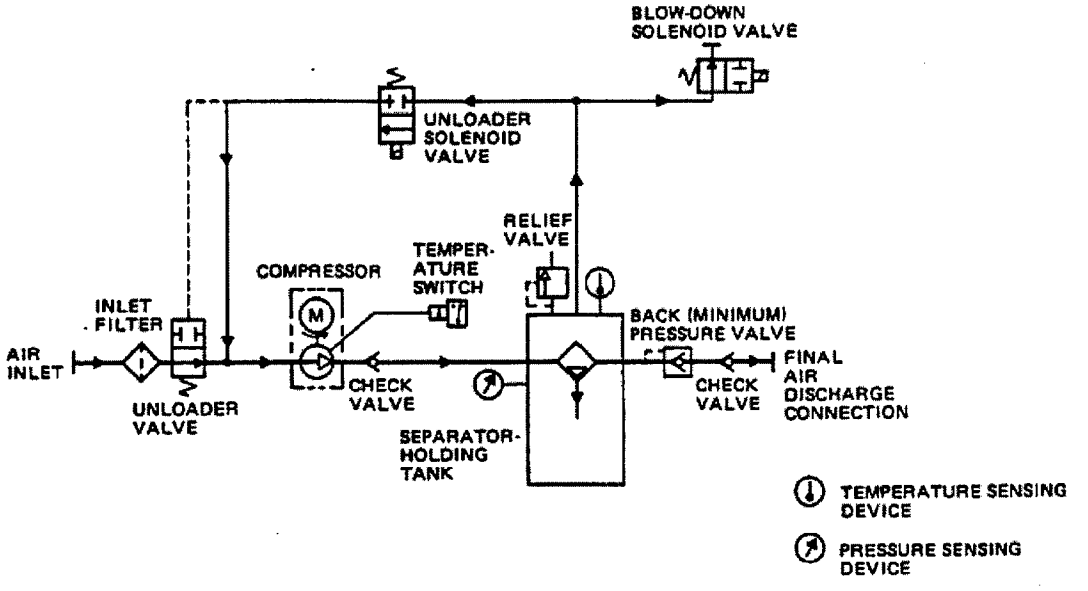

Figure 3-13: Compressor Air Flow Diagram

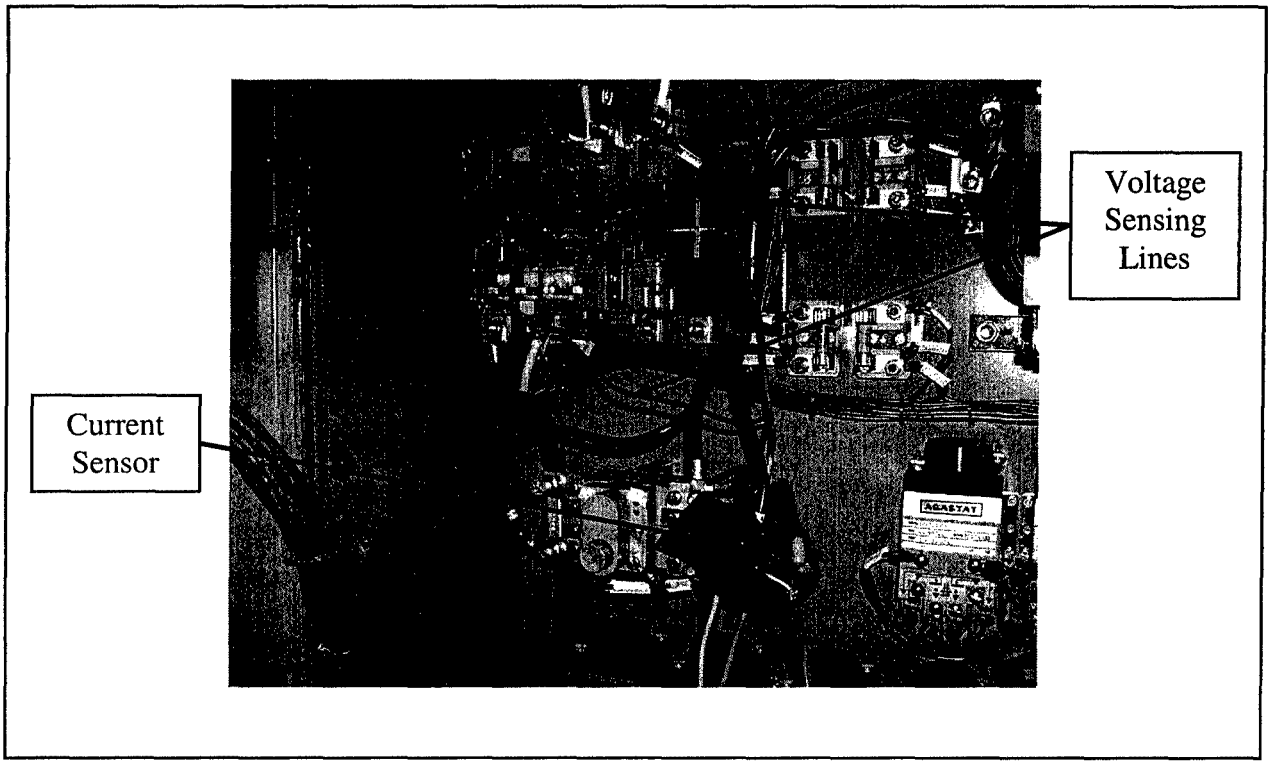

Figure 3-14: LPAC Motor Controller with NILM Sensors Installed

The NILM was configured as follows:

Table 3-9: NILM Configuration for LPAC Monitoring

NILM Channel	Measurement	Resistors	Reference Resistors	Transducers	Current Transducer Conversion
1	Voltage	180Ω (pins 34-68)	62Ω (pins 34-26)	LEM LV-25P	2500/1000
2	Current	36Ω (pins 33-67)	62Ω (pins 33-26)	LEM LA-305S	1/2500

The LPAC was monitored by a NILM installation at the motor controller panel. NILM voltage sensing was connected line to line across phase 1 and phase 2 (terminals L1 – black, and L2 - red) of the motor contactor as shown in Figure 3-14. The current transducer was installed on phase 3 (L3). The compressor was operated per the test plan titled Non-intrusive Load Monitor and ICAS Component Monitoring in Appendix D.

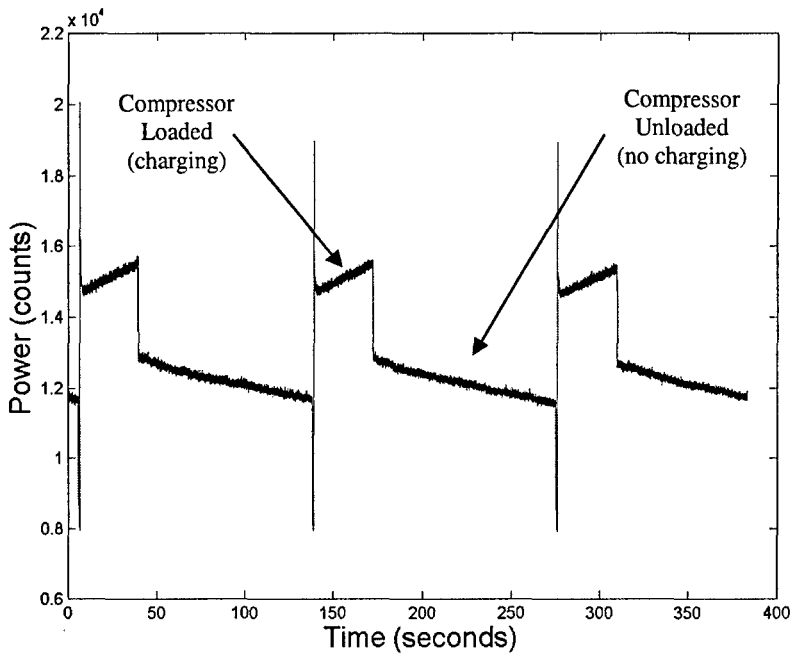

Figure 3-15: LPAC in Automatic 125PSIG Operation

Figure 3-15 shows the spectral power envelope of three cycles of the LPAC operating in Automatic 125 PSIG mode. The compressor is loaded where the power signature is increasing in magnitude and is unloading where the power signature is decreasing in magnitude. The loading and unloading times are dependant on system demand. The principle low pressure air loads at LBES are pneumatically operated Leslie valves on the Water Brake (2), Lube Oil Service System (temperature regulating valve), and Fuel Oil Service System (unloading valve), as well as GTM bleed air pressure regulating valves.

3.6 NILM Installations

Two NILMs were constructed for this testing using the methods outlined in [11]. These NILMs are configured as described in Section 3.3 and 3.5. Further information on the current and voltage transducer specifications is available in reference [26]. Each NILM system included a 133MHz Mini-Q PC with 120G hard drive, DVD+RW drive, 14 inch flat panel monitor, keyboard and uninterruptible power supply (UPS). After individual component monitoring was accomplished, permanent installations were made to the 2A Fuel Oil Pump motor controller and the LPAC motor controller. This involved adding a penetration to each controller to route the

voltage and current sensing lines to the NILM box. The installations are shown in Figure 3-16 and Figure 3-17. Each NILM can collect pre-processed data for up to seven months without operator action.

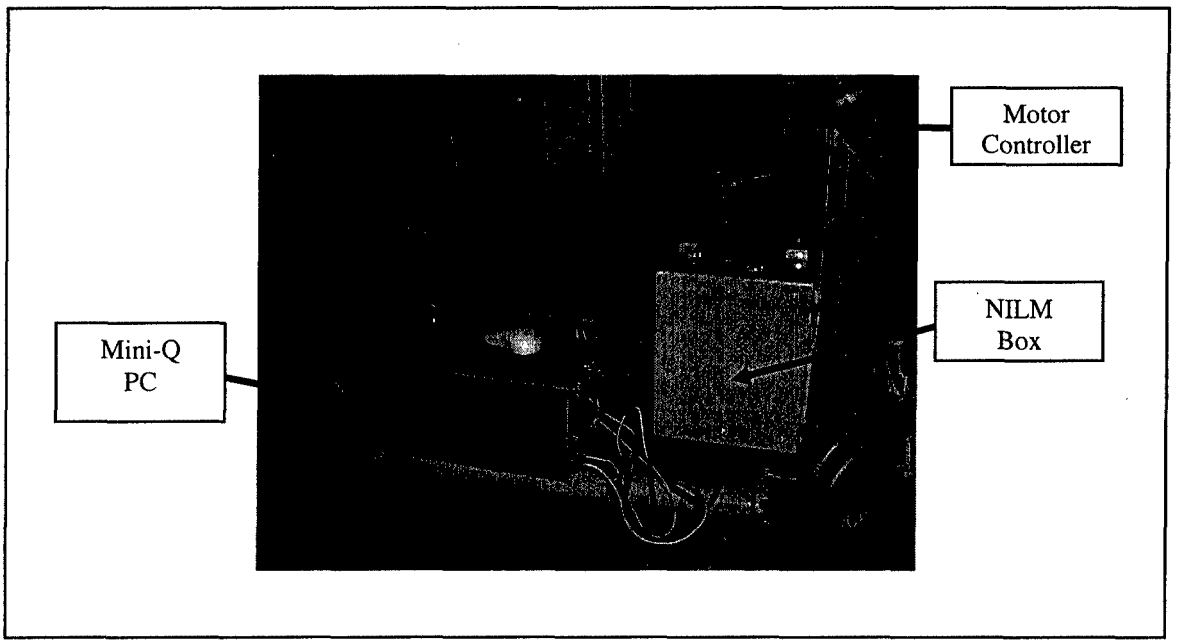

Figure 3-16: NILM Installation on 2A Fuel Oil Pump Motor Controller

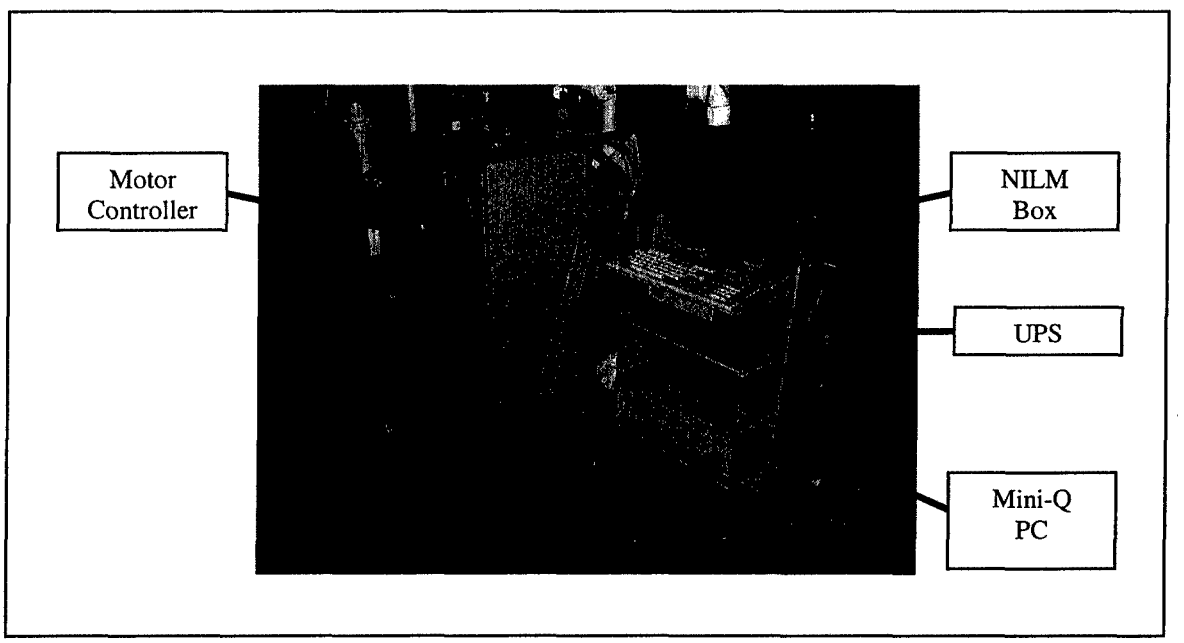

Figure 3-17: NILM Installation on LPAC Motor Controller

Chapter 4 NILM Applications on US Navy Propulsion Plant Machinery

4.1 Evaluation of Fuel Oil System Mechanical Transients

4.1.1 Significance of Mechanical Transients in Navy Propulsion Plants

Mechanical transients are of significant interest to both maintenance providers and war fighters. To the maintenance provider, they are an indication that equipment is not operating properly. To war fighters, mechanical transients can lead to detection and prosecution by enemy forces using advanced sonar systems. An abnormal configuration of the LBES Fuel Oil Service System allowed an opportunity to evaluate mechanical transients with the NILM. Specifically, the objective was to determine if the transients generated mechanical vibrations of sufficient magnitude to induce frequency modulations in the motor power spectrum that are detectable by the NILM. If successful, this could indicate one way in which the NILM could be employed in a CBM scheme.

4.1.2 Background

During the construction of the LBES, the lift check valve (FS-V016) on the discharge of the 2B Fuel Oil Service Pump was installed upside down (Figure 4-1). This caused the lift check to fail open as gravity pulled the check away from its seat. Correcting the error by cutting out the valve and replacing it would have resulted in significant cost and schedule impact, since the entire system would have to be drained and certified gas free prior to perform the hot work necessary to remove the valve. Additionally, the cleanliness of the system would also have to be re-certified after the valve repair. Alternative corrective action was taken by installing a second lift check valve in series with the first, with the second attached to one of two rubber flex-hoses on the discharge of the 2B pump. Because it was mounted on a flex-hose, no welding was required to make the repair. Thus the upside down lift check remains in place. Fuel oil flow past the lift check valve sometimes causes it to vibrate, resulting in a significant mechanical transient that can be audibly detected. This transient was occasionally observed when the 2A Fuel Oil Service

Pump was started in fast speed. The transient typically started about one second after the pump was started, and continued for several seconds.

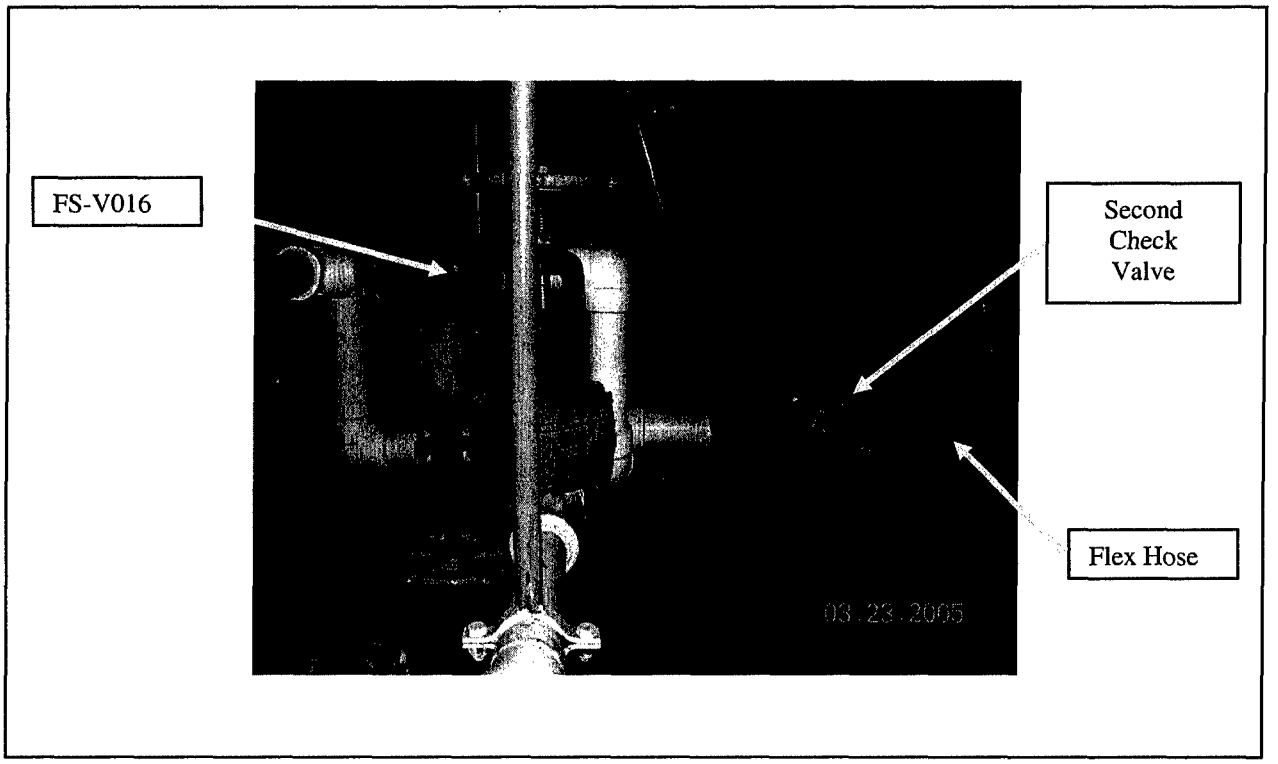

Figure 4-1: Fuel Oil Service System Lift Check Valve FS-V016

4.1.3 Investigation

Testing was conducted while the propulsion plant was shutdown (i.e. fuel oil was not required at the GTMs and GTGs) with the Fuel Oil Service System lined up in a recirculation mode. Fuel was discharged from the pump to the header and then through the fuel oil unloading valve (FS-VO-96) and back to the service tank. The bypass valve FS-VO95 remained shut during the tests (see system diagram in Appendix C). A series of pump runs was conducted with the 2A Fuel Oil Service Pump being started in fast speed. The NILM was set to collect pre-processed data and was configured as described in Section 3.3. The detection and duration of mechanical transients from the lift check valve FS-V016 was recorded. A summary of the test runs is contained in table Table 4-1. Transient duration was measured with a stopwatch and referenced to the associated pump start as time zero.

Table 4-1: 2A Fuel Oil Pump Fast Speed Runs

Pump Run	Audible Transient Detected	Transient Start (seconds)	Transient Stop (seconds)
1	No	0	0
2	Yes	1	11
3	No	0	0
4	Yes	1	9
5	Yes	1	11
6	No	0	0
7	Yes	1	6
8	No	0	0
9	No	0	0
10	No	0	0
11	No	0	0
12	No	0	0
13	No	0	0
14	Yes	1	8
15	No	0	0
16	Yes	1	9

The NILM data was processed in MATLAB and real power data was separated. Three different sections of the power spectrum for each pump run in Table 4-1 were evaluated. The data was zero padded to create 1024 data points (N=1024) and then multiplied by a 1024 point Hanning window before the Fast Fourier Transform (FFT) was applied. This prevents the aliasing of artifacts that occur in cases where the start and end points of the data do not match. A Hanning window of length N is shown in equation below [27]:

$$h(k) = \frac{1}{2}(1 - \cos(2\pi k / N)) \tag{4-1}$$

The frequency spectrum was then generated using a FFT (see MATLAB script in Appendix E). These evaluations are presented in the following sections.

4.1.3.1 240 Count Steady State Windows

First 240 count (2 second) windows of steady state data from the pump runs in Table 4-1 were considered. With the pump start marking time zero (t_o), the data was evaluated from 240 counts (time = t_o + 2 seconds) to 480 counts (time = t_o + 4 seconds). This isolated the period of time in which the mechanical transients were audible (all started at time t = 1 second and lasted until a minimum of t = 6 seconds) and eliminated interference from the motor start transient. An example of the FFT of transient and non-transient power spectrums is shown in Figure 4-2. No characteristics that would consistently distinguish the transient runs from the non-transient runs were identified using the 240 count window.

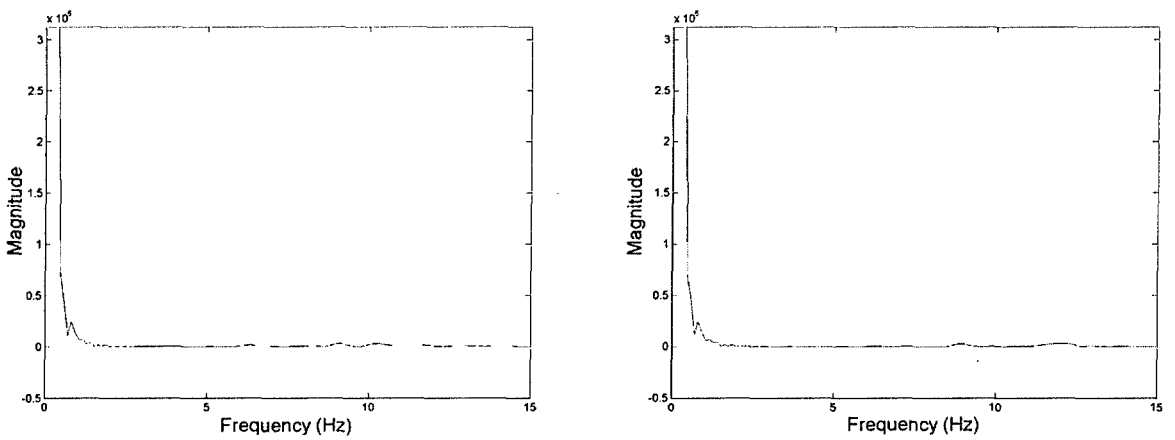

Audible Transient No Transient

Figure 4-2: Comparison of Typical 240 Count Steady State Windows

4.1.3.2 30 Count Steady State Windows

Next, 30 count (0.25 second) windows of steady state data from the pump runs in Table 4-1 were considered. With the pump start marking time zero (t_o), the data was evaluated from 450 counts (time = t_o + 3.75 seconds) to 480 counts (time = t_o + 4.00 seconds). This isolated a shorter period

of time in which the mechanical transients were detected and moved the data set further away from the motor start transient. An example of the FFT of transient and non-transient power spectrums is shown in Figure 4-3.

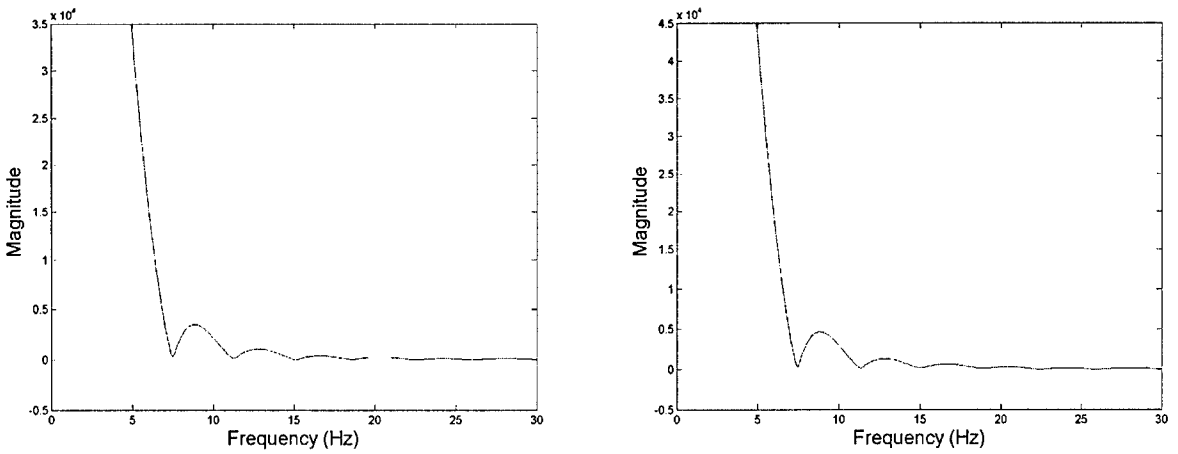

Audible Transient No Transient

Figure 4-3: Comparison of Typical 30 Count Steady State Windows

Again, no characteristics that would distinguish the transient runs from the non-transient runs were identified using the 30 count window. However, the most prominent feature of the 2A Fuel Oil Pump signature, a peak at 9 Hz that is visible in the graphs of Figure 4-3, was observed to shift slightly between pump runs. Additional analysis was conducted to determine if these shifts could be correlated to the detection of audible mechanical transients. The center frequency and magnitude of the peaks were measured for each run and are presented in Table 4-2 below. With one exception, the frequency of the peak was fixed at 8.906 Hz, while the variation in magnitude appeared to be random.

Table 4-2: Variation in 9 Hz Peak

Pump Run	Audible Transient Detected	Magnitude	Frequency (Hz)
1	No	4640	8.906
2	Yes	3492	8.906
3	No	3324	8.906
4	Yes	3231	8.789
5	Yes	3660	8.906
6	No	3880	8.906
7	Yes	4945	8.906
8	No	3937	8.906
9	No	3781	8.906
10	No	3739	8.906
11	No	3868	8.906
12	No	4039	8.906
13	No	3790	8.906
14	Yes	3975	8.906
15	No	4052	8.906
16	Yes	4464	8.906

4.1.3.3 120 Count Motor Start Transient Windows

Finally, 120 count (1 second) windows of motor start transient data from the pump runs in Table 4-1 were considered. With the pump start marking time zero (t_o), the data was evaluated from time = t_o to t = 120 counts. An example of the FFT of transient and non-transient power spectrums is shown in Figure 4-4. Again, no diagnostic indicators of the mechanical transient condition were identified.

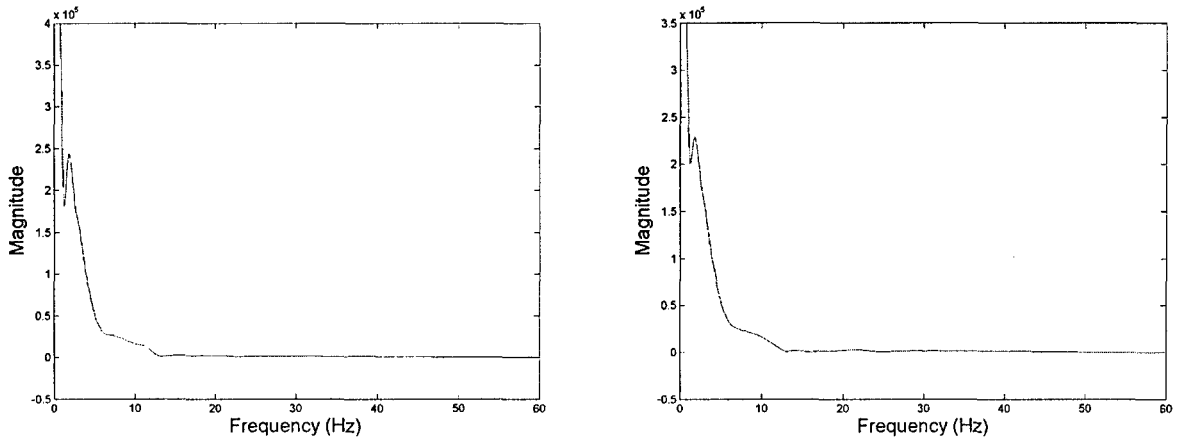

Audible Transient

No Transient

Figure 4-4: Comparison of Typical 120 Count Motor Start Windows

4.1.4 Results of Mechanical Transient Evaluation

No features in the spectral power envelopes of the 2A Fuel Oil Pump motor consistently appeared that would distinguish the pump runs with audible mechanical transients from the runs where transients were not detected. This implies that the mechanical vibrations from these transients do not appear as oscillations in the motor power spectrum. One possible explanation is that the magnitude of the transients is simply too small to have a detectable effect on the motor. This may be due to the location of the check valve which is not directly in the flow path of the 2A pump (see Figure 4-5).

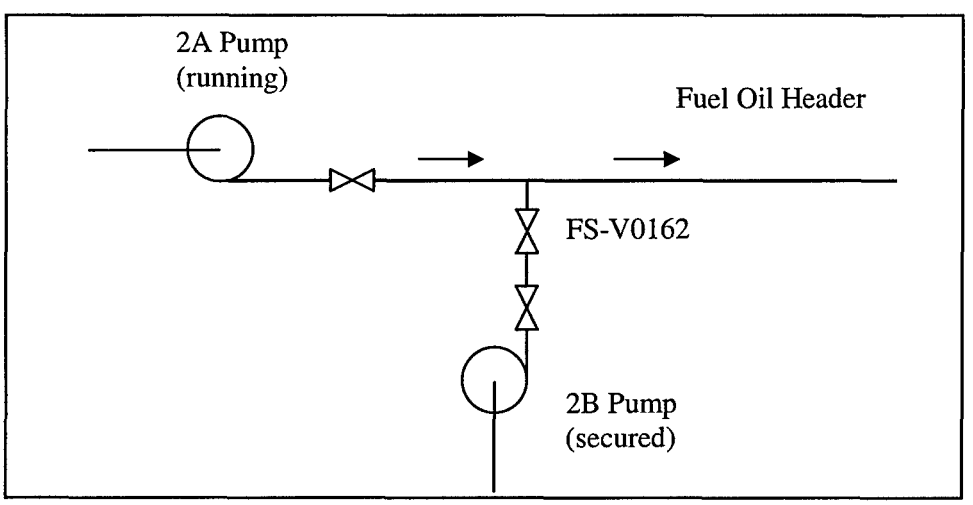

Figure 4-5: Fuel Oil Flow in relation to FS-V016

4.1.5 Effects of System Valve Lineup on Pump Motor Power

During initial evaluations of the mechanical transients from FS-V016, the bypass valve FS-VO95 was set in various positions. It was determined that the transients were most frequent when the bypass was shut, the position set for the pump runs in Table 4-1. However, it was observed that the position of the bypass valve had a noticeable effect on the motor spectral power envelope as seen in Figure 4-6. With the bypass open, the pump motor achieves steady state quickly, with a mean power of 6994 counts. With the bypass shut, a second peak is observed after the initial induction motor starting surge. This second peak reaches a value of 11552 counts and is characteristic of operation with the bypass valve closed. Additionally, power following this peak is observed to slowly ramp down from a range of 8600 counts to 7700 counts when the pump is secured. This results in the motor operating at a higher mean steady state power of 8028 counts with the bypass closed. These observations illustrate the potential of the NILM for identifying a particular valve lineup through the evaluation of the motor spectral power envelope.

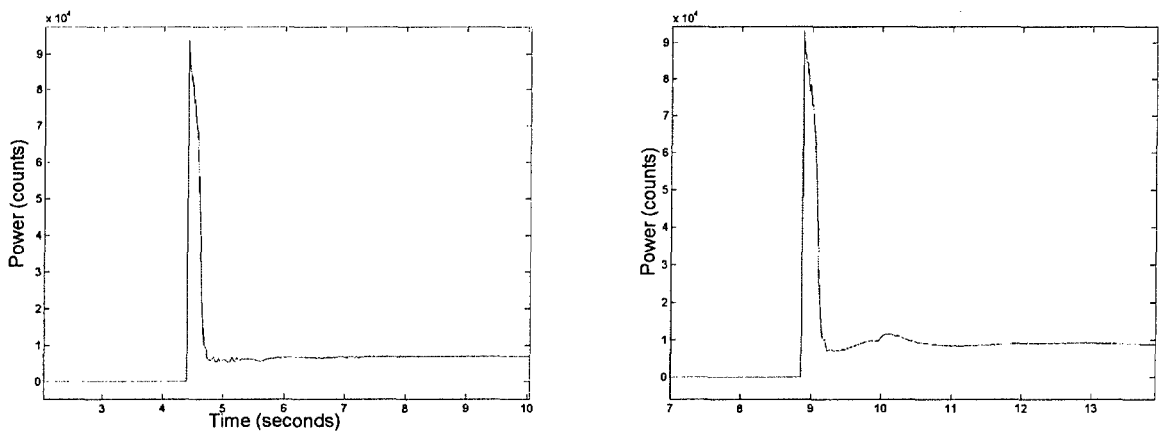

Bypass Open

Bypass Closed

Figure 4-6: Effect of System Valve Lineup on Pump Motor Power

4.2 Low Pressure Air System Leak Test

4.2.1 Significance of Compressed Air Systems on Navy Ships

Compressed air systems are extremely important to the operation of modern warships. Just a few examples of critical air loads include the ship's whistle, gas turbine generator start air, numerous pneumatically controlled propulsion plant valves, and 4500 PSI emergency main ballast tank blow air for nuclear submarines. At the same time, DDG-51 Class maintenance providers report air compressors as among the components requiring the most frequent maintenance actions in the propulsion plan [28]. Leaks in compressed air systems result in unnecessary wear on the compressor and can degrade system performance. Any diagnostic tool that can detect leaks in these systems has the potential to enhance propulsion plant reliability and reduce maintenance costs.

4.2.2 Background

A diagnostic was developed from NILM data collected during the operation of the sewage pumps on the *SENECA*. The methodology uses the statistics of pump runs to detect a fault (vacuum leak) in the system and is discussed in references [11] and [12]. The objective of this section is to describe an attempt to further validate this diagnostic on another shipboard cycling system, namely a compressed air system.

The NILM installation on the LBES Low Pressure Service Air system described in Section 3.5 was used for this study. Because the majority of the air loads on the system are used to support main propulsion equipment, the testing needed to be conducted during a period when the full propulsion plant was in operation.

4.2.3 Investigation

A week long LBES crew certification period (for *USS BAINBRIDGE (DDG-96)*) provided an opportunity to observe the Low Pressure Service Air system during normal operations. The test plan titled LBES Non-intrusive Load Monitor LPAC Testing included in Appendix D was

submitted and approved by the LBES Test Director. This plan called for the installation of flow meters that would allow venting of a measured rate of low pressure air to simulate a leak condition. Two different flow meters were installed and are shown in Figure 4-7. Flow Meter 1 on the left provides small leaks up to 90 SCFH (1.5 SCFM) and was installed at a hose between ALP-V033 and the air dehydrator. Flow Meter 2 on the right provides larger leaks, up to 25 SCFM, and was installed at the pneumatic tool station connection downstream of ALP-V055 (see system diagram in Appendix C).

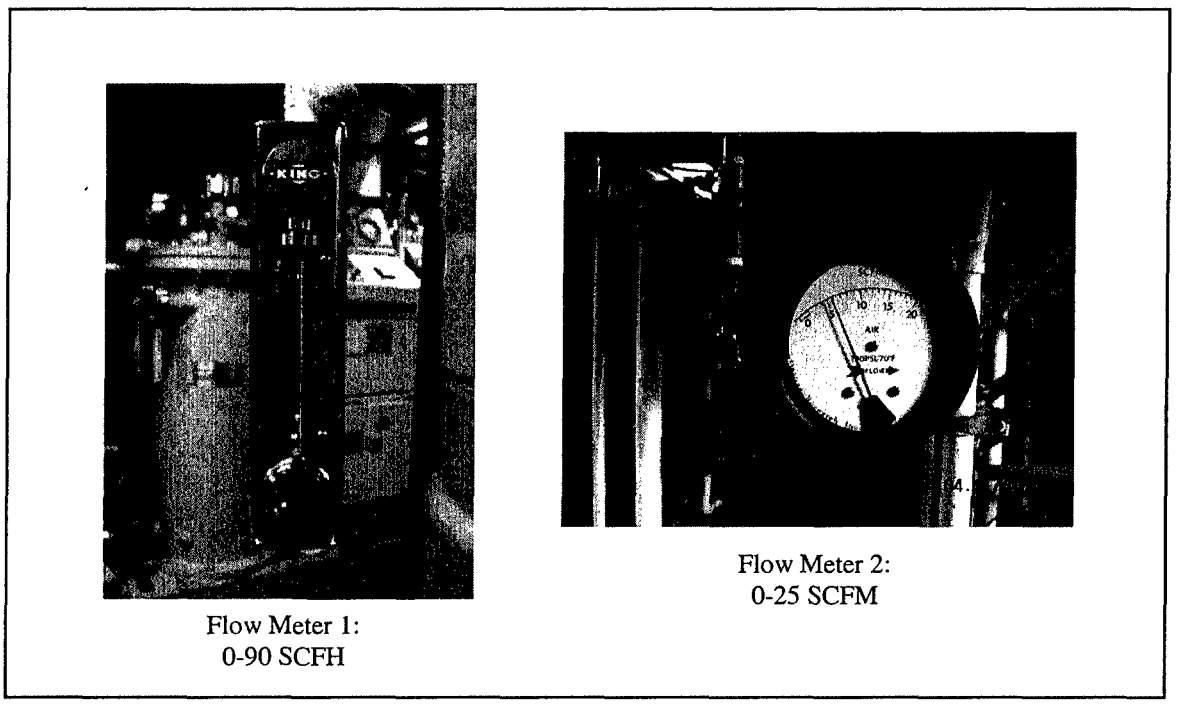

Flow Meter 1:
0-90 SCFH

Flow Meter 2:
0-25 SCFM

Figure 4-7: Flow Meters installed in the Low Pressure Air System

Prior to testing, the shop air system was isolated at FA-V007 (Appendix C) to prevent the possibility of an additional supply of air to the Low Pressure Air Service system that was not generated by the compressor. Several leak conditions were assessed in Table 4-3 to ensure that the test leak in combination with normal plant loads did not exceed the capacity of the LPAC. The compressor's operating profile is also illustrates by this table. As the demand on the system increases, loaded compressor run time increases and unloaded compressor run time decreases. After a review of this data it was determined that the test leak rate would be 12.5 SCFM. This

was considered a "significant leak rate" (one LBES mechanic stated "if I found this leak, I would try to fix it") and represents just over 10% of the compressors capacity. It also falls at the mid-point of the "large leak" flow meter gage range, and therefore allows the most flexibility in setting leak rates for future tests.

Table 4-3: Test Leak Rate Determination

Operational Air Loads	Test Leak Rate (SCFM)	Compressor Run Time – Loaded (seconds)	Compressor Run Time – Unloaded (seconds)
None	0	27	161
None	1.25	28	158
Startup (Small Load)	12.5	31	123
Full Ops (Large Load)	0	35	77

4.2.3.1 Procedure

This section supplements the test procedure Appendix D. Each morning civilian technicians at the LBES would begin the plant startup. Then the operation was turned over to the crew of the *BAINBRIDGE*, who rotated through three watches with the objective of repeating the day's scheduled certification evolutions. At the end of the day, the crew on watch would initiate the plant shutdown and turn the watch over to the civilians who would complete the evolution. The test leak rate of 12.5 SCFM was initiated for approximately the last four hours of each day in an effort to obtain an equal amount of data from baseline "no leak" operations and operations with the test leak inserted. Pre-processed data was collected from the NILM in one hour snapshots during plant operations. The snapshots were then sorted to separate the no leak and leak conditions. The Perl script used in [12] was modified to evaluate the spectral envelopes of the compressor motor. The script counts the time between loaded compressor runs, which are equal to the time of unloaded compressor operation (see Appendix E). This method of analysis was chosen over simply counting the number of compressor starts which may not differentiate various load conditions as illustrated by Figure 4-8. The script output was then processed in MATLAB to generate histograms of compressor operation. The analysis of this data is presented in the following sections.

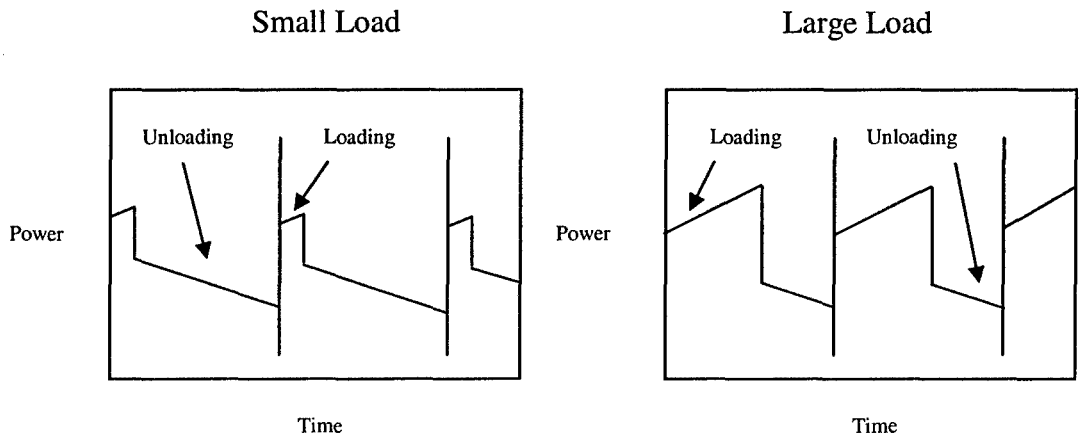

Figure 4-8: Illustration of Equal Time between Starts for Different Load Conditions

4.2.3.2 Analysis of Compressor Data from 4/18 – 4/22 LBES Operations

A total of 19 hours and 21 minutes of baseline plant operations data and 19 hours and 55 minutes of operation with the test leak present were collected. Equal bin size histograms showing the number of compressor cycles plotted against the duration of the unloaded compressor run times are shown below.

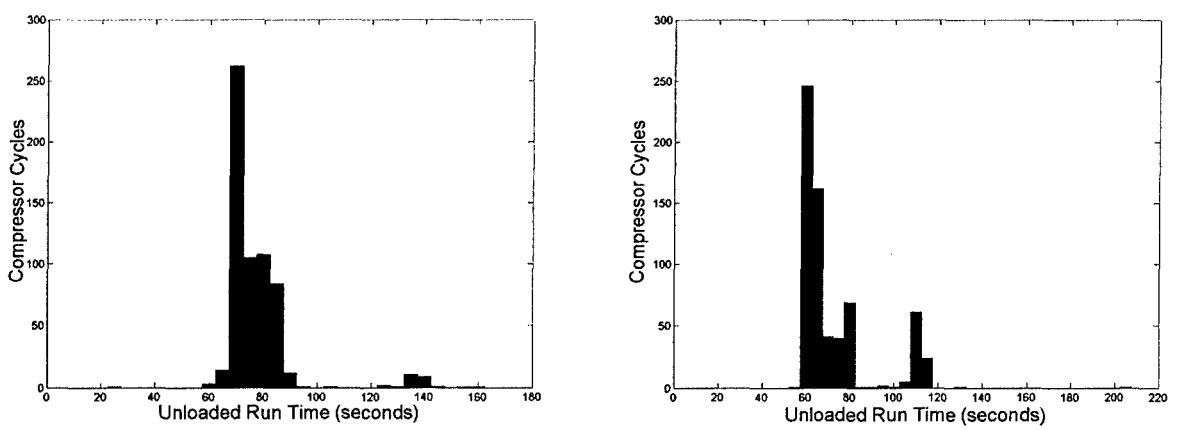

Baseline Case

Leak Case

Figure 4-9: LP Air Compressor Data 4/18-4/22 – 5 Second Bin Size

In Figure 4-9, the large peak in unloaded compressor run time to shifts to the left in the case where the leak is present. This follows the trend in Table 4-3 where additional loading causes the compressor to charge the system more often, decreasing the time between loaded compressor runs. The data from the leak case in Figure 4-9 could be used to continue the table with another row for a large load with a 12.5 SCFM leak and a corresponding unloaded compressor run time on the order of 70 seconds. Also observed in the Baseline case of Figure 4-9 is the presence of a small second peak in the range of 140 seconds. This secondary peak appears to grow and shift to the left (to a range of about 105 seconds) in the presence of the leak. More than two data sets will be needed before this behavior can be called a trend caused by the leak condition, and additional tests with wide range of leak rates are required to fully evaluate the phenomenon. However, it is interesting to note that if the system were to behave in a similar manner to the *SENECA* sewage system, this peak would be seen to continue to grow and shift left in the presence of larger and larger leaks.

4.2.3.3 Time between Runs and Histogram Bin Sizing

One significant difference between the *SENECA* sewage system data and the LBES Low Pressure Air system data is the amount of time observed between motor runs. The mean time between *SENECA* sewage pump runs was on the order of 5 minutes, while the mean time between LBES compressor runs was on the order of 1 minute. Because the frequency of the compressor cycles is so much higher than the sewage pumps, small bin sizes were deemed more appropriate for evaluating trends in the data. Two and one second bin sizes are shown in Figure 4-10 below.

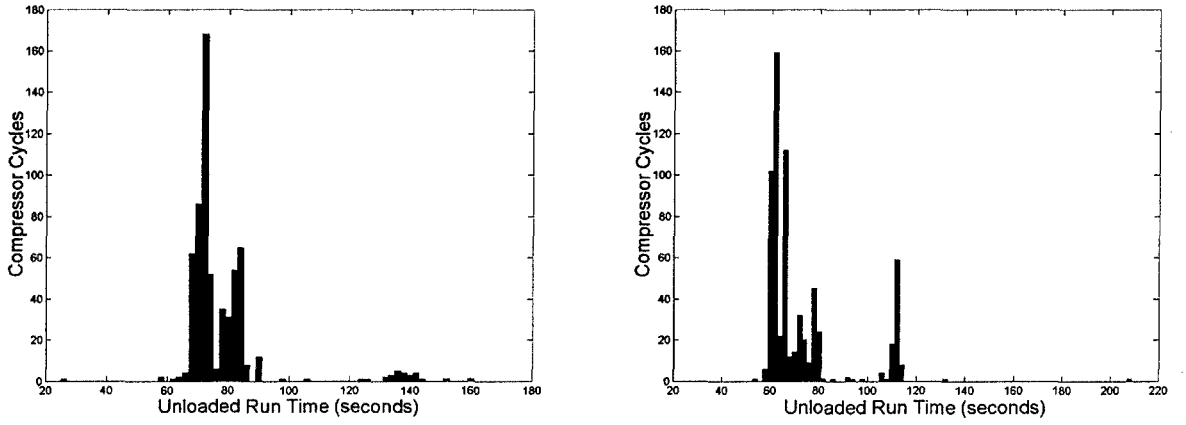

Baseline Case Leak Case

Figure 4-10: LP Air Compressor Data 4/18-4/22 – 2 Second Bin Size

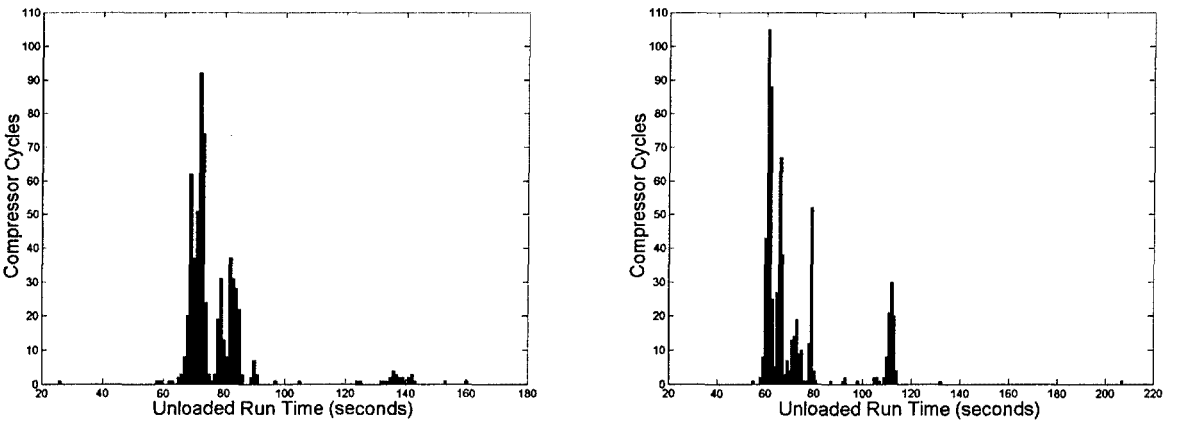

Baseline Case Leak Case

Figure 4-11: LP Air Compressor Data 4/18-4/22 – 1 Second Bin Size

In Figure 4-11 the leak case more clearly illustrates the behavior of the primary peak not only shifting to the left, but also growing larger. The characteristics of the secondary peak are also better defined. Details of Figure 4-11 are as follows: Baseline – Peak at 92 cycles occurring at an interval of 72 seconds, mean unloaded run time 77.6 seconds, Leak – Peak at 105 cycles occurring at an interval of 61 seconds, mean unloaded run time 73.4 seconds.

4.2.3.4 The Influence of Throttle Position on Compressor Operation

As discussed in Section 3.5, the variable loads on the LBES Low Pressure Air system are from pneumatic control valves associated with main propulsion. It should be noted that pneumatic tool stations were also installed at the LBES, but were not in use. Propulsion orders on ships are referred to as bells, and this will be the terminology used in this chapter. Some examples of common bell orders used in the LBES operations log are listed in Table 4-4 below.

Table 4-4: Standard Ship Propulsion Bells

Propulsion Order (Bell)	Shorthand Symbol
All Stop	A/S
Ahead One Third	A1/3
Ahead Two Thirds	A2/3
Ahead Standard	AI
Ahead Full	AII
Ahead Flank	AIII

When the bell is increased, the throttles are opened and the propulsion plant's Machinery Control System ensures several actions take place:

1. The pneumatically controlled Fuel Oil Service System unloading valve repositions, supplying additional fuel to the main engines.
2. As the shaft spins faster, the two pneumatic Water Brake control valves reposition, providing additional resistance.
3. As the shaft generates more friction, the propulsion lube oil temperature increases, and the pneumatically controlled Lube Oil Service System temperature regulating valve repositions to allow more lube oil to be directed to the coolers.

In order to employ the NILM as a diagnostic tool to detect leaks, we must be able to differentiate between large system loads and fault conditions (i.e. leaks). As an initial evaluation of this situation, two operating profiles were compared. The first profile consisted of the plant operating with large bells and no leak present. Here the large bells were 6 minutes at AII followed by 8 minutes at AIII. The second profile consisted of operations at a small bell (A2/3) and the test leak present (Figure 4-12).

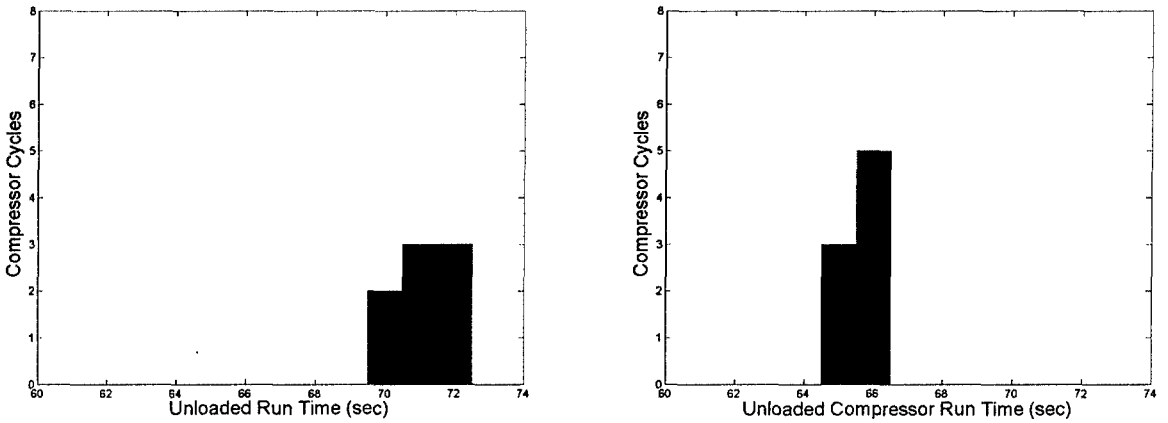

Large Bells, No Leak

Small Bell with Leak

Figure 4-12: Comparison of Two 14 Minutes Operating Profiles

The histograms shown in Figure 4-12 only represent eight compressor runs and this may not be sufficient to indicate a trend. However, they provide a preliminary indication that the test leak has a greater impact on compressor operation than does the large bell. If this small data set is representative of normal operations, a large bell would not be expected to mask the effect of the test leak.

4.2.3.5 Evaluation of Combinations of Bell Changes and Leak Conditions

The operating logs from the crew certification were reviewed and four two hour periods were identified for the following cases: 1) no leak, no bell changes 2) no leak, 8 bell changes, 3) leak and no bell changes, and 4) leak and 8 bell changes. The histograms of compressor performance for each case are shown in Figure 4-13.

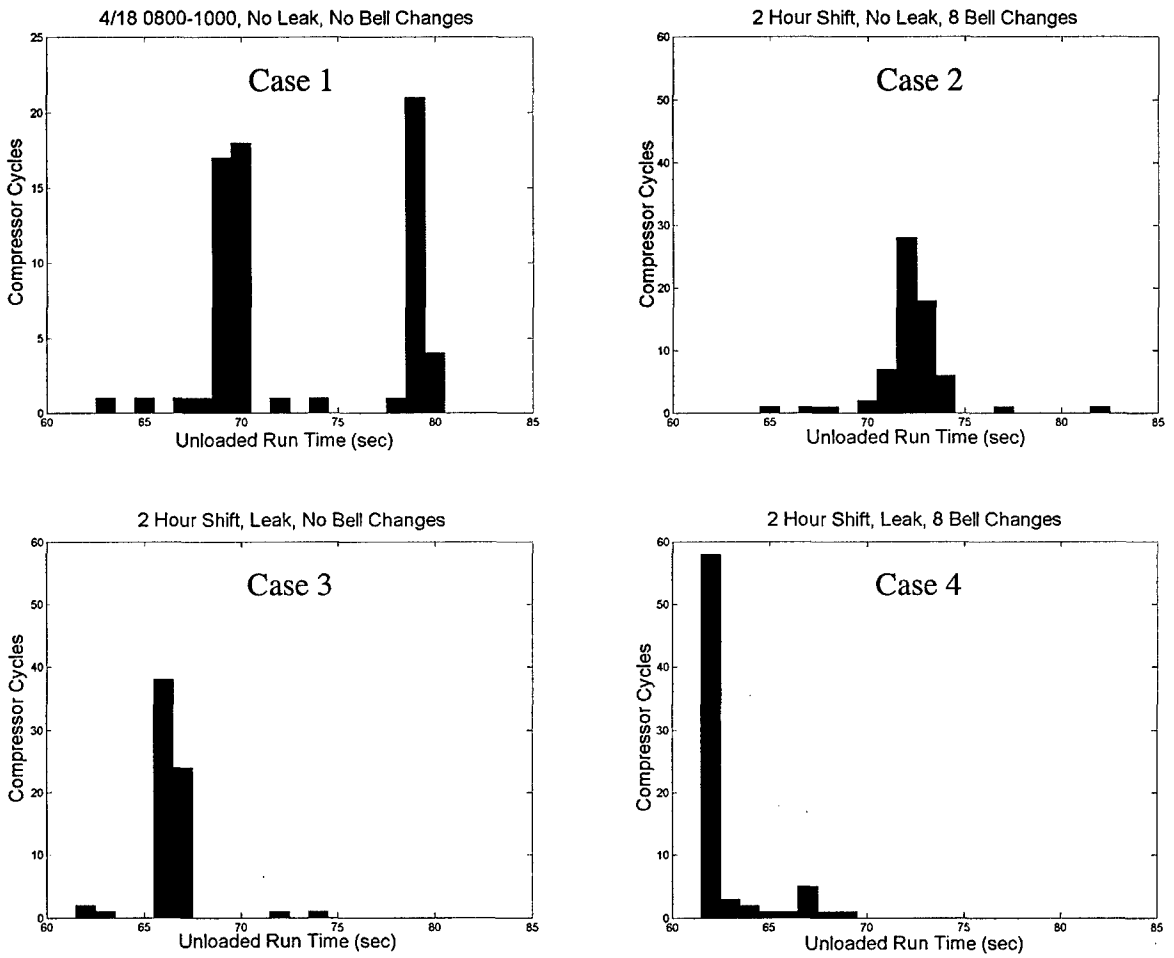

Figure 4-13: Two Hour Data Sets Comparing Combinations of Bell Changes and Leak Conditions

These histograms show demand on the air system increasing for each case. Case 2 appears to have a distribution similar to that of the full baseline data set in Figure 4-11. Comparing cases 2 and 3 indicates the test leak generates more demand than the bell changes. The peak demand on the air system is seen in case 4, which bears a striking similarity to the leak case in the full 19 hour data set shown in Figure 4-11. The details of case 2 and 4 are defined as follows: Case 2 – Peak of 28 cycles occurring at an interval of 72 seconds, Case 4 – Peak of 58 cycles occurring at an interval of 62 seconds.

One anomaly in the data is the apparent bimodal distribution of case 1. A further review of the operating logs reveals an explanation. At approximately 0900, the bleed air system was started. This system uses air from the gas turbine's compressor to perform many shipboard functions that require large volumes of compressed air (see Figure 4-14) [29]. It should be noted that these loads are not present at the LBES and bleed air at the facility is vented to atmosphere.

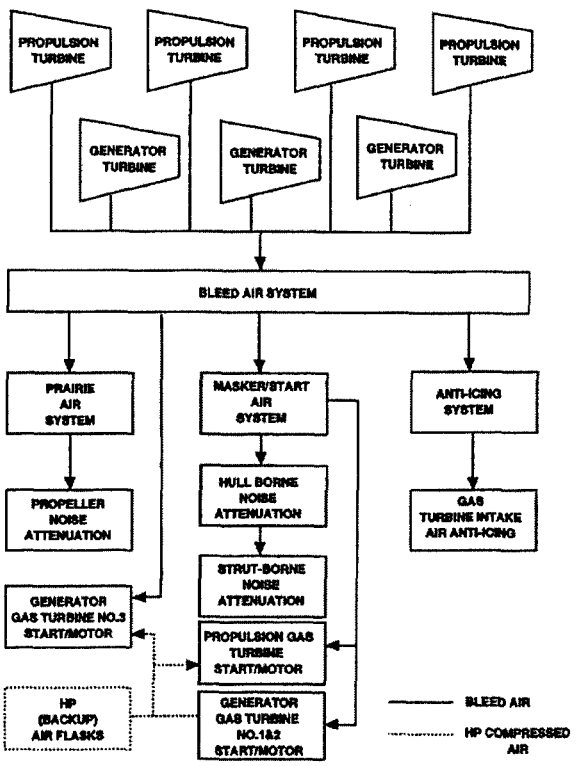

Figure 4-14: Simplified Block Diagram of the DDG-51 Bleed Air System

The bleed air discharge line from each gas turbine contains a pressure regulating valve (Figure 4-15) [29] in the shipboard piping. The pressure regulating valves reduce the gas turbine compressor discharge pressure to the nominal system pressure of 75 PSIG. The valves contain a butterfly valve-type wafer for pressure regulation, activated by ship service air to the valve actuator. An external sensing line from the actuator senses the bleed air main pressure downstream of the valve. Based on this sensed pressure, the valve actuator modulates the valve position to maintain the nominal system pressure of 75±2 PSIG accordingly. The bleed air pressure regulating valve is normally open, and may be operated manually [21]. These valves

are configured with two small vents that constantly bleed off the low pressure control air to atmosphere until it is needed to reposition the valve. The effect is a very large load on the system that is better approximated as a constant leak than the more discrete demands of other types of control valves.

To isolate the effect of the bleed air system, the data from case 1 was divided into two sections, from 0800-0900 and from 0900-1000, as shown in Figure 4-16.

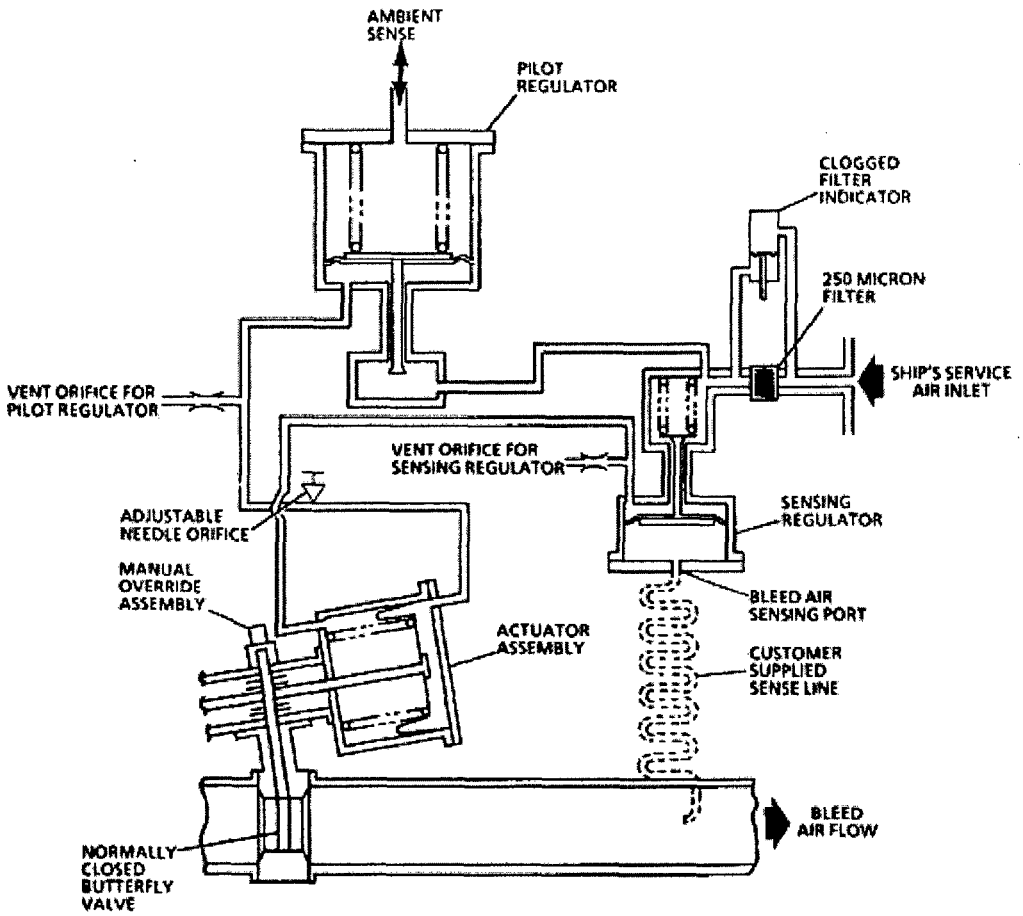

Figure 4-15: Functional Schematic of the Bleed Air Pressure Regulating Valve

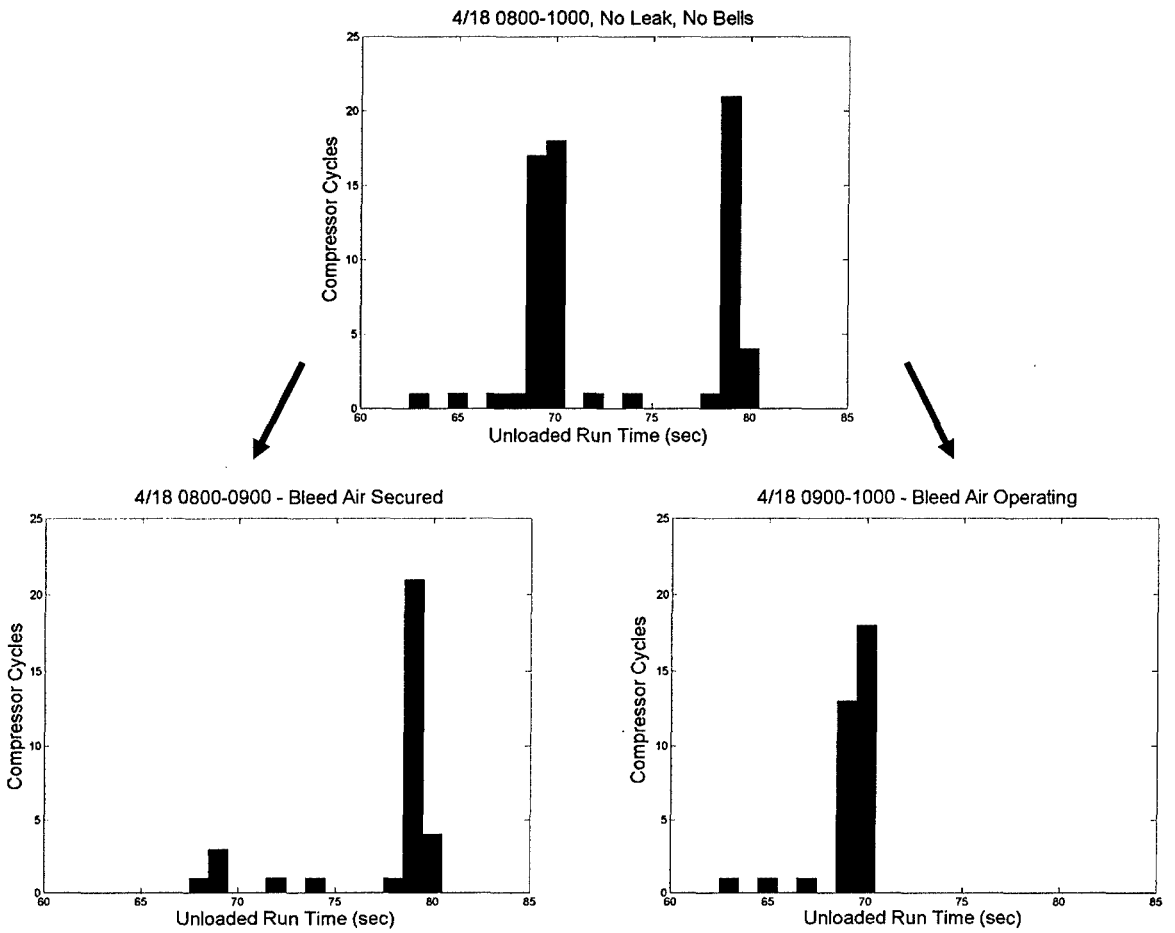

Figure 4-16: Case 1 from Figure 4-13 Split into One Hour Periods

The plot on the lower left of Figure 4-16 shows operation of the LPAC with the bleed air system secured, no bells and no test leak. The plot on the lower right shows the bleed air system operating, again with no bells and no leak. The load from the bleed air system is large enough to drive the peak of compressor cycles down from 79 seconds to 70 seconds. Because bleed air is such a large load, it may also provide an explanation for the smaller peaks seen around 80 seconds in the full 19 hour data sets in Figure 4-11.

4.2.3.6 MATLAB Low Pressure Air System Simulation

In order to obtain a better understanding of the operation of the LBES Low Pressure Air System, the random nature of the loads caused by propulsion plant air operated valves must be controlled. In order to accomplish this, a MATLAB simulation developed for the SENECA Sewage System [12] was modified to reflect the operating parameters of the Low Pressure Air System. In this case the following assumptions were made:

- Pneumatic control valve cycles provide the variable load on the system and their arrival times are normally distributed random variables.
- Each valve cycle reduces system pressure by an equal amount.
- The only pressure source is provided by the single LBES low pressure air compressor.
- The leak rate is constant and does not depend on system pressure.

Additionally, system set points and loads were changed as shown in Table 4-5.

Table 4-5: LBES Low Pressure Air System Parameters

Parameter	Value
P_{high}	125 PSIG
P_{low}	110 PSIG
Pressure drop	0.7-2.0 PSIG/valve cycle
Compressor Rate	33 PSIG/min
μ time between valve cycles	10 seconds
σ time between valve cycles	0.005 seconds

A normal random variable was applied to the simulation. This was chosen based on the Central Limit Theorem which states:

> If $\{X_i\}$ are independent and identically distributed random variables with mean μ and finite variance σ^2, then the random variable
>
> $$Z = \frac{(X_1 + X_2 + \cdots + X_n) - n\mu}{\sigma\sqrt{n}} \tag{4-2}$$
>
> tends (as $n \rightarrow \infty$) to a normal random variable with mean zero and variance one.

This implies that if we collect enough data on the compressor operation, it will tend towards a normal or Gaussian distribution. A normal random variable Y with zero mean and unit variance is called a standard normal random variable. In this case we need to scale the variable to account for the estimated mean and variance of the control valve cycles. This is possible because normality is preserved by linear transformation as follows [30]:

> If X is a normal random variable with mean μ and variance σ^2, and if $a \neq 0$, b are scalars, then the random variable
>
> $$Y = aX + b \tag{4-3}$$
>
> is also normal, with mean and variance
>
> $$E[Y] = a\mu + b \qquad \text{var}(Y) = a^2\sigma^2 \tag{4-4), (4-5}$$

A standard normal random variable was called from MATLAB and was then scaled as described above. The simulation provided an approximation of baseline system performance using a pressure drop of 0.7 PSI/valve cycle, but would not generate mean unloaded compressor run times less than 105 seconds (Figure 4-17). With a leak inserted, the simulation provided histograms with trends similar to the LBES data, but again, the mean unloaded compressor run times were about 45 seconds above the expected values. Figure 4-18 models the conditions of case 4 in Figure 4-13. Here a pressure drop of 2 PSI/valve cycle generated the most comparable trends. The simulation also broke down at higher leak rates. As the leak rate was increased, the mean unloaded compressor run time first increased as expected, but the decreased as the leak rate exceeded 11 PSIG/min.

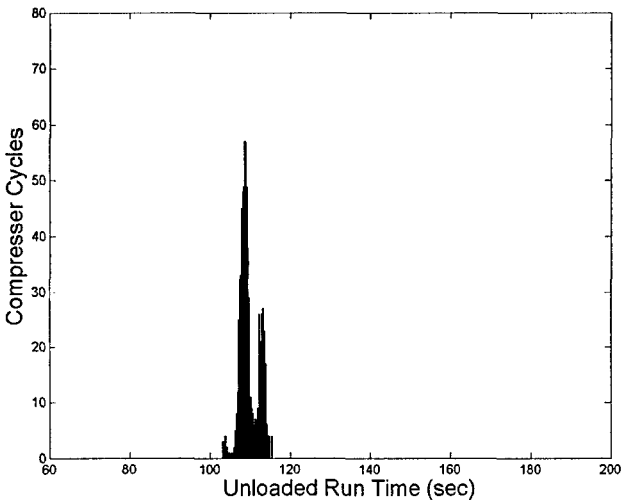

Figure 4-17: 19 hour MATLAB Simulation with no Leak Condition

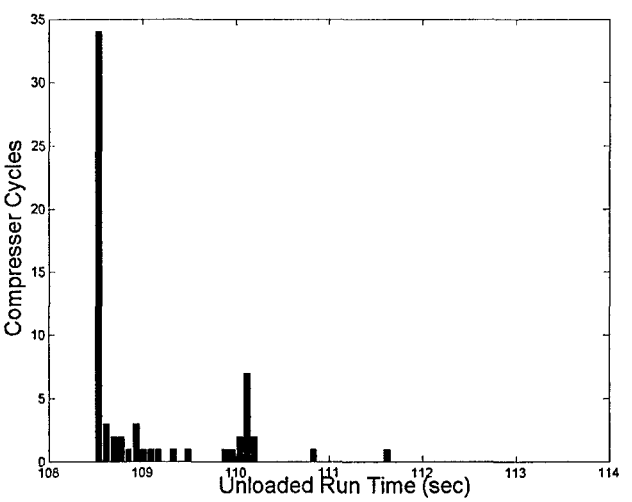

Figure 4-18: 2 hour MATLAB Simulation with 7 PSIG/min Leak

4.3 Chapter Summary

While the results presented in this chapter are preliminary, they show the potential of the NILM in evaluating system performance factors based on evaluation of motor spectral envelopes. The analysis of the Fuel Oil System demonstrates how changes in system valve lineups can be observed using the NILM. This capability to remotely verify valve lineups would be especially valuable for systems with many valves on minimally manned ships, or in systems where valves are not always accessible, such as in the reactor compartment of a nuclear powered submarine or aircraft carrier. The Low Pressure Air System data shows that the NILM can provide useful information on the health of the system (compressor loading) and even determine the source of the loads, as in the case of the bleed air system. Further development of the Low Pressure Air System simulation may provide additional information on the system's performance and could lead to the development of a diagnostic tool to detect the presence of air leaks. More data is needed from the LBES to obtain a better understanding of the preliminary results in this chapter as well as the potential of the NILM as a CBM tool for the US Navy. However, based on the data collected in this study, a recommendation has been passed to the LBES Test Director to either modify operation of the bleed air valves (i.e. place then in manual mode) or replace them with a new style of valve. Either of these actions would prevent the loss of low pressure air from the Bleed Air Pressure Regulating Valves and should significantly reduce wear on the LBES Low Pressure Air Compressor. Quantitatively, assuming operation for one 8 hour shift 50 weeks per year, a reduction of approximately 50 compressor cycles per day or 250,000 cycles over a nominal 20 year component life could be realized.

Chapter 5 The Multi-Function Monitor (MFM)

5.1 Introduction

The Multi-Function Monitor (MFM) is the central component in the electrical protection systems of modern surface warships that employ the Zonal Electrical Distribution System (ZEDS). Because the MFM uses current sensors located on the main busses of the shipboard electric distribution system, it is considered a natural entry point for the NILM in monitoring multiple loads as discussed in Chapter 2. In addition to CBM, the NILM may also have applications in ship reconfiguration and survivability. The MFM is one of the ways the Navy is moving towards systems that can automatically assess battle damage conditions and reconfigure for optimal performance. The NILM's potential to disaggregate individual loads from bus current and voltage may provide future electrical protection systems with valuable information on critical loads, such as which loads are running, secured, have power available, or are running but underpowered. This information would allow more sophisticated decisions to be made on by the protection system logic during automatic reconfiguration. Therefore, integration of the NILM and the MFM may provide a duel benefit to the Navy. In order to facilitate future research in this area, the following information on the MFM is provided.

5.2 Background

The MFM was developed in part to provide "fight through" capability for warships that experienced major electrical faults as a result of battle damage. Traditional electric plant fault isolation methods rely on over current or under voltage settings to trip circuit breakers and protect loads from damage. During battle damage scenarios involving major bus faults, ships were losing critical loads, such as those associated with combat systems, due to low voltage protective actions. Additionally, these major bus faults could draw such a large amount of current that feeder breakers that should trip to improve the survivability of the ship would not see enough current to initiate a protective action. Further challenges were imposed when the Navy began to employ the Zonal Electrical Distribution System (ZEDS) on the Flight IIA DDG-51 Class and the LPD-17 Class of ships. The physical arrangement of this system results in zones

where current can flow in different directions on a given bus, depending on the electric plant configuration. This led to the requirement for a protective system with the capability to discern the direction of current in order to provide "intelligent fault detection and isolation" [31]. The baseline MFM, designated MFM I, has been upgraded and the improved version, or MFM III will be discussed in this chapter.

5.3 MFM III Description

The MFM III is built to military specifications and enclosed in a small (roughly 1 ft3) case which is then mounted in cabinet adjacent to its related switchgear (Figure 5-1). The case houses a processor and terminals for current and voltage sensor input, Ethernet communications, and shunt trip signal output (Figure 5-2).

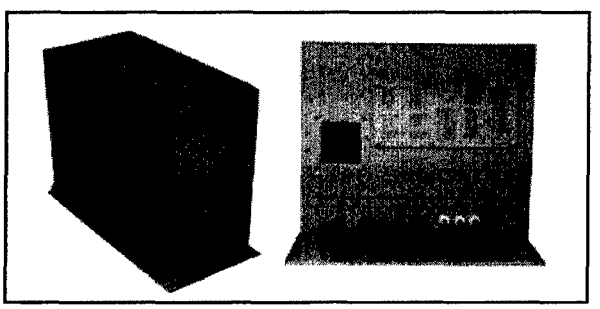

Figure 5-1: Exterior of MFM III Unit

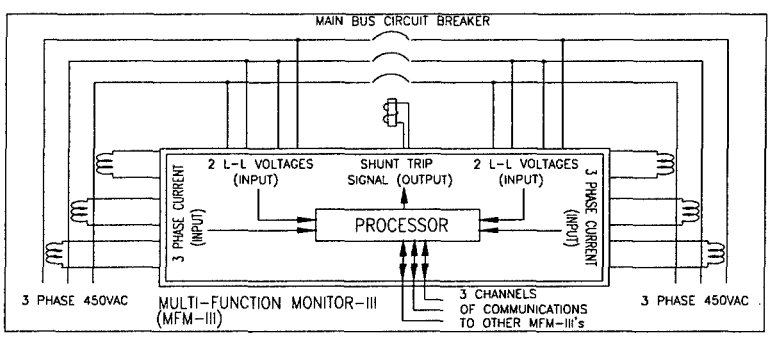

Figure 5-2: MFM III Functional Diagram

Individual MFM III units are installed with each main bus breaker in the DDG-51 Flight IIA ZEDS for a total of 11 units in the electric plant. Each unit has two channels of voltage and current input, one on each side of its associated circuit breaker. Line to line voltage is sensed through two potential transformers (440:110) and line current for each phase is sensed by two sets of current transformers (6000:5). The MFM also receives input on the status of its adjacent circuit breaker. For reliability, the MFM units communicate via Ethernet in both a point to point mode (directly with each of their two immediate neighbors) and in a ring mode (all 11 MFMs on the same ring). There are four different types of MFM III units and all employ the same software. The type of MFM used depends on its physical location in the electric plant (generator breaker, etc). Each unit is assigned an address based on its unit number, location and type. The software routines executed by the MFM are determined in part by this address (Figure 5-3) [32].

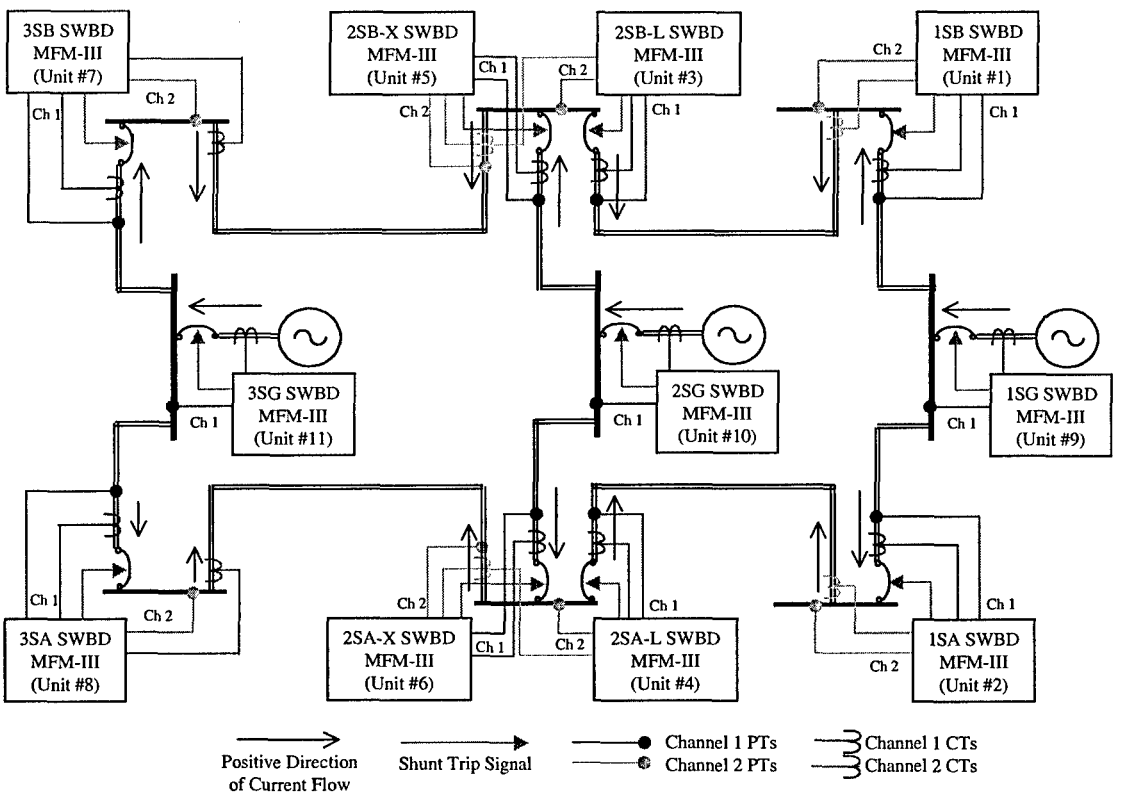

Figure 5-3: DDG-51 FLTIIA ZEDS MFM III Locations and Inputs

5.4 MFM III Operation

The MFM III is designed to determine if a fault exists in 0.5 ms, determine the location of the fault, and execute a coordinated shunt trip decision in 10 ms. To perform this function the MFM III uses two primary algorithms: the High Speed Relay (HSR) fault detection algorithm and the Integrated Protective Coordination System (IPCS) algorithm.

5.4.1 High Speed Relay Algorithm

The HSR algorithm is used for fault detection and to establish "fault direction" (the direction of fault current the bus). Bus voltage is sampled by each MFM channel at a frequency of 1000Hz. The algorithm uses the Park Transformation to map the balanced AC input voltages (V_a, V_b, V_c) to constant values in the *d-q* (direct and quadrature axis) domain through the use of a moving reference frame. When the Park Transformation is applied to each voltage sample, a phasor is produced. Reference [33] describes the process as follows:

The Park Transformation from the stationary to the rotating reference frame is given by

$$\begin{bmatrix} f_0 \\ f_d \\ f_q \end{bmatrix} = \sqrt{\frac{2}{3}} \begin{bmatrix} \frac{1}{\sqrt{2}} & \frac{1}{\sqrt{2}} & \frac{1}{\sqrt{2}} \\ \cos\theta & \cos(\theta - 2\pi/3) & \cos(\theta + 2\pi/3) \\ \sin\theta & \sin(\theta - 2\pi/3) & \sin(\theta + 2\pi/3) \end{bmatrix} \begin{bmatrix} f_a \\ f_b \\ f_c \end{bmatrix} \tag{5-1}$$

where the *f*'s represent the line-to-line voltages in the three-phase system. The three line-to-line voltages should sum to zero in accordance with Kirchoff's Voltage Law (KVL). "The first Park Transformation equation is essentially a check to see whether or not the voltages sum to zero. The HSR algorithm, which assumes the voltages do sum to zero, uses this information to bias the line-to-line voltages, as will be discussed later in this section. The two other Park Transformation equations involve projecting the fixed coordinate values onto a rotating reference frame. Given:

$$\theta = \omega_0 t \tag{5-2}$$

$$f_a = F_a \cos(\omega t + \phi) \tag{5-3}$$

$$f_b = F_b \cos(\omega t - 2\pi/3 + \phi) \tag{5-4}$$

$$f_c = F_c \cos(\omega t + 2\pi/3 + \phi) \tag{5-5}$$

then

$$\begin{aligned} f_d = &\sqrt{\frac{2}{3}}\{\frac{F_a}{2}\cos([\omega_0 - \omega]t - \phi) + \frac{F_a}{2}\cos([\omega_0 + \omega]t + \phi)\} \\ &+ \sqrt{\frac{2}{3}}\{\frac{F_b}{2}\cos([\omega_0 - \omega]t - \phi) + \frac{F_b}{2}\cos([\omega_0 + \omega]t + 2\pi/3 + \phi)\} \\ &+ \sqrt{\frac{2}{3}}\{\frac{F_c}{2}\cos([\omega_0 - \omega]t - \phi) + \frac{F_c}{2}\cos([\omega_0 + \omega]t - 2\pi/3 + \phi)\} \end{aligned} \tag{5-6}$$

If $F=F_a= F_b= F_c$, then the terms in the first column are identical and those in the second column represent a balanced three-phase set and therefore sum to zero. Thus f_d becomes

$$f_d = \sqrt{\frac{2}{3}}\{\frac{3}{2}F\cos([\omega_0 - \omega]t - \phi)\} \tag{5-7}$$

which, if $\omega = \omega_0$, reduces to

$$f_d = \sqrt{\frac{2}{3}}\{\frac{3}{2}F\cos(-\phi)\} \tag{5-8}$$

Similarly for f_q

$$f_d = \sqrt{\frac{2}{3}}\{\frac{3}{2}F\sin(-\phi)\} \tag{5-9}$$

Therefore, for a balanced three-phase system where KVL applies

$$\begin{bmatrix} f_0 \\ f_d \\ f_q \end{bmatrix} = \begin{bmatrix} 0 \\ \sqrt{3/2}F\cos\phi \\ -\sqrt{3/2}F\sin\phi \end{bmatrix} \tag{5-10}$$

Dropping the f_0 component, the resulting constant vector (phasor) in a two dimensional plane is

$$F_{dq} = \left|\sqrt{3/2}F\right| \angle -\phi \tag{5-11}$$

F determines the system voltage and magnitude, whereas ϕ relates the start of the three-phase voltage cycle to the initial angle of the rotating coordinate axes of the Park Transformation."

A typical 60Hz AC voltage phasor would rotate counter clockwise with the input signal, but the transformed phasor is effectively held stationary in the d-q domain (Figure 5-4).

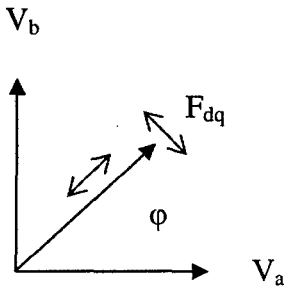

Figure 5-4: HSR Park Transformation Phasor Diagram

A buffer is used to evaluate the change in the phasor over the past eight samples. If the phasor changes by a pre-determined threshold in either angle, magnitude, or both, a given event is classified as a fault. Once a fault is detected, the present power is designated as the "fault power". The previous power calculation is saved and designated "steady state power" (i.e. the power before the fault). A comparison of these two power values is made and if the power has decreased, the fault is presumed to be "down-line" from the MFM. If the power has increased, the fault is presumed to be "up-line" of the MFM [33].

The calculations made by the HSR algorithm are based on KVL and assume that the three-phase voltages sum to zero. Reference [33] states "Although only two voltages are used to compute the Park Transformation's magnitude and angle, all three phases are sampled by the algorithm to deal with non-zero closed loop voltages. The average of these three values is computed and then subtracted from the two phases actually used by the Park Transformation. In this way, disruptions common to all three phases are removed." This statement is critical to the operation of the MFM, as changes in electric plant lineups and changes in three-phase loads can be discriminated from fault conditions. However, single phase and line-to-line faults result in significant changes to the phasor, allowing the identification of a fault.

5.4.2 Integrated Protective Coordination System (IPCS) Algorithm

The IPCS algorithm provides the MFM III with the means to evaluate local information from its own sensors and remote information from other MFM units via the Ethernet and if necessary execute a coordinated shunt trip response. The algorithm has six separate routines 1) Fault Counter and Direction Assignment, 2) Topology and Generator Line-up Assessment, 3) Switchboard Fault Detection, 4) Bus-Tie Fault Detection, 5) Catastrophic Switchboard Fault Detection, and 6) Shunt Trip. These routines are executed ever 0.1ms and generate flags and counters that populate logic tables in the IPCS program. The Shunt Trip routine "looks up" values of the internal/downstream switchboard fault detection, bus-tie fault detection, and catastrophic switchboard fault detection sections of the IPCS routine (as well as back up algorithms from the original MFM I algorithm) and if certain conditions are met, it sends a signal to initiate voltage to the shunt trip coil of its associated circuit breaker. The logic tables for each of the above routines are contained in reference [32].

5.5 Exploration of NILM/MFM Integration

A review of the construction, arrangement, source code and operation of the MFM III leads to the conclusion that it does have the potential as an interface for the NILM with the ship's electric distribution system. The NILM could take advantage of the MFM IIIs existing voltage and current sensors and their centralized locations. It is also conceivable that the NILM could augment the inputs to the MFM. For example, NILM data columns could be added to existing MFM logic tables to provide detailed status on critical loads. The use of this information could be incorporated into the IPCS routines improve automatic reconfiguration actions. Discussions with the lead electrical test engineer at the LBES indicate that detailed technical reviews would be required prior to obtaining authorization to connect the NILM with the MFM because of the MFM's status as a "safety of ship" device [34]. It was recommended that prior to moving forward with testing on an MFM in the LBES ZEDS, the LEES Navy team should first consider interfacing with the installed current meters used to monitor bus current at the electric plant control panel. These meters are reported to use the same type of current transformers employed by the MFM III and would allow for validation of equipment setup and operation. Another issue

that needs to be addressed is the difference in sample rates between the two systems (120Hz for NILM pre-processed data and 1000Hz for the MFM). Some additional resources for evaluating the NILM/MFM interface prior to pursuing approval for full scale testing are discussed in Chapter 7.

Chapter 6 The Navy's Integrated Condition Assessment System (ICAS)

6.1 Objective

The previous chapters show that the NILM is well suited for shipboard machinery monitoring and has significant potential as an input to a Navy CBM scheme. If the NILM is going to be installed on ships, it will likely interface with ICAS. To facilitate shipboard implementation of the NILM, this chapter briefly describes the ICAS system. To help make an initial evaluation of how the unique capabilities of the NILM could be used to augment data collected by existing or future ICAS installations, a simple side by side comparison of machinery monitoring data from both systems was made.

6.2 Background

ICAS is a system which monitors equipment operating parameters from shipboard HM&E equipment and transforms this data into information useful to operators and maintenance providers. ICAS uses a CBM approach to reduce the burden of preventive maintenance practices on crews while improving coordination with shore-based maintenance providers. ICAS machinery monitoring data is used by operators for indication and warning as well as diagnostics. It is also transmitted off the ship to shore-based support facilities on a periodic basis, or immediately in the event of a key equipment failure. Once on shore, ICAS data is also stored on the Navy's Maintenance Engineering Library Server (MELS) and used to improve the accuracy of future shipyard work packages and Class Maintenance Plans (CMPs). MELS also allows access to the data so it can to be trended and evaluated by system experts to assist ship's force or technical support fly-away teams in evaluating fault conditions.

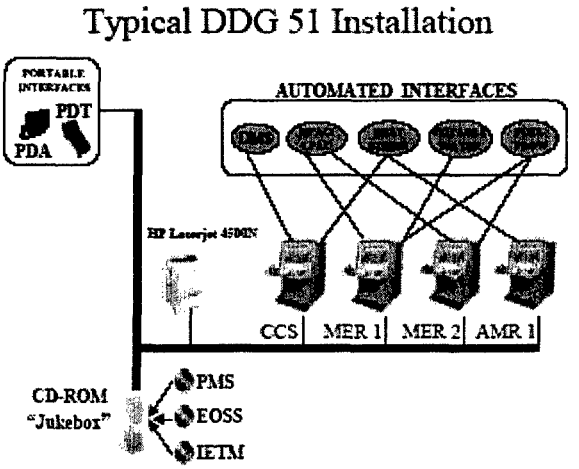

Figure 6-1: Shipboard ICAS Configuration

A typical shipboard ICAS installation is made up of several Windows NT workstations, printers, portable (manual, i.e. palm pilots) and installed (automatic or online) data acquisition devices, and a CD-ROM tower of other Navy maintenance related software, all linked by a fiber-optic Local Area Network (Figure 6-1). ICAS is designed to have a flexible architecture to allow the system to monitor a wide variety of parameters including temperature, pressure, speed, voltage, vibration, and level data. Sensor information is received automatically from traditional hard-wired sensors. Additional data from stand alone sensors (such as locally installed pressure and temperature gages) are manually collected, stored in portable devices, and uploaded to ICAS workstations. A complete list of equipment monitored on DDG-51 Class Destroyers can be seen in Appendix E. Because the sensor information collected is subsequently relied on for so many applications (trending, troubleshooting, work package forecasting and indication and warning), it is critical that the data be accurate [31].

6.3 ICAS Monitoring

ICAS uses proprietary rule-based software that evaluates input from individual sensors. The system compares real time machinery monitoring data against expected equipment operational profiles to identify out of specification conditions or performance degradation prior to an equipment failure. The software can be customized by the operator to select data collection rates

and alarm set points, although these are generally promulgated in the ship's operating procedures. ICAS has several categories of monitoring, including events and trends. In event monitoring, data from selected system sensors can be sampled as frequently as once per second, and stored for an interval of up to six minutes. When a trigger event occurs, (for example an out of specification reading or a command to start a pump in fast speed) the data from up to three minutes before and three minutes after an event is stored. The event can also trigger an alarm or warning to operators at the ICAS workstation. Trend monitoring, as the name implies, is used for longer term trend analysis of the data. Trend data can be sampled as frequently as every minute, and can be collected on all sensors, including those sampled manually. This mode also records machinery run hours. Both Event and Trend monitoring data can be plotted using the proprietary software at a workstation, (additional graphs can be generated using MELS) and exported to commercial programs such as Microsoft Excel in a comma separated values (.cvs) file format. Additionally, both types of monitoring are performed simultaneously by the system. Other ICAS monitoring functions include Hybrid Decision Support (HDS) and Vibration. HDS uses Boolean Logic. It takes inputs from several gates (such as sensor inputs, alarms, or machinery status), assigns pre-defined triggers that instruct ICAS when to evaluate the logic, and uses a variety of Boolean logic gates (AND, OR, NOR, NOT, etc.) to determine when an alert should be sent to operators. Vibration monitoring uses trending of component displacement, velocity and acceleration data to analyze for conditions such as equipment imbalance or misalignment.

6.4 Investigation

In the following tests, components on the LBES Fuel Oil and Lube Oil Service Systems were monitored simultaneously with both the NILM and ICAS. Monitoring was conducted during steady state and transient pump operations as outlined in the test plan titled Non-intrusive Load Monitor and ICAS Component Monitoring contained in Appendix C. Because the GTMs and GTGs were not operating at the time of data collection, both the systems were run in a recirculation mode for the duration of the testing. Details of the selected fluid systems and NILM installations can be found in Chapter 3.

6.4.1 Event Monitoring

The LBES ICAS system was set up for event monitoring by an ICAS technician. The type of event to be monitored, time duration of the event, and sensors selected to provide input to the system were all entered at an ICAS workstation (Figure 6-2). The specific event of a Fuel Oil or Lube Oil Service Pump starting based on either a low or high speed indication being received was designated as the trigger. This would result in the collection of monitoring data 60 seconds prior to and 60 seconds after the event was sensed by the system. The maximum sample rate of once per second was used. Several sensor inputs were selected, although due to plant conditions, some were in isolated portions of the system.

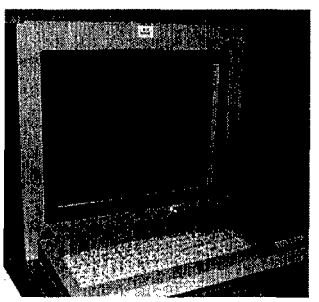

Figure 6-2: LBES ICAS Workstation

As an illustration, the raw ICAS data (presented in Appendix G) was plotted using MS Excel and is shown in Figure 6-3. The trigger event is at time zero. Pump indications for fast speed (-56 to -29 seconds), pump stop (-28 to -1 seconds), pump start in slow (the trigger) (0 to 13 seconds), a shift to fast speed (14 to 29 seconds), and another pump stop indication (30 to 60 seconds) are shown in the bottom half of the plot. Pump indications are represented by a non-zero integer (1 for slow speed indication, 2 for stop indication and 16 for fast speed indication). These non-dimensional values were plotted with reference to the left hand vertical axis for convenience. Also shown are discharge pressure, sump temperature and 'most remote bearing' (MRB) pressure. Discharge pressure can be seen to rise during pump starts as expected. Sump temperature also rises during fast speed pump operation (fast speed pumps are used to warm up the lube oil systems during recirculation operations). The slight dip in temperature may be due to a slug of cooler oil entering the sump as a result of the somewhat erratic nature pump operations during the testing. Figure 6-4 shows the real power spectral envelope collected simultaneously by the NILM. Time zero in Figure 6-3 corresponds to time 60 seconds in Figure 6-4.

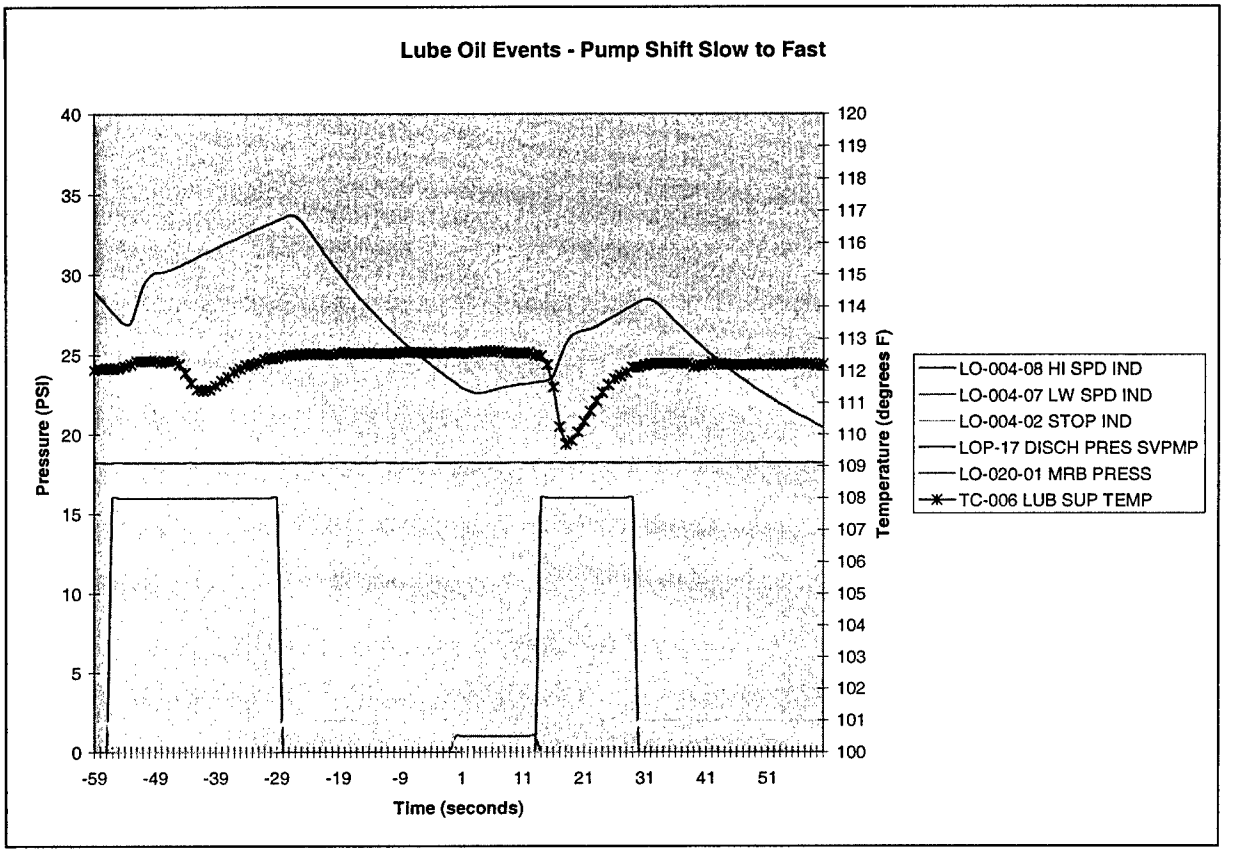

Figure 6-3: ICAS Event Data for Lube Oil Pump 2B Shifting Speed

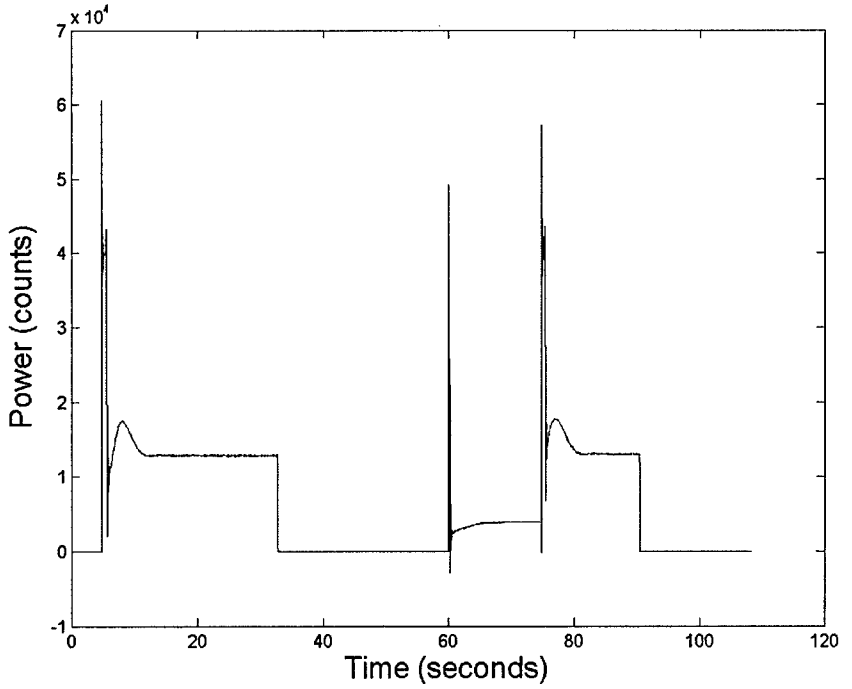

Figure 6-4: NILM Monitoring Data for Lube Oil Pump 2B Shifting Speed

6.4.2 Trend Monitoring

The LBES ICAS system was set up for trend monitoring at the same time it was set up for event monitoring. The sample rate of the monitoring and the sensors selected to provide input to the system were again entered at the ICAS workstation. The sample rate was specified at once per minute due to the short duration of the test period. This is the maximum frequency the system is capable of, as most systems in the fleet are only monitored once per hour. Sensors inputs of system pressure, oil temperature and pump indication (stop, slow, fast) were chosen. In contrast with event monitoring which operates for discrete periods, trend monitoring collects data continuously.

Again, the raw ICAS data (Appendix G) was plotted, using MS Excel. The results are shown in Figure 6-5. The raw data shows the non-zero integers representing pump operations are 128 for slow speed indication and 64 for fast speed indication. The plot represents a nine minute monitoring period, from 1416 to 1425 (local time) in one minute intervals. The 2A Fuel Oil Service pump is started at time 1416, and is run in steady state for the duration of the test. Also shown are fuel service header pressure and header temperature. Again, due to plant conditions, this data shows system startup parameters (normally the fuel oil is maintained between 85 and 120 °F by electric heaters). Figure 6-6 shows the real power spectral envelope collected simultaneously by the NILM. Time zero in Figure 6-6 corresponds to time 14:16:14 in Figure 6-5.

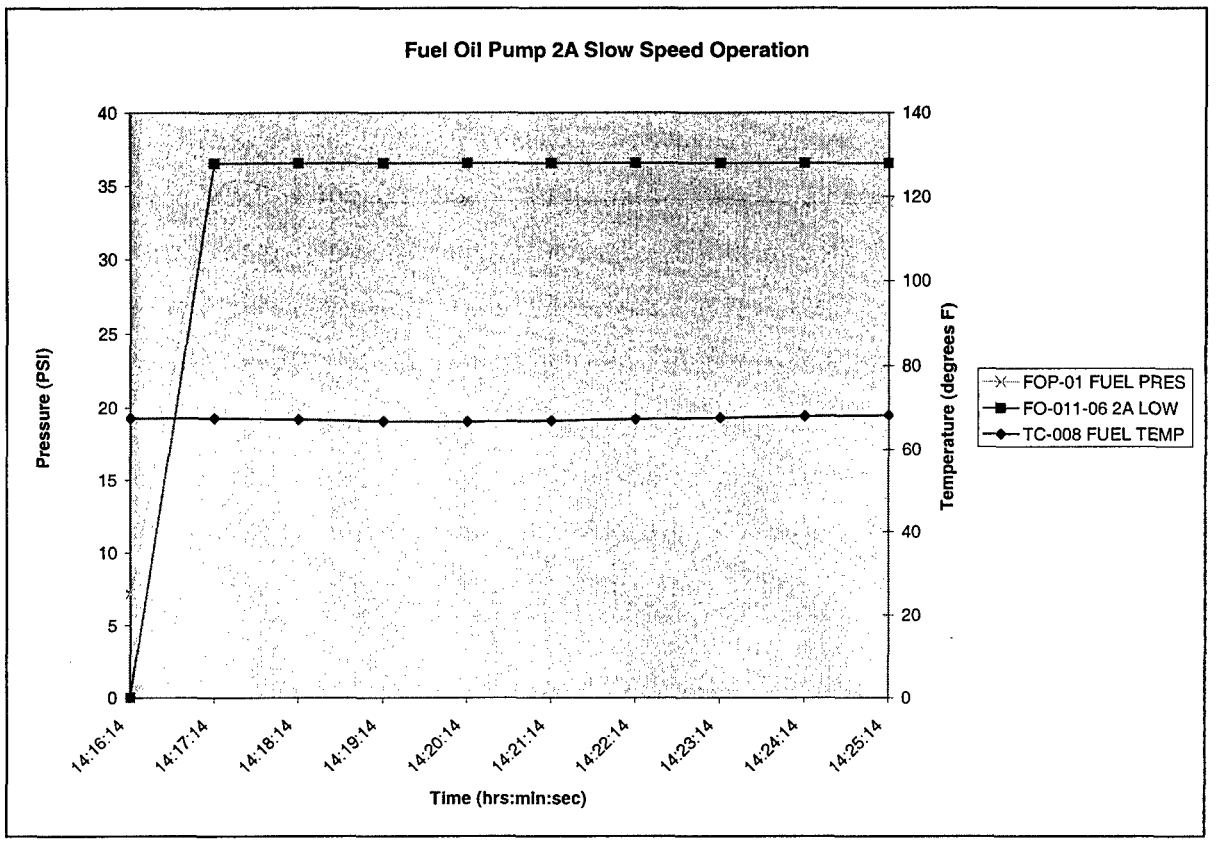

Figure 6-5: ICAS Trend Data for Fuel Oil Pump 2A Slow Speed Operation

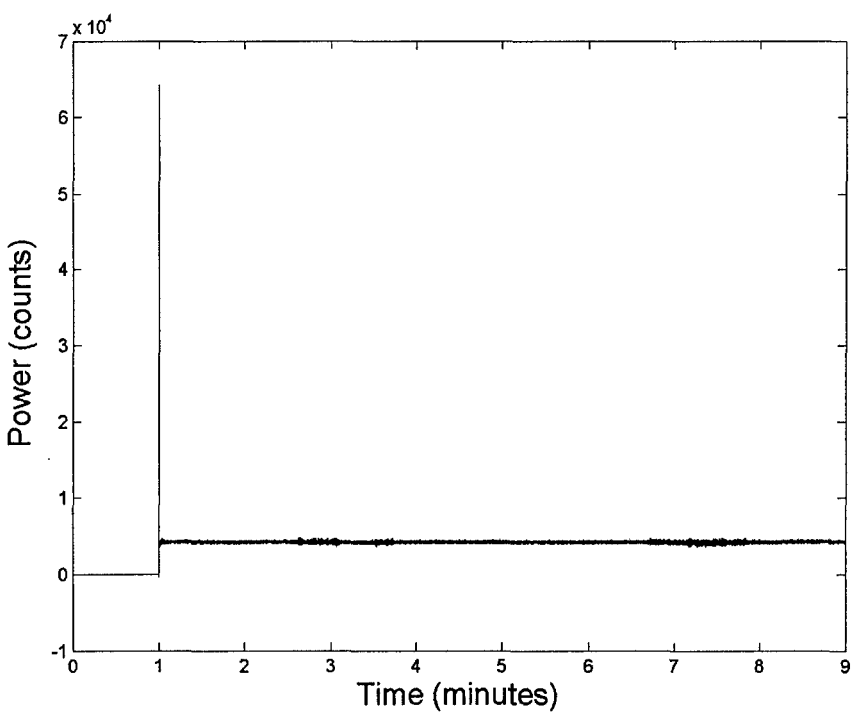

Figure 6-6: NILM Monitoring Data for Fuel Oil Pump 2A Slow Speed Operation

6.5 Chapter Summary

The developers of ICAS envision that eventually, all shipboard systems will interface with ICAS. If this is the case, the LEES Navy Team needs to continue to evaluate how to interface the NILM and ICAS so that the capabilities of the NILM can be employed fleet wide as soon as possible. The comparison of ICAS event monitoring and NILM data in Figure 6-3 and Figure 6-4 illustrate the striking difference between the input of an analog device such as a pressure sensor, and the NILM. They also show the limits of ICAS in event monitoring. The much higher sample rates (120Hz for pre-processed data and 8KHz for raw data), allow the NILM to detect system abnormalities that would be invisible to sensors currently available to ICAS. A prime example of this is the NILM's detection of high frequency data that diagnosed an Auxiliary Sea Water Pump coupling failure on the *SENECA* as discussed in references [11] and [12]. Section 6.3.2 is presented to illustrate the concept of ICAS trend monitoring, but is not representative of the long time periods typically associated with machinery monitoring trend analysis. However, the discussion of the implementation of ICAS indicates that data from the NILM would be a valuable input in trending machinery performance on US Navy Ships.

Chapter 7 Future Research

7.1 Limitations of Non-intrusive Monitoring

In exploring the limits of non-intrusive monitoring, this thesis shows that the NILM has the potential to provide meaningful information in support of CBM programs while being employed to monitor multiple loads. Several opportunities to further evaluate this concept are outlined below.

7.1.1 Multiple Load Monitoring in the Laboratory

The LEES Fluid Test System NILM can be used to monitor multiple loads by installing large scale current transducers (LEM LA 205-S or LA 305-S) in a laboratory load center. Various small loads are available to generate an aggregate test signal. The Fluid Test System Motor, air conditioning plant compressor motor, light banks and various smaller motors are all good candidates for these loads. The three channel data collection method discussed in Chapter 2 should then be used to verify the scaling factor of the LA-55P (installed in the Fluid Test System NILM) to the larger current transducer. This scale factor can in turn be applied to selected high quality templates generated from individual component monitoring in an attempt to disaggregate the fluid test system motor using the Machinery Space Simulation. Additionally, templates of steady state and shut off signatures should be investigated.

7.1.2 Load Center Monitoring

The installation of a NILM employing a large current transducer on an LBES load center would allow for a full scale test of multiple load monitoring. Panel 3-280-1 powered by switchboard 3SA is an excellent candidate because it supplies the 2A Fuel Oil Service Pump. This component would serve as the "target" as it has a permanent NILM installed and the motor's high quality templates have already been cataloged. The Machinery Space Simulation could then be used to evaluate the quality of the disaggregated signal.

7.1.3 Main Bus Monitoring

The NILM can be installed on existing current and voltage sensors used to monitor the busses that power the LBES auxiliary components. This would help complete an evaluation of the spectrum of non-intrusive monitoring from component level to load center level and finally to the main bus level. It should be noted again that this is a separate electrical distribution system from the full DDG-51 LBES ZEDS.

7.2 Testing Navy Systems

7.2.1 LBES Fuel Oil Service System

The permanent installation of a NILM on the LBES Fuel Oil Service System provides an opportunity to conduct additional tests of various NILM applications. For example, data collection runs could be conducted to generate a library of motor power spectral envelopes for normal and abnormal system valve lineups. Then blind tests could be conducted to determine if the NILM can recognize the current valve lineup based solely on the patterns of these spectral envelopes. Additionally the "dry start" phenomenon mentioned in Chapter 3 could be evaluated in more detail. A simple doubling test could be run to determine how long in takes for the pump impeller to reach what appears to be a dry state.

7.2.2 LBES Lube Oil Service System

The LBES Lube Oil Service System is an excellent candidate for cross-system validation of fluid system diagnostics explored in references [11] and [12]. Specifically, the techniques used to evaluate the clogging of the Auxiliary Sea Water heat exchangers on *SENECA* through frequency domain analysis of pump motor signatures could be used to attempt to identify test conditions where lube oil flow to an individual bearing was restricted. Of course these tests would need to be conducted with the main engines secured to prevent damage to the bearings. A diagnostic in this area would be particularly valuable to the Navy as inadequate lube oil flow to a bearing on the main propulsion train can result in a "hot bearing" condition. The immediate actions for this casualty typically call for the main propulsion shaft to be stopped and locked,

resulting in a loss of propulsion. As the name implies, a hot bearing is detected by an out of specification temperature condition at the bearing. If the NILM could provide a more timely indication that a clogging condition was developing, a hot bearing and associated loss of propulsion might be avoided.

7.2.3 LBES Low Pressure Service Air System

The baseline and test leak data gathered for Chapter 4 provided some preliminary insight into the operation of the Low Pressure Service Air System. However, to develop a meaningful diagnostic of a leak condition in this system, many more test runs need to be conducted with various test leak rates applied. Additionally, NILM test data without the bleed air system operating would assist in the further development of the MATLAB system simulation by helping to characterize the influence of bleed air operations on the frequency of air compressor cycles.

7.2.4 Other LBES Facilities

There are several facilities available at NSWCCD Philadelphia that would aid the progress of NILM research.

1. The Technical Acquisition Data Center (TDAC) is a local machinery monitoring system used at the DDG-51 LBES. TDAC "piggybacks" on the existing DDG-51 Machinery Control System, and can collect tailored data on parameters such as system pressure, temperature, and flow, as well as individual machinery status. TDAC can be used to help evaluate NILM data from LBES components. The ability to time stamp key plant parameters and compare them to NILM indications opens up new possibilities in the development of NILM diagnostics. The ICAS system can be used in a similar manner.

2. As discussed in Chapter 6, the ICAS system is designed to collect machinery monitoring data and transmit this data to a remote server for access by system experts and maintenance planners. This system could be utilized at the LBES to allow remote monitoring of NILM data. Although other remote monitoring techniques have been used with NILM installations at other sites, this method would allow a preview of the procedures necessary for remote monitoring of a NILM installed on a US Navy ship.

3. There are several stand alone facilities at the LBES that could be used for additional research on the application of the NILM on US Navy shipboard propulsion plant components. Two sites of interest are the compressed air facility and the air conditioning plant test facility. The compressed air facility has two 4500 PSI High Pressure Air Compressors similar to those used on Trident Class Ballistic Missile Submarines. The air conditioning facility has two 200 ton air conditioning plants of the same type currently in use on US Navy DDGs. The load on each plant can be varied between 50 and 200 tons for test purposes.

7.3 NILM-MFM Integration

Some additional resources for evaluating the NILM/MFM interface prior to pursuing approval for full scale testing are included below:

1. Use of the NSWCCD Philadelphia Distributed Heterogeneous Simulation (DHS) Laboratory. The DHS Lab would allow access to both electric plant and MFM simulation software that was developed locally to test the MFM III algorithms. It includes simulation models of Navy circuit breakers, MFM-III logic, various faults, and the DDG-91 ZEDS.

2. Use of the LBES Generator Protection Test Laboratory. The Generator Protection Lab is used to "bench test" communications and shunt trip actions for up to eleven full scale MFMs without having them installed in the ZEDS.

7.4 Moving towards testing NILM on a US Navy Ship

By conducting tests with the NILM at a Navy land based prototype, it is hoped that the research conducted for this thesis will provide a path to testing the NILM on a commissioned warship. Developing meaningful diagnostics that show the value of the NILM in Navy CBM schemes will be critical to achieving this goal. Additionally, briefing the commanding officers of crews training at the DDG-51 LBES on the capabilities of the NILM may help generate both interest and allies for future test proposals. Finally, another platform to consider for initial trials of the NILM is the ex-*USS ARTHUR W. RADFORD (DD 968).* This ship has a long history as a test platform and is currently being reconfigured to test various components of the Navy's future destroyer, the DD(X), including testing of the Integrated Power System [36].

7.5 Conclusion

Present machinery monitoring programs are laying the foundation for future systems that will one day provide a fully integrated ship control system. NILM is a sensor technology that has the potential to provide a great deal of operational and diagnostic information when in a "stand-alone" mode or when tied into existing machinery-monitoring systems such as ICAS. The testing conducted for this thesis indicates that NILM also has the potential to help reduce the number of sensors in current and future warships by monitoring multiple components simultaneously. This in turn could greatly reduce the installation and maintenance costs associated with machinery monitoring. Finally, using the ability to associate observed waveform features with the operation of particular loads, it may be possible to compute many diagnostic indicators and employ the NILM as a platform for condition based monitoring.

Page Intentionally Left Blank

List of References

[1] S.B. Leeb, S. R. Shaw, and J. L. Kirtley, Jr. 1995. "Transient Event Detection in Spectral Envelope Estimates for Noninstrusive Load Monitoring," *IEEE Transactions on Power Delivery* Vol. 10 No. 3, pp. 1200-1210.

[2] C.R. Laughman, K. Lee, R. Cox, S. Shaw, S.B. Leeb, and L. Norford, "Power Signature Analysis," IEEE Power and Energy Magazine, March/April 2003, pp. 56-63.

[3] Norford, L. K. and S. B. Leeb. 1996. "Nonintrusive Electrical Load Monitoring." *Energy and Buildings*, Vol. 24, pp. 51-64.

[4] K.D. Lee, S.B. Leeb, L.K. Norford, P. Armstrong, J. Holloway and S.R. Shaw, Estimation of Variable Speed Drive Power Consumption from Harmonic Content, accepted for publication, *IEEE Transactions on Energy Conversion.*

[5] Shaw, S.R., D. Evangelista, S.B. Leeb, and C.R. Laughman, Nonintrusive Load Monitoring and Identification in an Automotive Environment, *Proceedings of ELECTRIMACS 1999*, Lisbon, Portugal, pp. 199-204, September 1999

[6] S.R. Shaw, M. Keppler, S.B. Leeb, Pre-Estimation for Better Initial Guesses, *IEEE Transactions on Instrumentation and Measurement*, Volume 53, No. 3, June 2004, pp. 762-769.

[7] S.R. Shaw, S.B. Leeb, Identification of Induction Motor Parameters from Transient Stator Current Measurements, *IEEE Transactions on Industrial Electronics*, Volume 46, No. 1, February 1999, pp. 139-149.

[8] P. Armstrong, "Model Identification with Application to Building Control and Fault Detection", Building Technology, Massachusetts Institute of Technology, Cambridge, MA, 1993.

[9] Abler, C., R Lepard, S. Shaw, D. Luo, S. Leeb, and L. Norford. 1998. "Instrumentation for High-Performance Nonintrusive Electrical Load Monitoring." ASME *J. Solar Energy Engineering.*

[10] S.R. Shaw, R.F. Lepard, S.B. Leeb, and C.R. Laughman, A Power Quality Prediction System, *IEEE Transactions on Industrial Electronics*, Volume 47, No. 3, June 2000, pp. 511-517.

[11] J. Steven Ramsey, "Shipboard Applications of Non-Intrusive Load Monitoring", MIT NSEE/S.M. EECS thesis, June 2004.

[12] Tom DeNucci, "Diagnostic Indicators for Shipboard Systems Using Non-Intrusive Load Monitoring", MIT S.M. OE/S.M. ME thesis, June 2005.

[13] Shaw, S.R., "System Identification Techniques and Modeling for Nonintrusive Load Diagnostics," Ph.D. Dissertation, Department of Electrical Engineering and Computer Science, Massachusetts Institute of Technology, Cambridge, MA, February, 2000.

[14] DiUlio, M., Savage, C. and Schneider, E. "Taking the Integrated Condition Assessment System into the Year 2010," *13th Ship Control Symposium, Orlando FL,* 2003.

[15] Stanton, M., Captain, USN. Commanding Officer, Supervisor of Shipbuilding, Bath Maine. Interview with author, 21 January 2005.

[16] Davidson Instruments webpage. Available: http://www.davidson-instruments.com/news. July 10, 2002.

[17] Harmon, R. and Clark, D. "Wireless Machinery Monitoring Systems for Shipboard and Power Plant Applications," *13th Ship Control Symposium, Orlando FL,* 2003.

[18] Brooks, T. and Lee, K. "IEEE 1451 Smart Wireless Machinery Monitoring and Control for Naval Vessels," *13th Ship Control Symposium, Orlando FL,* 2003.
[19] M. Wickenheiser, ""Huge Ballet' Goes into Details of Building a Ship," Maine Sunday Telegraph, 11 April 2004, pg 7A.
[20] Carins, Andrew, DDG-51 LBES Test Director, 21 April 2005.
[21] Naval Sea Systems Command, Ship Information Book, USS FITZGERALD (DDG-61), Change C, 12 September 2001.
[22] United States Government Printing Office, USS ROOSEVELT (DDG-80) Damage Control and Engineering Handbook, 2000.
[23] Naval Sea Systems Command, Technical Manual for Fuel Service Pump, S6226-DE-MMA-010/07524, 5 July 2000.
[24] Naval Sea Systems Command, Technical Repair Standard for Lube Oil Service Pump (applicable to DDG-51/52/53/54), S6225-KH-TRS-010, 1 October 1992.
[25] Naval Sea Systems Command, Technical Manual for Air Compressor, Low Pressure, Oil Free, Model NAXI-100-4A, S6220-DQ-MMA-010/88663, 1 August 1989.
[26] LEM USA website, Current Transducers for Industrial Applications. Available at <http://www.lemusa.com/category/1>, April 2005.
[27] Wikepedia Website, Available at <http://en.wikipedia.org/wiki/Hanning_window>, April 2005.
[28] Rawstron David A, Supervisor of Shipbuilding, Bath Maine. E-mail correspondence, 10 June 2004.
[29] Naval Sea Systems Command, Technical Manual for Propulsion Gas Turbine and Ship Service Gas Turbine Generator Bleed Air Pressure Regulating Valves, S6435-M7-MMA-010/09790, 1 February 1990
[30] Bertsekas, Dimitri P., Tsitsiklis, John N. *Introduction to Probability*, Athens Scientific, (2002) page 154.
[31] Plesnick, Lyle, Hannon, Tracy, Devine, Daniel, An Intelligent Fault Detection Device for Shipboard Power Applications, Naval Sea Systems Command, Naval Surface Warfare Center, Carderock Division, Philadelphia.
[32] Guide to MFM Operations. Naval Sea Systems Command, Naval Surface Warfare Center, Carderock Division, Philadelphia, 2003.
[33] Wipf, David P., Parker, Eugene B., Demonstration and Assessment of High Speed Relay Algorithm, Barron Associates, Inc (for NSWCCD, Bethesda, MD). 30 June 1997.
[34] Checchio, Toni, Lead Electrical Test Engineer, DDG51 LBES, NSWCCD Philadelphia. Interview with author, 22 April 2005.
[35] Integrated Condition Assessment System webpage. Naval Surface Warfare Center, Carderock Division, Philadelphia. Available: <https://icas.navsses.navy.mil>. August 2004.
[36] DD 968 Arthur W Radford, Globalsecurity.org website. Available: <https://www.globalsecurity.org/military/agency/navy/dd-968.htm>. April 2005.

Appendix A. Machinery Space Simulation MATLAB Scripts

A.1 Requant

```
% This script calculates the re-quantized component signal (W) and the
% re-quantized template (Wt).  This is used when evaluating the monitoring of
% multiple pre-processed loads with no specific information
% about the size of the CT to be used.  The output of this script should then
% be called as an input to the "recognition" script.
function [W,Wt]=requant(maxY,X,t)
% Evaluate the graph of the high quality component signal.  Determine the
% peak power in watts and enter this value for "maxY".
a=1/maxY;
% This step transforms the scale of the HQ component signal (X) into values
% between 0 and 1.
Y=a*X;
% This step make a second transformation to the scale of the component
% signal (now identified as Y), to values between 0 and 4095.  This
% represents the window of the 12 bit analog to digital converter used by
% the NILM.
Z=Y*4095;
% This step quantizes the rescaled aggregate signal (now designated Z) by
% applying the floor function.  Floor rounds the elements of Z to the nearest
% integers towards minus infinity.
W=floor(Z);
% Again, use the peak power from the component data for "maxY".  The rest of
% the steps are similar to the steps above, except they are applied to the
% high quality template data vice the component data.  The template must be
% re-scaled and re-quantized in order to be applied to the aggregate
% signal.
Yt=a*t;
Zt=Yt*4096;
Wt=floor(Zt);
```

A.2 Recognition

```
% This script acts as a Transient Event Detector (TED)for the Machinery
% Space Simulation.
% The script takes the input "section", the template (i.e. N(8900:9400)
% where N is the column of pre-processed real power data output by the NILM),
% and "data", the aggregate signal (i.e. X = C+D+E+F), and outputs "test 1"
% (the flipped and re-quantized template), and "recog", (the convolution of
% test 1 and the aggregate signal).
function [test1, recog]=template(section,data)
% Input a representative section of a data field (such as a transient) and
% set this equal to the template designation (ex.template 2)
% t2 = N(8900:9400);
orig = section;
% convert template to AC coupled data (here the sum of this "work" is zero,
% i.e. the waveform is centered at zero)
work = section - sum(section)/length(section);
% check result, should equal zero (or some very small number)
sum(work)
% normalize the template
work = work/(norm(work)*norm(work));
% check that the inner product of work and the original section is equal
% to 1.0 (work' is the transpose)
work'*orig
% apply transversal filter:
% determine the lenght of the final template
finalt = work;
length(finalt)
% flip the final template for convolution
for count = 1:length(finalt),
flipfinalt(count) = finalt(1+length(finalt)-count);
end
plot(flipfinalt)
figure(2)
plot(conv(flipfinalt,data));
xlabel('Time (counts)')
ylabel('Match Factor')
title('Recognition')
test1=flipfinalt;
recog=conv(test1,data);
```

Appendix B. Process Instruction for Machinery Space Simulation

Process for Generating Templates from High Quality (Individual Component) Data and Assessing the Ability of the NILM to Disaggregate those Loads from an Aggregate Signal using MATLAB

1) Evaluate HQ snapshots of individual components.
    a. Note: when fingerprinting a component for the first time you must calibrate the NILM power measurements (i.e. measure the power output of the device during a brief period of steady state operation). This can be accomplished by using a power meter as described by [11] or by collecting raw voltage and current data to calculate steady state power and compare it to steady state counts). See step f.
    b. Unzip the file and save as a Winword text document.
    c. Strip headers (use Cygwin software as described in [12]).
    d. Load in MATLAB {ex: load ('snapshot-20050316-164256.txt'); }
    e. Save real power (column 2) array with component name. (note array size) {ex: brute205s=(snapshot_20050316_164256(:,2));}. Note also the change in format of "-" to "_" in the snapshot text.
    f. Plot array {ex: plot(brute205s);}. This will be in power (counts) on the y-axis and samples on the x-axis. Look for the section of steady state operation where you monitored the power in paragraph 1.a.
    g. Choose a representative section and save it as an array called "counts". {ex. counts205s=brute205s(7500:17500);}.
    h. Determine the average number of counts in this array using the "mean" command. {ex. mean(counts205s) }.
    i. Divide the average power in watts (as measured in paragraph 1.a) by the average counts to give you the scaling factor in watts/ADC count.
    j. Set the time scale to minutes or seconds. For example, to set it to minutes, generate a new array t. To do this, first look at the size of your snapshot in the MATLAB workspace window. Our example of brute205 is 35100 counts. Let t start at zero, increase with a step of 1/(120*60) {this changes the NILM sampling rate of 120Hz to

minutes}, all the way to 1 minus the array size (in minutes). The command looks like this: t=[0:1/(120*60):35099*(1/(120*60))]; .

k. Now you can plot your data in power vs. time (watts per minute) format as follows: plot(t2,brute205s*5.345); , where 5.345 is the scale factor in watts/ADC for the NILM/CT combination used to collect the data (see paragraph 1.i. above). Note that if you monitor the same load with a different CT, the scale factor must be re-computed.

2) Generate templates of each component.

a. Plot the data for a given component as in paragraph 1.f.

b. Select a representative section of transient (on the order of 200 to 700 counts in size, see Chapter 2, paragraph 2.4). For example: brute55p(16300:16500);

c. Save the template so it can be used in the script. Ensure you add the scale factor {i.e. t55p=(brute55p(16300:16500)*0.078);}.

3) Process the loads using the *"requant"* script.

a. Determine the maximum power in the aggregate signal. Multiply this by the scale factor to change the units to watts if necessary {ex. max(X)*0.078=1.6362e+003}. Round up to the nearest 10s place (i.e. 1640 watts).

b. Save this value as "maxY" {maxY=1640}.

c. Run the *requant* script. This will calculate the rescaled and re-quantized aggregate signal and the rescaled and re-quantized template of the component you are trying to identify. These arrays will be automatically loaded into your workspace. The script is executed by entering the designations you have chosen for these two arrays in brackets and setting them equal to the *requant* function. This function is expressed in terms of the maximum expected power in the aggregate signal, the designation of the aggregate signal, and the designation of the template of the target component. {ex. [W55p, Wt55p]=requant(1640,brute55p*0.078,t55p); }. Be sure to use the same units of power throughout (watts or counts). Here watts are used and the scale factor is included.

4) Process the loads and templates using the "*recognition*" script.

a. Determine the individual loads that are to comprise the simulated machinery space (ex. Pump1, Motor2, LoadA, etc).

b. Sum up the loads {ex: X = Pump1+Motor2+LoadA}. Again, ensure you are consistent with units. If using watts, multiply each load by its scale factor.
c. Now enter the "section" from paragraph 2.c. and the 'data" from paragraph 4.b and run the script.
d. The MATLAB output will be a series of checks and two plots. The first is the flipped, re-quantized template. The second is the plot of the match values and gives an estimate of the ability of the NILM to recognize the template against the given aggregate loads.

Page Intentionally Left Blank

Appendix C. Selected LBES System Drawings

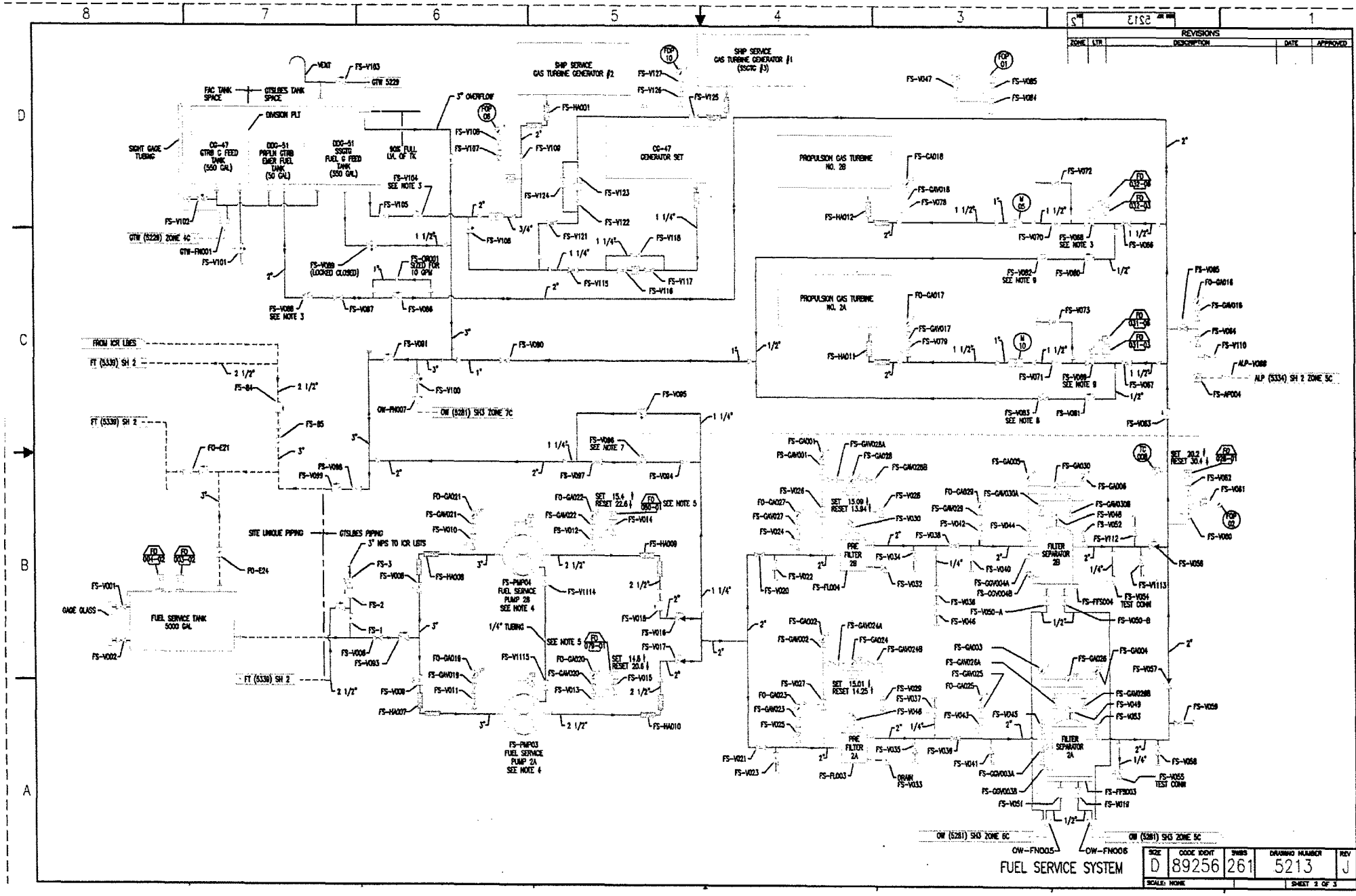
REVISIONS
ZONE | LTR | DESCRIPTION | DATE | APPROVED
FUEL SERVICE SYSTEM
SIZE D | CODE IDENT 89256 | SHEET 2 OF 3 | DRAWING NUMBER 5213 | REV J
SCALE: NONE
SHIP SERVICE GAS TURBINE GENERATOR #2
SHIP SERVICE GAS TURBINE GENERATOR #1 (SSGTG #3)
CC-47 GTRB C FEED TANK (550 GAL)
DDG-51 PROPLN GTRB EMCR FUEL TANK (50 GAL)
DDG-51 SSGTG FUEL G FEED TANK (550 GAL)
CC-47 GENERATOR SET
PROPULSION GAS TURBINE NO. 2B
PROPULSION GAS TURBINE NO. 2A
FUEL SERVICE TANK 5000 GAL
FS-PMP04 FUEL SERVICE PUMP 2B SEE NOTE 4
FS-PMP03 FUEL SERVICE PUMP 2A SEE NOTE 4
PRE FILTER 2B
PRE FILTER 2A
FILTER SEPARATOR 2B
FILTER SEPARATOR 2A
SITE UNIQUE PIPING — GTSLBES PIPING
FROM ICR LBES
OW (5281) SH3 ZONE 7C
OW (5281) SH3 ZONE 8C
OW (5281) SH3 ZONE 5C
ALP (5334) SH 2 ZONE 5C
FT (5339) SH 2
GTW (5228) ZONE 4C
SEE NOTE 3
SEE NOTE 5
SEE NOTE 7
SEE NOTE 8
SEE NOTE 9
TEST CONN
DRAIN FS-V033

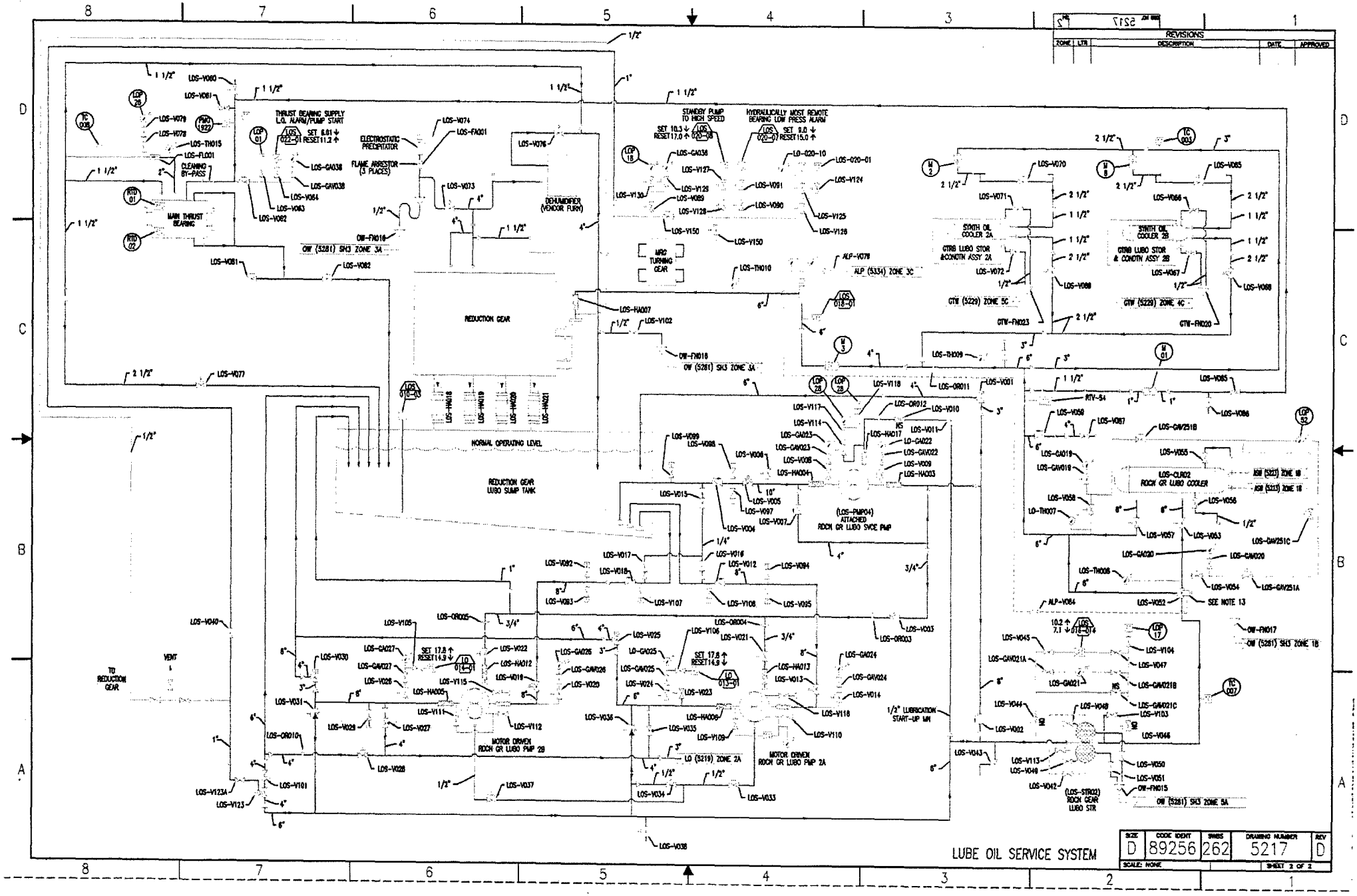
REVISIONS
ZONE | LTR | DESCRIPTION | DATE | APPROVED
LUBE OIL SERVICE SYSTEM
SIZE D | CODE IDENT 89256 | SHEET 262 | DRAWING NUMBER 5217 | REV D
SCALE: NONE
SHEET 2 OF 2
REDUCTION GEAR
REDUCTION GEAR LUBO SUMP TANK
NORMAL OPERATING LEVEL
MAIN THRUST BEARING
THRUST BEARING SUPPLY L.O. ALARM/PUMP START
STANDBY PUMP TO HIGH SPEED
HYDRAULICALLY MOST REMOTE BEARING LOW PRESS ALARM
ELECTROSTATIC PRECIPITATOR
FLAME ARRESTOR (3 PLACES)
DEHUMIDIFIER (VENDOR FURN)
CLEANING BY-PASS
MPR TURNING GEAR
SYNTH OIL COOLER 2A
SYNTH OIL COOLER 2B
GTRB LUBO STOR &CONDTN ASSY 2A
GTRB LUBO STOR & CONDTN ASSY 2B
(LOS-PMP04) ATTACHED ROCH GR LUBO SVCE PMP
ROCH GR LUBO COOLER
MOTOR DRIVEN ROCH GR LUBO PMP 2B
MOTOR DRIVEN ROCH GR LUBO PMP 2A
1/2" LUBRICATION START-UP MN
(LOS-STR02) ROCH GEAR LUBO STR
TO REDUCTION GEAR
VENT
SEE NOTE 13

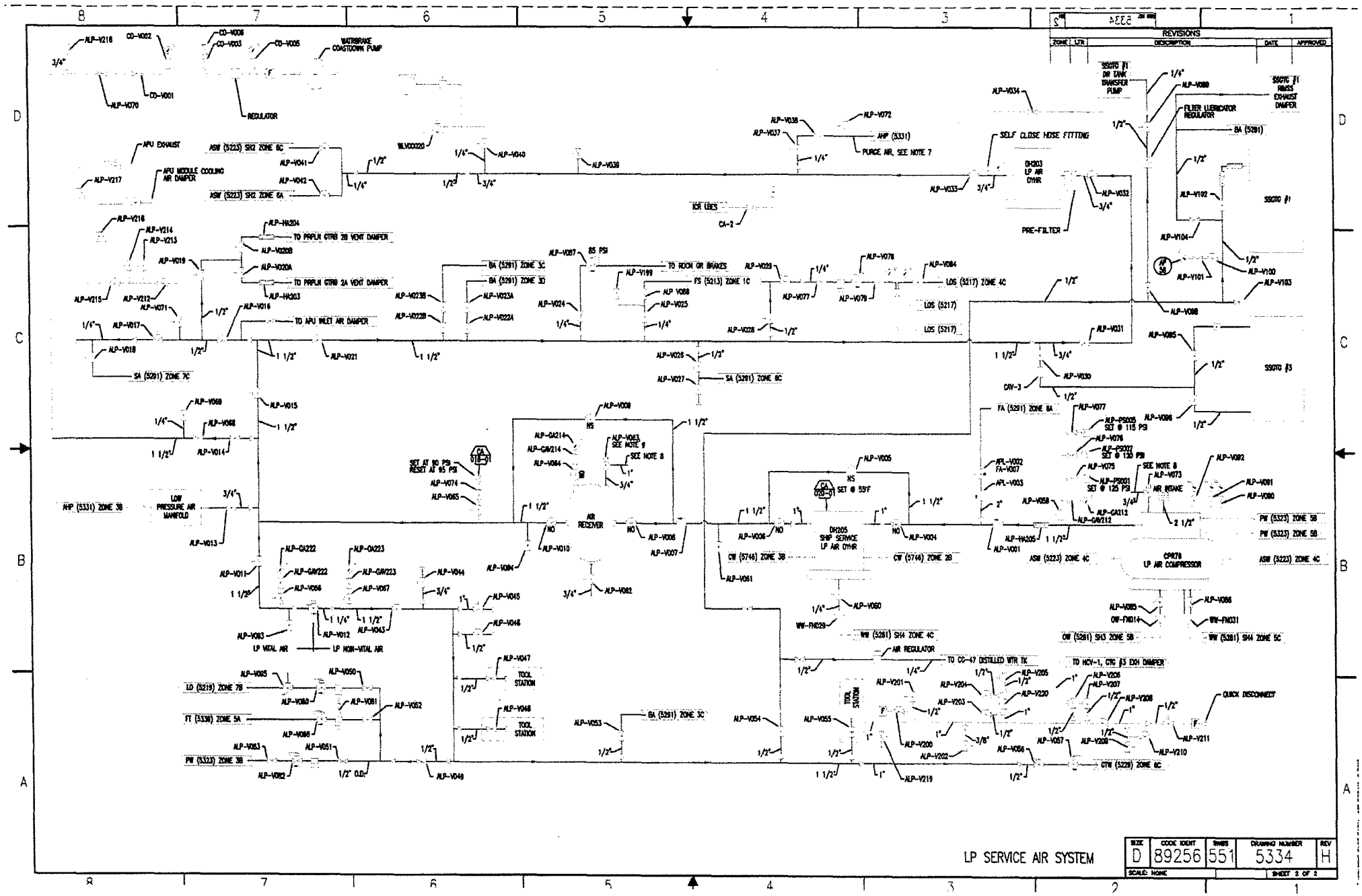
REVISIONS
ZONE | LTR | DESCRIPTION | DATE | APPROVED
LP SERVICE AIR SYSTEM
SIZE D | CODE IDENT 89256 | SHEET 551 | DRAWING NUMBER 5334 | REV H
SCALE: NONE
SHEET 2 OF 2
AIR RECEIVER
LOW PRESSURE AIR MANIFOLD
DH205 SHIP SERVICE LP AIR DYHR
DH203 LP AIR DYHR
CP478 LP AIR COMPRESSOR
AIR REGULATOR
PRE-FILTER
FILTER LUBRICATOR REGULATOR
SELF CLOSE HOSE FITTING
QUICK DISCONNECT
TOOL STATION
LP VITAL AIR
LP NON-VITAL AIR
SET @ 55°F
SET @ 115 PSI
SET @ 125 PSI
SET @ 130 PSI
SET AT 80 PSI RESET AT 65 PSI
PURGE AIR, SEE NOTE 7
SEE NOTE 8
SEE NOTE 9
TO HCV-1, CTG #3 EXH DAMPER
TO CC-47 DISTILLED WTR TK
TO APU INLET AIR DAMPER
TO FRPLN CTRB 2A VENT DAMPER
TO FRPLN CTRB 2B VENT DAMPER
TO ROOM OR BRAKES
APU EXHAUST
APU MODULE COOLING AIR DAMPER
WATERBRAKE COASTDOWN PUMP
ICR LOCS
CA-2
ALP-V001
ALP-V002
ALP-V003
ALP-V004
ALP-V005
ALP-V006
ALP-V007
ALP-V008
ALP-V009
ALP-V010
ALP-V011
ALP-V012
ALP-V013
ALP-V014
ALP-V015
ALP-V016
ALP-V017
ALP-V018
ALP-V019
ALP-V021
ALP-V022
ALP-V023
ALP-V024
ALP-V025
ALP-V026
ALP-V027
ALP-V028
ALP-V029
ALP-V030
ALP-V031
ALP-V032
ALP-V033
ALP-V034
ALP-V035
ALP-V036
ALP-V037
ALP-V038
ALP-V039
ALP-V040
ALP-V041
ALP-V042
ALP-V043
ALP-V044
ALP-V045
ALP-V046
ALP-V047
ALP-V048
ALP-V049
ALP-V050
ALP-V051
ALP-V052
ALP-V053
ALP-V054
ALP-V055
ALP-V056
ALP-V057
ALP-V058
ALP-V060
ALP-V061
ALP-V062
ALP-V063
ALP-V064
ALP-V065
ALP-V066
ALP-V067
ALP-V068
ALP-V069
ALP-V070
ALP-V071
ALP-V072
ALP-V073
ALP-V074
ALP-V075
ALP-V076
ALP-V077
ALP-V078
ALP-V079
ALP-V080
ALP-V081
ALP-V082
ALP-V083
ALP-V084
ALP-V085
ALP-V086
ALP-V087
ALP-V088
ALP-V091
ALP-V092
ALP-V096
ALP-V099
ALP-V100
ALP-V101
ALP-V102
ALP-V103
ALP-V104
ALP-V200
ALP-V201
ALP-V202
ALP-V203
ALP-V204
ALP-V205
ALP-V206
ALP-V207
ALP-V208
ALP-V209
ALP-V210
ALP-V211
ALP-V212
ALP-V213
ALP-V214
ALP-V215
ALP-V216
ALP-V217
ALP-V219
ALP-V220
ALP-V222
ALP-V223
ALP-V228
ALP-V238
ALP-GA211
ALP-GA212
ALP-GA214
ALP-GA222
ALP-GA223
ALP-GW212
ALP-GW214
ALP-GW222
ALP-GW223
ALP-HA203
ALP-HA204
ALP-HA205
ALP-PS001
ALP-PS002
ALP-PS005
APL-V002
APL-V003
FA-V007
CD-V001
CD-V002
CD-V003
CD-V005
CD-V006
CW-3
WLVD0020
ASW (5223) SH2 ZONE 6C
ASW (5223) SH2 ZONE 6A
ASW (5223) ZONE 4C
BA (5291) ZONE 3C
BA (5291) ZONE 3D
SA (5291) ZONE 7C
SA (5291) ZONE 6C
FA (5291) ZONE 8A
LOS (5217)
LOS (5217) ZONE 4C
PS (5213) ZONE 1C
AHP (5331)
AHP (5331) ZONE 3B
LD (5219) ZONE 7B
FT (5338) ZONE 5A
PW (5323) ZONE 3B
PW (5323) ZONE 5B
CW (5746) ZONE 3B
CW (5746) ZONE 2B
CW (5281) SH3 ZONE 5B
WW (5281) SH4 ZONE 4C
WW (5281) SH4 ZONE 5C
GTW (5229) ZONE 6C
SSGTG #1
SSGTG #1 EXHAUST DAMPER
SSGTG #1 DR TANK TRANSFER PUMP
SSGTG #3
WW-FN029
WW-FN031
OW-FN014
1/4"
1/2"
3/4"
1"
1 1/2"
2"
2 1/2"
3/8"
1/2" O.D.

Appendix D. LBES Test Plans

Non-intrusive Load Monitor and ICAS Component Monitoring

Test No.: _____ Revision: 0 Date: 9 February 2005

A. OBJECTIVE:

Collect voltage and current data on selected individual loads during stead state and transient operation using a NILM installed immediately upstream of the components power supply (typically in the component controller). This data will be compared with ICAS data collected on selected systems at the same time. The following components will be observed: 1) Fuel Oil Service Pump, 2) Lube Oil Pump, 3) Low Pressure Air Compressor, other components as recommended.

B. BACKGROUND:

The NILM was originally developed to monitor electrical power usage in buildings. The NILM measures voltage and current at the utility service entry and generates power envelopes such as the one shown in Figure 1.

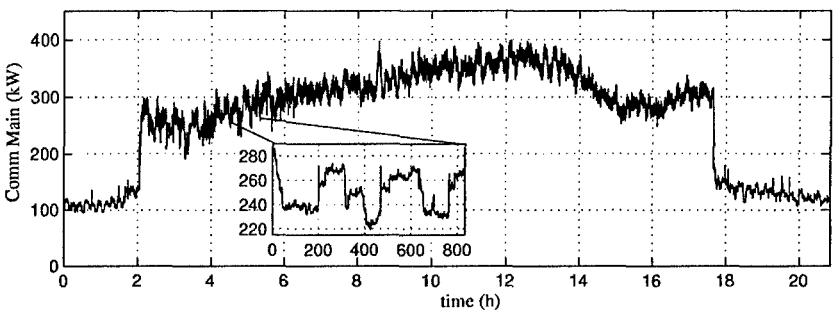

FIGURE 1: NILM Data from a Large Commercial Building

It can be seen in Figure 1 that in addition to providing gross power usage, the NILM captures data on the operation of individual loads. When the NILM is connected to a power supply immediately upstream of a single component, the NILM will provide the power envelope of just that individual load. Figure 2 shows an ASW Pump being started and stopped.

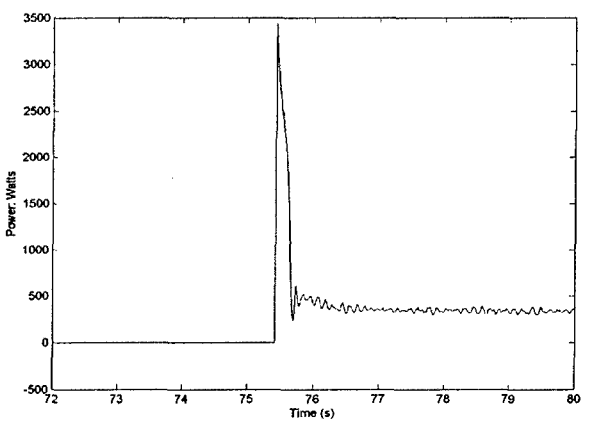

FIGURE 2: NILM Data from an ASW Pump Start

These power envelopes look different and can be used like "fingerprints" to identify individual loads. The NILM uses a sophisticated transient event detector that can be trained to recognize these fingerprints during system installation. Once trained, the NILM can differentiate between the operation individual loads, even when other loads on the same service are operating or being cycled on and off. However, the limits of this capability have not been explored. In theory, a few NILMs may be able to provide machinery monitoring information for an entire engineering space.

Component Monitoring:

Test #1: 2A Fuel Oil Service Pump Operation

C. PREREQUISTES:

1. Set up ICAS for event and trend monitoring of the Fuel Oil Service System.
2. Fuel Oil System lined up to support operation of the 2A Fuel Oil Service Pump.
3. De-energize and power panel 1-283-1 at 1SA SWBD.
4. Verify NILM voltage board and current resistors are set up to monitor 440VAC and 5.75/7.5 FLA (slow and fast speed).
5. Install NILM voltage and current transformer at the LPAC motor controller.
6. Restore power to power panel 1-283-1.

D. PRELIMINARY:

1. Conduct NILM system checks.
2. Read through the procedure in its entirety prior to beginning the test.

E. PROCEDURE:

1. Energize the NILM and initialize data acquisition.
2. Collect steady state data.
   a. Start the 2A Fuel Oil Service Pump in slow speed and allow it to operate normally for 5 minutes.
   b. Secure the pump.

c. Repeat steps 2.a and 2.b for fast speed operation.

3. Collect transient data.
   a. Start the pump and run for 1 minute.
   b. Secure the pump for 1 minute.
   c. Repeat steps 3.a and 3.b for a total of three slow speed and three fast speed starts.
   d. Start the pump in slow speed, run for 1 minute, and shift to fast speed.
   e. Run for 1 minute and secure the pump.
   f. Start the pump in fast speed, run for 1 minute, and shift to slow speed.
   g. Run for 1 minute and secure the pump.

Test #2: 2B Lube Oil Service Pump Operation

F. PREREQUISTES:

1. Set up ICAS for event and trend monitoring of the Lube Oil Service System
2. Lube Oil System lined up to support operation of the 2B Lube Oil Service Pump.
3. De-energize power panel 3-254-4 at 3SA SWBD.
4. Verify NILM voltage board and current resistors are set up to monitor 440VAC and 61/72 FLA (slow and fast speed).
5. Install NILM voltage and current transformer at the 2B Motor Control Panel. Note: this may require additional cable access to the panel.
6. Restore power to power panel 3-254-4.

G. PRELIMINARY:

1. Conduct NILM system checks.
2. Read through the procedure in its entirety prior to beginning the test.

H. PROCEDURE:

1. Energize the NILM and initialize data acquisition.

2. Collect steady state data.
   a. Start the 2B Lube Oil Pump in slow speed and allow it to operate normally for 5 minutes.
   b. Secure the pump.
   c. Repeat steps 2.a and 2.b for fast speed operation.
3. Collect transient data.
   a. Start the pump and run for 1 minute.
   b. Secure the pump for 1 minute.
   c. Repeat steps 3.a and 3.b for a total of three slow speed and three fast speed starts.
   d. Start the pump in slow speed, run for 1 minute, and shift to fast speed.
   e. Run for 1 minute and secure the pump.
   f. Start the pump in fast speed, run for 1 minute, and shift to slow speed.
   g. Run for 1 minute and secure the pump.
4. End Test 2.

Test 3: Low Pressure Air Compressor Operation

I. PREREQUISTES:

1. Low Pressure Air System lined up to support operation of the Low Pressure Air Compressor.
2. De-energize and tag out power to power panel 3-254-4 at 3SA SWBD.
3. Verify NILM voltage board and current resistors are set up to monitor 440VAC and 35 FLA.
4. Install NILM voltage and current transformer at the 2A Fuel Oil motor controller. Note: this may require additional cable access to the panel.
5. Clear tags at 3SA SWBD and re-energize power panel 3-254-4.

J. PRELIMINARY:

1. Conduct NILM system checks.
2. Read through the procedure in its entirety prior to beginning the test.

Test No.: _____ Revision: 0 Date: 9 February 2005

K. PROCEDURE:

1. Energize the NILM and initialize data acquisition.
2. Collect steady state data.
   a. Start the Low Pressure Air Compressor and allow it to operate normally for 15 minutes.
   b. Secure the compressor.
3. Collect transient data.
   a. Start the compressor and run for 2 minutes.
   b. Secure the compressor for 2 minutes.
   c. Repeat steps 3.a and 3.b for a total of five compressor starts.
4. End Test 3.

LBES Non-intrusive Load Monitor LPAC Testing

Test No.: _____ Revision: 2 Date: 31 March 2005

A. OBJECTIVE:

Evaluate the use of the non-intrusive load monitor (NILM) in detecting leaks in the Low Pressure Air System by monitoring voltage and current input to the Low Pressure Air Compressor (LPAC). This test is to be conducted during a crew certification to ensure adequate loads are applied to the LP air system.

B. BACKGROUND:

Many cycling systems require periodic mechanical "charging" by an electromagnetic actuator like a motor. Examples include low-pressure and high-pressure air, some pneumatic actuators, and vacuum-assisted drains and disposals. Field experiments on the USCG Cutter *SENECA* indicate that the NILM can be used as a diagnostic tool to determine the difference between high system demand due to operations and demand caused by leaks.

C. PREREQUISTES (to be completed the week of 11 April):

6. Verify the Low Pressure Air System is lined up to support operation of the Low Pressure Air Compressor.
7. Ensure the compressor is running in Automatic 125 PSIG mode.
8. Ensure shop air is isolated by shutting FA-V007.
9. Verify LPAC NILM is operational.
10. Install flow meter in Low Pressure Air System. The flow meter to be used is a new air and gas dial type, rated to a maximum pressure of 3000 psi and a maximum temperature of 175° F. The scale is 0-25 scfm. Connections are ¼ inch NPT female. The installation will be made at an LP air tool station such as ALP-V047. The output of the flowmeter will be vented outboard of the building via the roof.
11. Verify leak rate to be used. If leak rate is too small, it will may not provide a statistically significant change to baseline loads on the system. If the leak rate is too large, the combination of the leak and large system loading could exceed the capacity of the LPAC. (Note: the introduction of shop air through check valve ALP-V003 would invalidate the test.) Based on the 100 scfm discharge capacity of the LPAC, an initial leak size of 5 scfm is proposed.

    F. Start the LPAC in Automatic 125 psi operating mode.

    G. Verify no loads are operating on the LP air system.

    H. Monitor the LPAC for 1 hour and determine the number of pump cycles.

    I. Open isolation to flow meter until 5 scfm is read on the gage.

* Sign and date as complete _____

J. Monitor the LPAC for 1 additional hour and determine the number of pump cycles.

K. Secure verification: isolate the flow meter and secure the LPAC.

If the number of pump cycles with the leak is more than double the number of pump runs with no leak, the leak rate should be reduced. If the number of pump runs with the leak does not change from the number without the leak, the leak rate should be increased.

D. PRELIMINARY (to be completed on 18 April at the start of plant operations):

2. Conduct NILM system checks.
3. Read through the procedure in its entirety prior to beginning the test.

E. PROCEDURE (to be completed on 18 April at the start of plant operations):

5. Verify the Low Pressure Air System is lined up to support operation of the Low Pressure Air Compressor.
6. Ensure the compressor is running in Automatic 125 PSIG mode.
7. Ensure shop air is isolated by shutting FA-V007.
8. Energize the NILM and initialize data acquisition for pre-processed data.
9. Collect data during the first half of operations each day with no leak in the system. Note number of LPAC pump cycles in each hour of operation and compare with logs from paragraph C.4.c.*
10. Insert leak in LP air system as described in paragraph C.4.d at the midpoint of each shift (approximately 1130 local time). Note number of LPAC pump cycles in each hour of operation and compare with logs from paragraph C.4.e.
11. Collect data with small system leak in system.
12. Secure monitoring when crew certification is complete.
13. Isolate flow meter.
14. Collect TDAC data and hand logs.
    a. Retrieve NILM data.
15. End Test.

* Leak rate may need to be adjusted based on system capacity.

Appendix E. LBES Data Analysis MATLAB and PERL Scripts

E.1 MATLAB Script Used in Fuel Oil Transient Analysis:

```
%This script zero pads the data set (PpX) with N=1024, applies a hanning
%window, calculates the FFT and plots the result.

function [spect]=freq_h(PpX,t_1024)
sPpXb=fft(hanning(length(PpX)).*PpX,1024);
plot(t_1024, abs(sPpXb));
xlabel('Frequency (Hz)')
ylabel('Magnitude')
spect=sPpXb;
title('Window: 0-120 counts -');
```

E.2 PERL Script Used In LPAC Data Analysis:

```
#!/usr/bin/perl

# Computes time between unloaded compressor runs for data given on stdin.

$edge_time = -1;
$last_val = 0;
$val = 0;
$last_rawval = -1;
$lines = 0;
while(<>)
{
    ($junk, $raw) = split(/\s+/);

    # $val should be 1 if the compressor is on,
    #                0 if the compressor is off.
    # On/off is determined by whether the power draw is above/below 14000
    # but only if it stays there for 2 seconds or longer

    if($raw < 14000) {
      $rawval = 0;
    } else {
      $rawval = 1;
    }
    if($rawval != $last_rawval) {
      # immediate change; reset the count
      $count = 0;
      $last_rawval = $rawval;
    } elsif($rawval != $val) {
      # raw value staying constant, increment count
      $count++;
      if($count > 240) {
          # stable, keep it
          $val = $rawval;
      }
    }

    if($val == 1 && $last_val == 0) {
      if($edge_time >= 0) {
          $diff = ($lines - $edge_time);
          print "$diff\n";
      }
    }
    if($val == 0 && $last_val == 1) {
      $edge_time = $lines;
    }

    $last_val = $val;
    $lines++;
}
```

E.3 MATLAB Script Used in Low Pressure Air System Leak Analysis:

E.3.1. Simulation_LPAC

```
% This is a modification of the script developed in reference [12].  It is
% designed to model the LBES Low Pressure Air Service System.  It assumes that
% air loads are due to the discrete cycles of control valves in the system.

% Parameters
global pump1_rate pump_low pump_high leak;
T = 19*60;          % simulation time (min) - up to 19 hours to match data runs
press_drop = 2;     % pressure drop of single control valve cycle (cvc) -
psi/min
pump1_rate = 33;    % rate for compressor - psi/min

pump_low = 110;     % compressor turns on

pump_high = 125;    % compressor turns off -
leak = 0;           % leak rate - psi/min
m = 10;             % estimated average cvc's per hour
v=0.005;            % estimated variance of cvc's per hour

clf;
colordef('white');
%Initialization
%for i=5:35
%    leak=i
pressure = pump_high;
pump_time = [];

% Simulate cvc's for the entire time period
t = 0;
lastt = 0;
while (t < T),
  % Run the pumping/leaking simulation to get us caught up
  [ pressure, tmptime ] = pumpleak(pressure, t - lastt);
  pump_time = [ pump_time, tmptime + lastt ];

  % Now we're caught up with pumping, so cycle a control valve.
  pressure = pressure - press_drop;

  % Jump forward to next valve cycle
  lastt = t;
   %scaling our random variable by v and m
  Y=((randn)*v)+1/m;
  t = t + Y;
end

[N, X] = hist(diff(pump_time),40);
figure(1);
whitebg(1,'white');
bar(X*60,N,'b');
xlabel('Unloaded Run Time (sec)','fontsize',18);
ylabel ('Compresser Cycles','fontsize',18);
%pause(0.25);
%end

for i=1:length(N)
   if N(i)==max(N)
       count=i;
   end
end
count;
```

E.3.1. Pumpleak

```
% This script is called by the LPAC simulation to determine compressor run
% time.  It was taken directly from reference [12] and was originally designed
for a
% system with 2 pumps.  Due to the modifications in global variables, the
% second pump is not called.

function [ pressure, turnons ] = pumpleak(pressure, T)
  % Simulate the pumping / leaking for 't' hours
  global pump1_rate pump2_rate pump_low pump_lower pump_high leak;

  persistent pumps_running;
  if (T == 0)
    pumps_running = 0;
  end

  if (pressure < 0)
    error('Pressure is negative!  Too much vavle cycling?\n');
  end

  t = 0;
  turnons = [];
  while(t < T),
    left = T - t;

    % Figure out the current pressure rate
    if (pressure <= pump_lower | pumps_running == 2)
      rate = pump1_rate + pump2_rate - leak;
      if(pumps_running ~= 2)
      turnons = [ turnons, t ];
      pumps_running = 2;
      end
    elseif (pressure <= pump_low | pumps_running == 1)
      rate = pump1_rate - leak;
      if(pumps_running ~= 1)
      turnons = [ turnons, t ];
      pumps_running = 1;
      end
    else
      rate = -leak;
      pumps_running = 0;
    end

    % Now jump forward until we run out of time or something may change
    if (rate == 0)
      t = T;
    else
      if (pumps_running == 2 & rate < 0)
      error('Both pumps running and still losing pressure due to leak!');
      elseif (pumps_running == 1 & rate < 0)
      % Run until we need two
      stop = pump_lower;
      elseif (rate < 0)
      % Run until we need one
      stop = pump_low;
      elseif (rate > 0)
      % Run until we need none
      stop = pump_high;
      end

      turnoff = (stop - pressure) / rate;
      if (t + turnoff < T)
      t = t + turnoff;
```

```
      pressure = stop;
      pumps_running = 0;
      else
      t = T;
      pressure = pressure + rate * left;
      end
    end
  end
end
```

Page Intentionally Left Blank

Appendix F. DDG-51 Class Destroyer ICAS Equipment Monitoring

CCS

- Dry Bulb Temp
- Wear Oil Analysis
- Potable Water
- Security (Intrusion)
- Sounding Level
- Sounding & Security
- Fuel Oil Panel
- MRG Humidity
- Heat Stress
- Laundry Heat Stress
- Ship Heat Stress
- Oily Drain Tanks
- Fire Pump 1
- Fire Pump 2
- Fire Pump 3
- Fire Pump 4
- Fire Pump 5
- Fire Pump 6
- SW Service System
- SW Service Pump 1
- SW Service Pump 2
- SW Service Pump 3
- SW Service Pump 4
- SW Service Pump 5

MER1

- HPAC 1
- LPAC 1
- Mark2 Dehyd #1
- Mark2 Dehyd #2
- GTM #1A
- GTM #1B
- MRG #1
- Stbd Lo Sys
- LOSP #1A
- LOSP #1B
- CRP #1
- Lo Purifier #1
- Stbd Line Shaft

MER2

- HPAC 2
- LPAC 2
- LPAC 3
- LPAD 3/T2
- LPAD 4/T2
- GTM 2A
- GTM 2B
- MRG #2
- Port Lo Sys
- LOSP #2A
- LOSP #2B
- Lo Purifier #2
- Port Line Shaft
- GTG #2
- GTG #3

AMR1

- AC Plant #1
- AC Plant #2
- AC Plant #3
- AC Plant #4
- RO Desal #1A
- RO Desal #1B
- Freezer/Chiller Box
- Ref Plant #1
- Ref Plant #2
- GTG #1
- Heat Stress
- Brominator
- RO Second Pass
- Potable Water

ICAS Technology Group.

Revised: August 23, 2002.

Appendix G. ICAS Machinery Monitoring Data

ICAS Event Monitoring - Lube Oil

TIME	LO-004-06 HI SPD CMD	LO-004-08 HI SPD IND	LO-004-05 LW SPD CMD	LO-004-07 LW SPD IND	LO-004-01 STOP CMD	LO-004-02 STOP IND	TC-006 LUB SUP TEMP	LOP-17 DISCH PRES SVPMP	LO-020-01 MRB PRESS	M-03 OIL FLOW TO MRG	M-01 OIL FLOW TO TBRG	LOP-01 OIL SUP TO TBRG
-59	0	0	0	0	0	2	112.03	28.987	18.227	102.56	6.502	6.931
-58	0	0	0	0	0	2	112.068	28.545	18.235	102.257	5.656	6.635
-57	0	0	0	0	0	2	112.091	28.093	18.21	90.286	5.024	6.376
-56	0	16	0	0	0	0	112.076	27.681	18.218	117.259	4.521	6.094
-55	0	16	0	0	0	0	112.091	27.278	18.241	115.037	7.497	5.8
-54	0	16	0	0	0	0	112.152	26.934	18.227	381.037	23.731	5.607
-53	0	16	0	0	0	0	112.213	26.997	18.216	538.384	33.028	5.763
-52	0	16	0	0	0	0	112.312	28.052	18.227	537.222	33.076	6.276
-51	0	16	0	0	0	0	112.312	29.226	18.218	474.94	29.721	6.766
-50	0	16	0	0	0	0	112.312	29.858	18.219	417.153	26.374	7.087
-49	0	16	0	0	0	0	112.328	30.115	18.211	385.785	24.525	7.27
-48	0	16	0	0	0	0	112.274	30.161	18.207	378.662	24.042	7.39
-47	0	16	0	0	0	0	112.32	30.256	18.21	379.824	24.209	7.465
-46	0	16	0	0	0	0	112.32	30.388	18.216	382.4	24.371	7.536
-45	0	16	0	0	0	0	112.213	30.571	18.21	381.239	24.274	7.607
-44	0	16	0	0	0	0	111.938	30.759	18.226	381.39	24.298	7.69
-43	0	16	0	0	0	0	111.626	30.918	18.239	381.592	24.355	7.747
-42	0	16	0	0	0	0	111.427	31.125	18.203	384.471	24.395	7.803
-41	0	16	0	0	0	0	111.382	31.321	18.218	381.895	24.299	7.859
-40	0	16	0	0	0	0	111.427	31.501	18.202	380.127	24.313	7.878
-39	0	16	0	0	0	0	111.549	31.672	18.216	381.643	24.315	7.939
-38	0	16	0	0	0	0	111.694	31.865	18.21	382.956	24.305	7.988
-37	0	16	0	0	0	0	111.809	32.058	18.208	381.087	24.305	8.039
-36	0	16	0	0	0	0	111.969	32.2	18.213	382.956	24.399	8.109
-35	0	16	0	0	0	0	112.068	32.405	18.217	382.501	24.403	8.14
-34	0	16	0	0	0	0	112.167	32.571	18.239	384.067	24.382	8.184
-33	0	16	0	0	0	0	112.213	32.754	18.245	382.299	24.443	8.239
-32	0	16	0	0	0	0	112.267	32.9	18.227	382.552	24.347	8.265
-31	0	16	0	0	0	0	112.373	33.074	18.209	381.138	24.337	8.293
-30	0	16	0	0	0	0	112.419	33.218	18.219	384.017	24.424	8.347
-29	0	16	0	0	0	0	112.404	33.401	18.213	383.007	24.482	8.362
-28	0	0	0	0	0	2	112.465	33.555	18.227	386.492	24.45	8.386

TIME	LO-004-06 HI SPD CMD	LO-004-08 HI SPD IND	LO-004-05 LW SPD CMD	LO-004-07 LW SPD IND	LO-004-01 STOP CMD	LO-004-02 STOP IND	TC-006 LUB SUP TEMP	LOP-17 DISCH PRES SVPMP	LO-020-01 MRB PRESS	M-03 OIL FLOW TO MRG	M-01 OIL FLOW TO TBRG	LOP-01 OIL SUP TO TBRG
-27	0	0	0	0	0	2	112.511	33.718	18.222	306.783	20.1	8.439
-26	0	0	0	0	0	2	112.495	33.66	18.218	243.086	16.495	8.365
-25	0	0	0	0	0	2	112.541	33.362	18.24	171.459	12.173	8.195
-24	0	0	0	0	0	2	112.518	32.874	18.215	120.694	9.098	7.917
-23	0	0	0	0	0	2	112.549	32.327	18.207	98.064	7.574	7.602
-22	0	0	0	0	0	2	112.526	31.765	18.226	86.295	6.475	7.273
-21	0	0	0	0	0	2	112.511	31.228	18.239	89.73	5.649	6.965
-20	0	0	0	0	0	2	112.511	30.684	18.224	101.045	5.017	6.646
-19	0	0	0	0	0	2	112.564	30.19	18.237	111.551	4.523	6.392
-18	0	0	0	0	0	2	112.587	29.685	18.218	110.39	4.14	6.1
-17	0	0	0	0	0	2	112.541	29.194	18.231	118.067	3.94	5.82
-16	0	0	0	0	0	2	112.564	28.765	18.21	135.09	3.829	5.507
-15	0	0	0	0	0	2	112.556	28.315	18.224	120.896	3.691	5.238
-14	0	0	0	0	0	2	112.572	27.913	18.213	130.797	3.544	4.969
-13	0	0	0	0	0	2	112.556	27.488	18.227	158.68	3.451	4.727
-12	0	0	0	0	0	2	112.556	27.087	18.234	21.336	3.401	4.489
-11	0	0	0	0	0	2	112.556	26.709	18.219	31.59	3.322	4.249
-10	0	0	0	0	0	2	112.556	26.321	18.222	-1.294	3.239	4.052
-9	0	0	0	0	0	2	112.587	25.974	18.211	2.292	3.131	3.84
-8	0	0	0	0	0	2	112.595	25.627	18.226	344.263	3.024	3.649
-7	0	0	0	0	0	2	112.595	25.317	18.2	4.869	2.927	3.469
-6	0	0	0	0	0	2	112.572	25.007	18.202	1.636	2.841	3.278
-5	0	0	0	0	0	2	112.572	24.69	18.226	1.585	2.772	3.122
-4	0	0	0	0	0	2	112.572	24.392	18.241	1.787	2.695	2.932
-3	0	0	0	0	0	2	112.549	24.087	18.227	1.585	2.643	2.78
-2	0	0	0	0	0	2	112.556	23.801	18.219	1.737	2.584	2.609
-1	0	0	0	0	0	2	112.572	23.513	18.223	1.787	2.524	2.451
0	0	0	0	[redacted]	0	0	112.587	23.228	18.221	84.78	3.868	2.285
1	0	0	0	[redacted]	0	0	112.556	22.957	18.251	175.702	8.146	2.258
2	0	0	0	[redacted]	0	0	112.556	22.771	18.232	216.416	10.572	2.416
3	0	0	0	[redacted]	0	0	112.602	22.632	18.218	211.819	13.658	2.702
4	0	0	0	[redacted]	0	0	112.587	22.622	18.207	246.117	16.141	3.047
5	0	0	0	[redacted]	0	0	112.633	22.686	18.227	265.363	17.367	3.41
6	0	0	0	[redacted]	0	0	112.587	22.793	18.198	274.758	17.946	3.72
7	0	0	0	[redacted]	0	0	112.633	22.896	18.206	276.879	18.187	3.983
8	0	0	0	[redacted]	0	0	112.564	22.993	18.208	280.062	18.35	4.218
9	0	0	0	[redacted]	0	0	112.572	23.062	18.233	282.385	18.431	4.395

TIME	LO-004-06 HI SPD CMD	LO-004-08 HI SPD IND	LO-004-05 LW SPD CMD	LO-004-07 LW SPD IND	LO-004-01 STOP CMD	LO-004-02 STOP IND	TC-006 LUB SUP TEMP	LOP-17 DISCH PRES SVPMP	LO-020-01 MRB PRESS	M-03 OIL FLOW TO MRG	M-01 OIL FLOW TO TBRG	LOP-01 OIL SUP TO TBRG
10	0	0	0	1	0	0	112.556	23.14	18.249	283.396	18.544	4.594
11	0	0	0	1	0	0	112.549	23.184	18.218	284.86	18.585	4.757
12	0	0	0	1	0	0	112.572	23.215	18.209	283.396	18.63	4.877
13	0	0	0	1	0	0	112.495	23.286	18.221	285.265	18.664	4.989
14	0	16	0	0	0	0	112.465	23.335	18.245	288.598	18.734	5.078
15	0	16	0	0	0	0	112.198	23.406	18.211	393.059	24.337	5.16
16	0	16	0	0	0	0	111.488	23.723	18.23	545.758	33.383	5.433
17	0	16	0	0	0	0	110.252	24.746	18.23	539.798	33.173	5.988
18	0	16	0	0	0	0	109.695	25.679	18.203	478.728	29.828	6.55
19	0	16	0	0	0	0	109.802	26.179	18.201	419.325	26.347	6.927
20	0	16	0	0	0	0	110.077	26.404	18.239	386.694	24.399	7.156
21	0	16	0	0	0	0	110.405	26.499	18.232	378.612	23.956	7.278
22	0	16	0	0	0	0	110.733	26.604	18.215	381.996	24.142	7.403
23	0	16	0	0	0	0	111.046	26.755	18.227	382.552	24.298	7.478
24	0	16	0	0	0	0	111.32	26.997	18.23	380.228	24.295	7.577
25	0	16	0	0	0	0	111.565	27.205	18.226	380.582	24.218	7.647
26	0	16	0	0	0	0	111.748	27.405	18.222	381.188	24.247	7.704
27	0	16	0	0	0	0	111.847	27.617	18.209	379.269	24.266	7.777
28	0	16	0	0	0	0	111.954	27.852	18.216	380.936	24.263	7.842
29	0	16	0	0	0	0	112.106	28.064	18.199	380.885	24.281	7.887
30	0	0	0	0	0	2	112.114	28.284	18.213	372.5	23.851	7.92
31	0	0	0	0	0	2	112.175	28.442	18.217	285.113	18.861	7.941
32	0	0	0	0	0	2	112.213	28.408	18.223	218.689	15.027	7.832
33	0	0	0	0	0	2	112.221	28.179	18.221	152.214	10.981	7.629
34	0	0	0	0	0	2	112.221	27.844	18.201	112.612	8.465	7.355
35	0	0	0	0	0	2	112.228	27.422	18.217	91.346	7.119	7.025
36	0	0	0	0	0	2	112.228	27.041	18.209	85.133	6.141	6.72
37	0	0	0	0	0	2	112.213	26.682	18.231	97.408	5.393	6.424
38	0	0	0	0	0	2	112.228	26.309	18.217	115.39	4.8	6.135
39	0	0	0	0	0	2	112.129	25.957	18.208	107.005	4.345	5.819
40	0	0	0	0	0	2	112.167	25.618	18.21	115.087	3.996	5.525
41	0	0	0	0	0	2	112.183	25.271	18.215	115.087	3.853	5.217
42	0	0	0	0	0	2	112.259	24.944	18.217	118.825	3.722	4.939
43	0	0	0	0	0	2	112.198	24.653	18.218	119.785	3.579	4.67
44	0	0	0	0	0	2	112.213	24.309	18.208	131.605	3.452	4.412
45	0	0	0	0	0	2	112.19	24.028	18.217	140.798	3.385	4.168
46	0	0	0	0	0	2	112.167	23.738	18.217	2.191	3.329	3.952

TIME	LO-004-06 HI SPD CMD	LO-004-08 HI SPD IND	LO-004-05 LW SPD CMD	LO-004-07 LW SPD IND	LO-004-01 STOP CMD	LO-004-02 STOP IND	TC-006 LUB SUP TEMP	LOP-17 DISCH PRES SVPMP	LO-020-01 MRB PRESS	M-03 OIL FLOW TO MRG	M-01 OIL FLOW TO TBRG	LOP-01 OIL SUP TO TBRG
47	0	0	0	0	0	2	112.198	23.459	18.21	95.034	3.256	3.73
48	0	0	0	0	0	2	112.175	23.188	18.218	-1.294	3.156	3.529
49	0	0	0	0	0	2	112.213	22.917	18.224	2.141	3.059	3.336
50	0	0	0	0	0	2	112.198	22.654	18.241	447.461	2.954	3.155
51	0	0	0	0	0	2	112.175	22.415	18.219	-1.294	2.858	2.988
52	0	0	0	0	0	2	112.213	22.166	18.218	1.484	2.781	2.811
53	0	0	0	0	0	2	112.175	21.912	18.216	1.686	2.708	2.644
54	0	0	0	0	0	2	112.213	21.709	18.221	1.636	2.626	2.466
55	0	0	0	0	0	2	112.206	21.46	18.202	1.686	2.578	2.324
56	0	0	0	0	0	2	112.228	21.245	18.199	1.585	2.528	2.165
57	0	0	0	0	0	2	112.19	21.047	18.214	1.585	2.48	2.065
58	0	0	0	0	0	2	112.228	20.847	18.23	1.636	2.453	2.026
59	0	0	0	0	0	2	112.175	20.63	18.21	1.585	2.406	1.981
60	0	0	0	0	0	2	112.213	20.435	18.211	1.737	2.366	1.95

ICAS Trend Monitoring – Fuel Oil

TIME	OPER. HOURS	FOP-01 FUEL PRES	TC-008 FUEL TEMP	FO-011-06 2A LOW	FO-011-07 2A HIGH	FO-012-06 2B LOW	FO-012-07 2B HIGH
14:16:14	0.196389	7.163	67.497	0	0	0	0
14:17:14	0.213056	34.263	67.497	128	0	0	0
14:18:14	0.229722	34.131	67.2	128	0	0	0
14:19:14	0.246389	33.896	66.75	128	0	0	0
14:20:14	0.263056	33.981	66.628	128	0	0	0
14:21:14	0.279722	33.995	66.879	128	0	0	0
14:22:14	0.296389	34.032	67.253	128	0	0	0
14:23:14	0.313056	34.098	67.619	128	0	0	0
14:24:14	0.329722	33.82	67.978	128	0	0	0
14:25:14	0.346389	33.856	68.23	128	0	0	0

Page Intentionally Left Blank

Appendix H. Points of Contact

Name	Title/Organization	Phone	E-mail
Dan Devine	Advanced Machinery Systems and Controls Branch Head	215-897-1890 215-514-3787 (c)	DevineDP@nswccd.navy.mil
Lyle Plesnick	Advanced Power & Propulsion Machinery R&D Branch Head	215-897-8602 215-205-3766 (c)	plesnicklr@nswccd.navy.mil
Andy Cairns	DDG-51 LBES Program Manager	215-897-7446 215-205-5886 (c)	CairnsJA@nswccd.navy.mil
Lee Skarbeck	Lead Test Engineer (Mechanical)	215-897-7299	SkarbekLF@nswccd.navy.mil
Frank Facciolo	LBES Technician (Mechanical)	215-897-7842	FaccioloFA@nswccd.navy.mil
Toni Checchio	Lead Test Engineer (Electrical)	215-897-1503	ChecchioTA@nswccd.navy.mil
Jack Eplin	Test Engineer (MFM)		
Chris Savage	Maintenance, Monitoring, and Information Systems Specialist (ICAS)	215-897-7460 215-806-6423 (c)	savagecj@nswccd.navy.mil
Mike McGovern	Code 921 Branch Head (POC for Air Conditioning Systems)	215-897-7213	michaelp.mcgovern@navy.mil
Keith Grimes	Compressed Air Systems Engineering	215-897-7248	GrimesKR@nswccd.navy.mil
GSCS(SW) Tim Wilson	Aegis Training and Readiness Center Detachment	215-897-1801	timothy.k.wilson1@navy.mil